Study Of The Effect Of Distributed Periodic Corrugation In A Semicoductor Injection Laser

A Thesis submitted to the Electrical and Electronic
Engineering Department of BUET, Dhaka,
in partial fulfilment
requirements for the degree of
Master of Science in Engineering
(Electrical and Electronic)

MD. MOHSIN MOLLAH

April 1994

Declaration

I hereby declare that this work has not been submitted elsewhere for the award of any degree or diploma or for publication.

Md. Mohsin Mollah

The thesis titled "STUDY OF THE EFFECT OF DISTRIBUTED PERIODIC CORRUGATION IN A SEMICONDUCTOR INJECTION LASER" submitted by Md. Mohsin Mollah, Roll No. 901337P, session '88-89 to the Electrical and Electronic Engineering Department of B.U.E.T. has been accepted as satisfactory for partial fulfilment of the requirements for the degree of Master of Science in Engineering (Electrical and Electronic).

Board of Examiners

1. Dr. Saiful Islam
   Professor
   Department of EEE
   B.U.E.T., Dhaka 1000

   Chairman Saiful Islam 12-4-94
   (Supervisor)

2. Dr. Syed Fazl-i Rahman
   Professor and Head
   Department of EEE
   B.U.E.T., Dhaka 1000

   Member 12.4.94
   (Ex-officio)

3. Dr. A. B. M. Siddique Hossain
   Professor
   Department of EEE
   B.U.E.T., Dhaka 1000

   Member 12/04/94

4. Dr. Shamsuddin Ahmed
   Head
   Department of EEE
   ICTVTR, Gazipur

   Member 12/04/94
   (External)

Acknowledgement

The author expresses his sincere and profound gratitude to Professor Dr. Saiful Islam of Electrical and Electronic Engineering Department of BUET for his incessant and meticulous guidance in completing this work. The author thanks him for his outstanding suggestions and expert opinions in the mathematical computation and design procedure of the periodic corrugation in a distributed feedback semiconductor laser.

Thanks are given to Professor Dr. Syed Fazl-i Rahman, Head of the Electrical and Electronic Engineering Department, BUET for his encouragement and cooperation.

The author thanks his friend Md. Shahadatullah Khan, Graduate Student, Department of Electrical and Computer Engineering, University of Victoria, Victoria, Canada for helping him by sending photocopies of Journals. Thanks are also given to M. Nazrul Islam, and Md. Ferdous Alam for their cooperation and encouragement.

Contents

List of principal symbols

$\overline{E}$	=	Electric field intensity Volts/m.
$\overline{H}$	=	Magnetic field intensity Amps/m.
k_0	=	Wave number in free space.
n	=	Refractive index.
$\overline{n}$	=	Average value of refractive index in an index corrugated layer.
Δn	=	Maximum variation of the refractive index in an index corrugated semiconductor layer, $\Delta n << \overline{n}$.
χ	=	Dielectric susceptibility; a complex quantity.
$\Delta\chi$	=	Maximum variation of the dielectric susceptibility; a complex quantity.
θ	=	Phase change experienced by a reflected wave within the external cavity.
ψ	=	Phase difference (in radians) between index corrugation κ_n and gain corrugation (corrugation of dielectric susceptibility) κ_g.
ϕ	=	Initial phase of index corrugation at z=0, radian.
ϕ_1, ϕ_2	=	The values of ϕ, the initial phase of corrugation at z=0 for regions 1 and 2 of a DFB laser, radian.
κ_n	=	$\frac{\kappa_0\lvert\Delta n\rvert}{2}$ = index coupling coefficient.
κ_g	=	$\frac{\kappa_0\lvert\Delta\chi\rvert}{2}$ = gain coupling coefficient.
γ	=	The complex propagation constant.
β	=	$\omega n/c_0$, the propagation constant in free space.
β_B	=	π/Λ, the propagation constant at the Bragg frequency.
$\Delta\beta$	=	Deviation from the propagation constant corresponding to the Bragg wavelength. $\approx (\beta - \beta_B)$.
$(\overline{g} - \alpha)$	=	Relative gain minus attenuation in a semiconductor laser.
r_1	=	The reflection coefficient at the inside of the left facet of a DFB semiconductor laser.

r_2	=	Is the reflection coefficient at the inside of the right facet of a DFB semiconductor laser.
R_2	=	Power reflection coefficient at $z = l_2 = l$, $\sqrt{R_2} = r_2$, if there is no reflection from external cavity.
Γ	=	Power reflection coefficient at the surface of a device external to the laser.
η	=	Coupling coefficient inside the laser for light entering from outside.
$\eta\Gamma$	=	The effective relfected light entering into the laser from external reflection of the laser cavity.
λ	=	$2\pi/k = 2\pi c/\omega = 2\pi c_0/n\omega$.
Λ	=	Grating period.
σ	=	Conductivity of the active layer of the laser.
σ'	=	$\sigma + j\omega\varepsilon_0\chi$.
$\eta\Gamma_c$	=	Critical feedback ratio above which the external cavity modes appear.
c_0	=	Phase velocity of EM wave in vacuum = velocity of light = 3×10^8 m/s.
ν	=	$\omega/2n$, the frequency of output light.
l	=	Length of laser (single section).
l_{ext}	=	Length of the external cavity.

Abstract

A general form of analytic expression for the oscillation condition of a pure index coupled distributed feedback (DFB) semiconductor laser has been derived following a recent work on DFB lasers. For this derivation a sinusoidal variation of refractive index corrugation along the length has been assumed and finite values of reflection at the front and back facets of the DFB semiconductor laser has been assumed.

Following the derivation of the equation for oscillation condition of a pure index coupled DFB laser, an equation representing oscillation condition for a 'gain plus index' coupled DFB semiconductor laser has been derived. In this type of laser, sinusoidal variation has been assumed for both index and gain coupling. An equation representing dispersion relation for such a laser has been presented. The equations for 'gain plus index' coupled DFB laser have been taken as a more general form of equation, since this can be used for (i) pure index coupled case by assuming zero value for gain coupling coefficient, (ii) pure gain coupled case by assuming zero value for index coupling coefficient and (iii) for a 'gain plus index' coupled case by assuming finite values for index as well as gain coupling coefficients.

Next, the generalized equations for 'gain plus index' coupled DFB semiconductor laser has been modified for taking into account of the effect of laser output signal entering back into the laser after facing partial reflection from a surface external to the laser. Such a reflection has been termed as external feedback.

A computer programme has been prepared using Quick Basic on 386 and 486 microcomputers for obtaining numerical solutions of the generalized equation representing oscillation in a 'gain plus index' coupled DFB semiconductor injection laser. The programme has been prepared in a way so that numerical computations and plots of relative gain vs. relative frequency of the results are obtained simultaneously. Solutions and plots for real part of the equation are obtained at first, and the solutions and plots of the imaginary part of the equation are obtained next on the same screen.

A number of combinations of parameters for (i) index coupled, (ii) gain coupled and (iii) 'gain plus index' coupled laser have been used for computation work without any external feedback. Then the computations for these examples have been repeated for various values of external feedback ratio. The values of critical feedback ratios of each type of DFB semiconductor laser have been obtained through computation work for lasers producing minimum value of threshold gain. The results for the three types of lasers have been analyzed and compared with each other.

CHAPTER 1

Introduction

1.1 Historical background of lasers

The introduction of ruby laser in 1960 [2] [4] and subsequent work on intense coherent optical sources during the following decades have stimulated researches in optical communication. Lasers of different types e.g., gas type, liquid type, solid-state ion type, semiconductor for both pulsed and continuous operations have been tried in optical communication besides various other applications.

The maser principle, which was originally developed in the microwave frequency range, is the basis for lasers [4]. Application of this principle to optical transitions provided the first method of achieving net gain at optical frequencies. Extension of the maser principle to optics was first proposed by Schawlow and Townes [1] in 1958. In 1960 Maiman [2] used maser principle in optical transitions to produce the first pulsed ruby laser.

Maiman's demonstration [2] was the beginning of a number of successes. Shortly after this, a second type of solid-state laser was reported by Sorokin and Stevenson (1960) at the IBM corporation. Trivalent uranium ions in calcium fluoride was used as a material in this solid-state laser. Approximately one year later, Javan et. al. [3] of Bell telephone Laboratories reported the first continuous wave (CW) He-Ne laser. This CW laser operated in the near infrared region.

The laser boom started in 1961. In this year, Johnson and Nassau [8] demonstrated the first solid-state Neodymium laser, in which the neodymium ion was a dopant in Calcium tungstate ($CaWO_4$) [4]. Johnson [5], Kiss and Pressley [6], and Goodwin and Heavens [7] reviewed various optically pumped crystalline lasers operated utilizing (i) transition metal ions such as Cr^{3+}, Ni^{2+}, and Co^{2+}; (ii) rare-earth ions such as Nd^{3+}, Pr^{3+}, Er^{3+}, Ho^{3+}, Tm^{3+}, Yb^{3+}, Sm^{2+}, Dy^{2+}; and (iii)

the actanide ion U^{3+}. Room temperature operation of a continuously pumped solid state laser was first reported in 1962 by Johnson et. al. [8] using Nd^{3+} in $CaWO_4$. Since then a number of CW solid state ion laser operation have been reported. Of these, solid-state ion lasers made of Cr^{3+} in Al_2O_3 (ruby) [9] [10], Nd^{3+} in glass [11] and $CaMO_4$ [12] are worth mentioning. Among these the most highly developed continuous solid state ion laser is the one made of Nd:YAG [13].

The first semiconductor diode laser was demonstrated nearly simultaneously by three separate groups in the fall of 1962 [4]. All three teams, one from the General Electric Research Laboratories in Schenectady (New York); another from the IBM Watson Research Centre in Yorktown Heights (New York), and the third from the MIT's Lincoln Laboratories in Lexington (Massachusetts) demonstrated similar Gallium Arsenide diodes cooled at 70^0K temperature of liquid Nitrogen [4]. During the next few years several more of today's most important lasers emerged.

Bridges [4] in (1964) observed laser transitions in the blue and green parts of the spectrum from singly ionized argon. This is the basis of today's argon ion lasers. Kumar and Patel [4] (1964) obtained a $10.6\mu m$ laser emission from carbon dioxide. Lasers of this type are still used as high power source in industry.

Sorokin and Lankard [29] at IBM Watson Research Centre in 1966 demonstrated the first organic dye laser, they used a giant pulse ruby laser to excite solutions of the dyes chloroaluminium phthalocynaine (CAP) which is a standard tool of laser spectroscopy now a days. The first chemical laser is the hydrogen chloride type which emitted at $3.7\mu m$ and was demonstrated in 1965 by Kaspar and Pimentel [4].

A simple p-n junction type semiconductor laser needs large forward currents and high dissipation, which required for cooling and pulsed operation. These disadvantages were overcome by using heterojunction laser structures. A further improvement was obtained with a double heterojunction (DH) structure (figure 1.1) in which an active GaAs layer is sandwiched between two layers of higher-band gap GaAs. The two most important DH lasers are (i) one with the active region made of $Ga_{1-x}Al_xAs$, (ii) the other one with the active region made of $Ga_{1-x}In_xAs_{1-y}P_y$. The first one emits light of wavelength ranging between $.75\mu m$ and $.88\mu m$. This spectral region is convenient for short-haul (<2 km) optical communication in silica

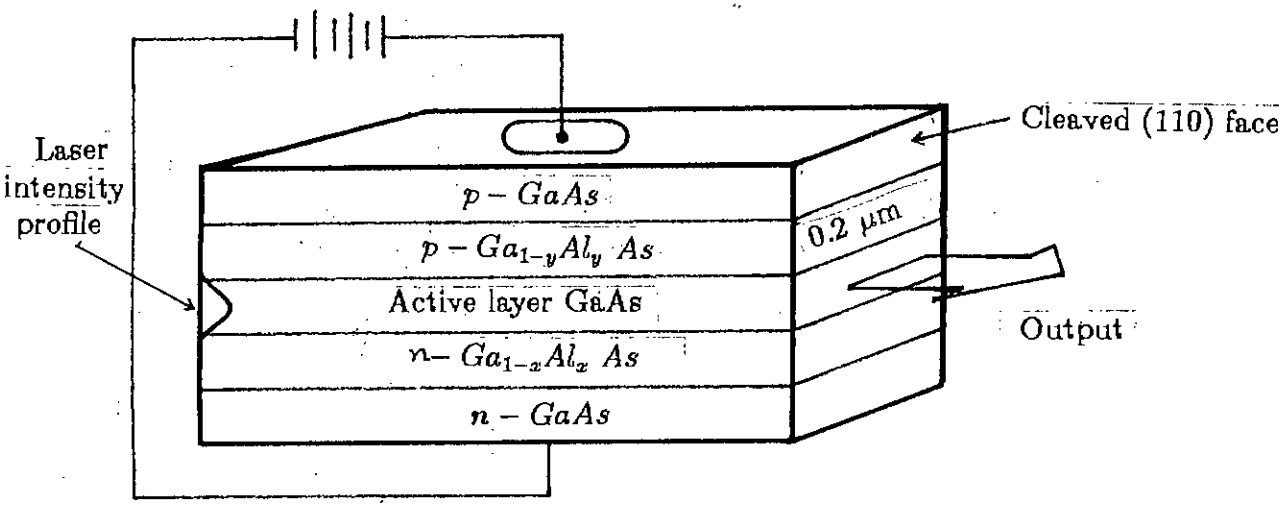

Figure 1.1: A typical double heterostructure (DH) GaAs-GaAlAs laser.

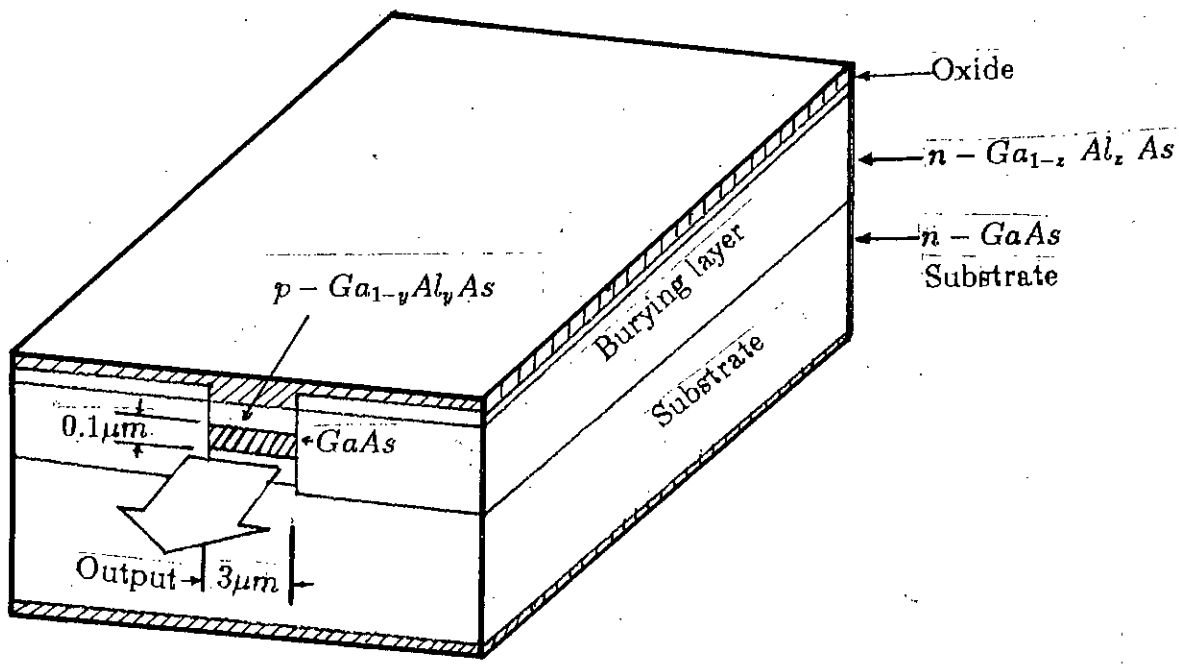

Figure 1.2: A typical buried heterostructure (BH) laser.

fibres. The second type laser has the wavelength between $1.1\mu m$ and $1.6\mu m$ depending on x and y. The region near $1.55\mu m$ is suitable in optical communication due to its low loss (0.15 dB/Km) [14].

Due to difficulties in confining current and radiation in the lateral (y) direction in heterojunction lasers more than one transverse (y) modes appeared thus mode hopping as well as spatial and temporal instabilities result. In order to circumvent these difficulties a new type of laser structure called buried heterostructure (BH) laser has been developed. The first of this kind of laser was successfully operated by Tsukada [15] in 1974. A basic structure of BH laser is shown in figure 1.2. Here the active region is surrounded on all sides by the lower index GaAlAs, so that electromagnetically the structure is that of a rectangular dielectric wave guide. The transverse dimensions of the active region and the index discontinuities (i.e. the molar fractions x, y, z) are so chosen that only the lower order transverse mode can propagate in the waveguide.

Usually, lasers contain three key elements, one is the laser medium itself, which generates the laser light. The second is the power supply, which delivers energy to the laser medium in the form needed to excite it (medium) to emit light. The third is the optical cavity or resonator, which concentrates the light to stimulate emission of laser radiation [4]. The laser oscillation is constructed by utilizing the laser gain medium inside an optical cavity as shown in figure 1.3. Optical regenerative gain occurs for light travelling along the cavity axis. The cavity length l is typically 10^3 to 10^6 times larger than the laser wavelength. Typically more than one axial or longitudinal cavity resonance fall within the laser gain profile. Oscillation occurs [16] at those cavity resonance lying within the inhomogeneous width of the laser transition for which the laser gain exceeds the cavity losses. This is depicted in figure 1.4, where the laser peak gain exceeds the single pass cavity losses for the two lowest order transition modes. The optical and temporal coherence of a laser source arises from the regenerative character of the combined laser gain medium and optical cavity. In the subsequent section we shall be dealing with semiconductor lasers as a result a discussion on the semiconductor materials is necessary at this stage.

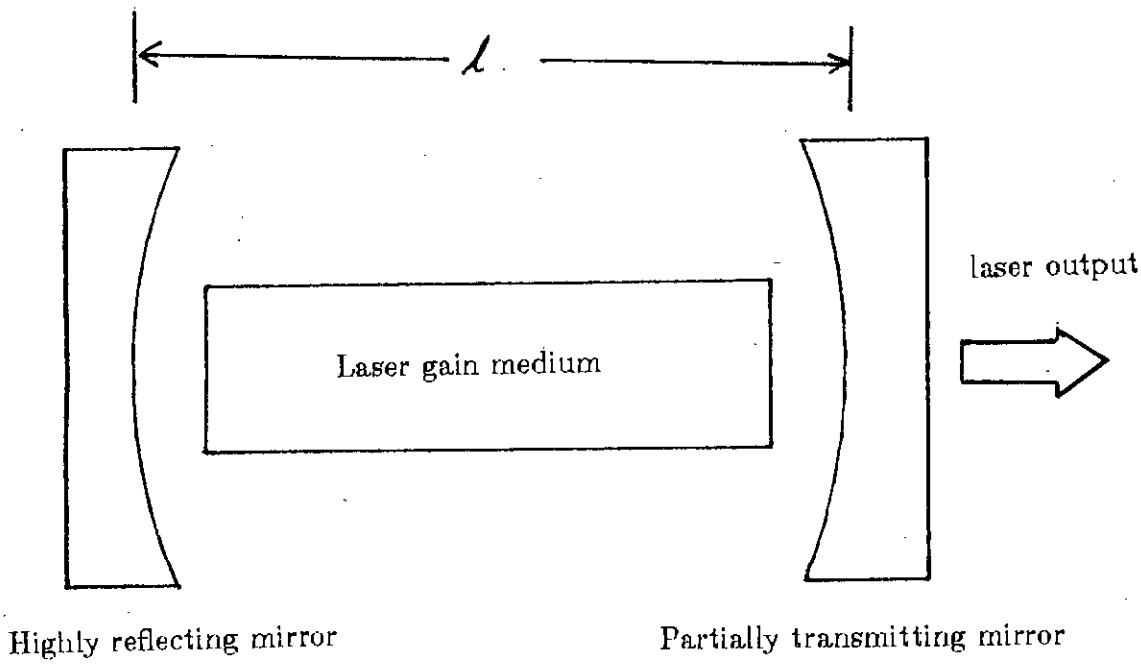

Figure 1.3: A scematic diagram of a simple laser oscillator.

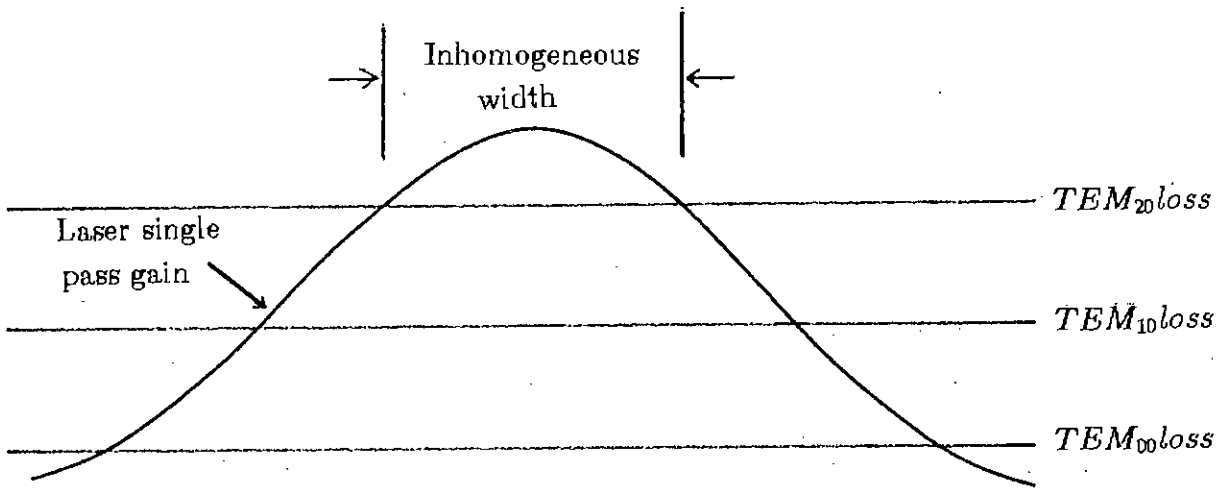

Figure 1.4: Laser gain and cavity losses for different cavity modes.

1.2 Semiconductor laser materials

A semiconductor laser consists of an appropriate type of semiconductor material within a suitable resonator having two reflecting mirrors. The semiconductor material should be such that one can get significant population inversion for obtaining stimulated emission. The very high population inversion obtainable in a semiconductor results in a large gain. The gain can be so large that the path length for the stimulated emission need not be long and the ends of the cavity need not be highly reflecting. Thus with cavity lengths of only a few hundred microns, semiconductor lasers are extremely small. In contrast to other types of lasers where the transitions occurs between discrete states of excited atoms, in a semiconductor laser, the transitions involve sets of banded states. The boundary of states results from the close packing of activated atoms. Hence a high density of population inversion is required to reach threshold conditions. The high gain required for laser action in semiconductor materials is observed in direct semiconductor than indirect semiconductor. The favourite direct semiconductor materials are GaAs, InGaP, AlGaAs, $Ga(As_xP_{1-x})$ etc.

The high gain associated with the direct gap semiconductor can be understood from the energy diagram of figure 1.5. Here, a minimum in the conduction band, at A for example, corresponds in the momentum scale to a minimum in the conduction band, at B. Hence, an electron can be elevated from the conduction band at A into the valance band at B with minimum energy and there is no change in momentum during the process. Similarly, the direct transition in the other direction i.e., from B to A, causes the emission of a photon without changing the momentum. For indirect-gap semiconductors, of which Si is the principle member, one gets a simplified energy band diagram as shown in figure 1.6. In this case, an electron transferred across the minimum energy gap from C to D or vice versa must also experience a simultaneous change in momentum as shown in the diagram. This momentum change is achieved by interaction with lattice phonon vibration. Such an indirect process is less likely than the direct transitions involving no change in momentum. In this section, we have discussed about the necessity of direct band gap semiconductor materials for constructing any type of semiconductor laser. In the next section we will discuss

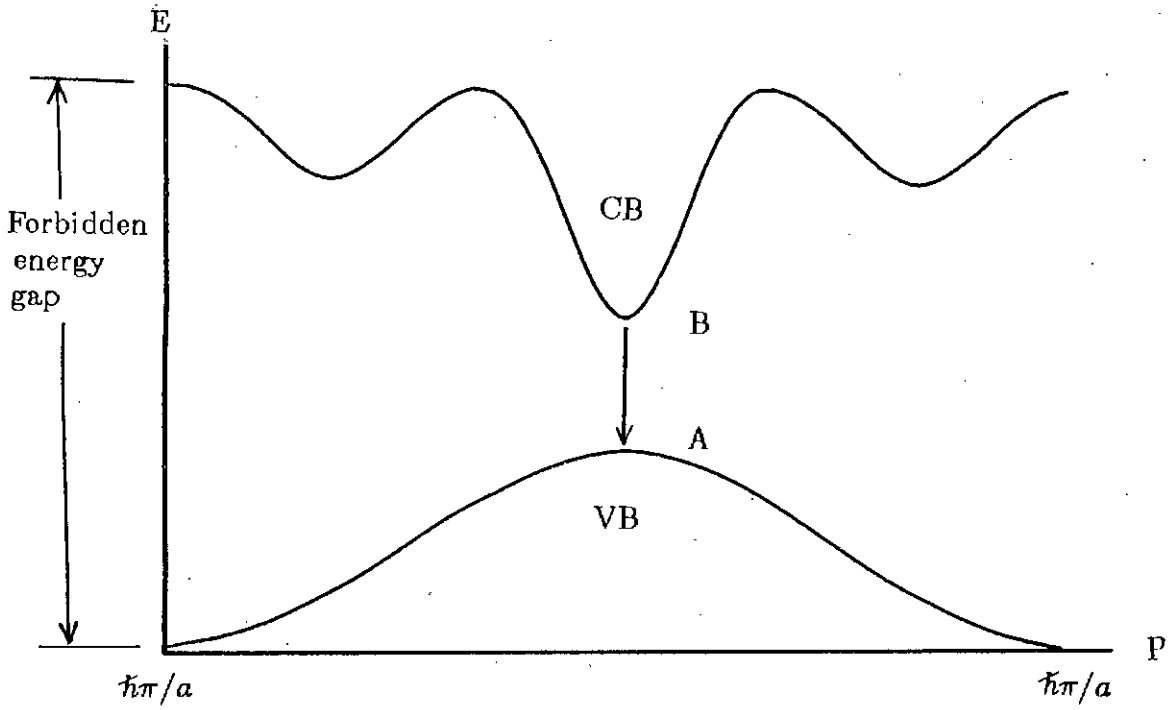

Figure 1.5: Energy diagram (Energy vs. momentum P) of a GaAs -a direct-gap semiconductor.

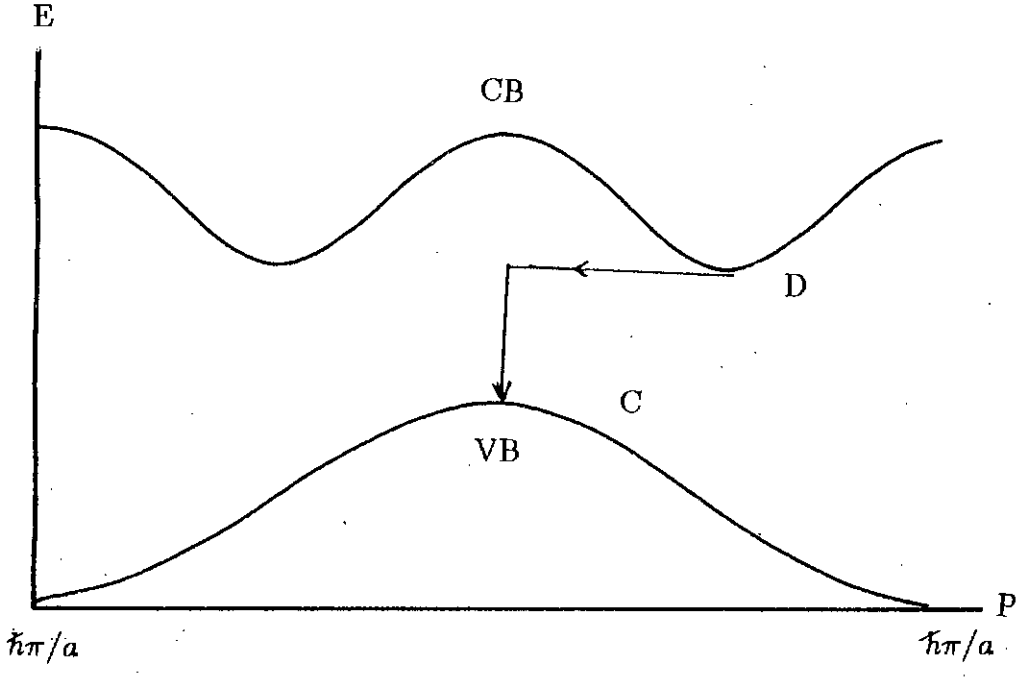

Figure 1.6: Simplified energy diagram of an indirect-gap semiconductor (silicon).

about a basic semiconductor laser diode structure.

1.3 Basic GaAs laser diode structure

When a photon interact with an electron, the electron can absorb energy to move to a higher excited state or alternatively with an equal probability, the electron can lose energy and in doing so emit a further photon, which leads to photon amplification [41]. Depending on the initial energy state of the interacting electron either absorption or amplification will occur. If it is a low energy state E_1 as shown in figure 1.7, an impinging photon with energy $h\nu \geq E_g$ will be absorbed, elevating the electron to an available higher energy state E_2. By pumping the lower energy electrons with energy to raise them to the excited state it is possible to have an unusually large number of electrons at the higher level. Such a situation is called a population inversion. This condition is illustrated in figure 1.7, the corresponding energy vs. density of state for an intrinsic semiconductor at equilibrium and at inverted condition is shown in figure 1.8. At this stage, an incident photon of the correct wavelength $\lambda_g = hc/E$ can stimulate an electron to fall to the lower energy state, resulting in a stimulated emission as shown in figure 1.9. In such stimulated emission the emitted photon has the same wavelength λ_g, phase, polarization and direction of propagation as the incident one. Devices that rely on this mechanism to generate coherent radiation are called lasers, which is an acronym for light amplification by stimulated emission of radiation [41]. It is to be noted that the highly coherent stimulated emission is the only responsible for laser.

The pumping mechanism for population inversion for semiconductor laser can easily be achieved by forward biasing the p-n junction as shown in figure 1.10. The energy band diagram without bias is shown in figure 1.11. When a forward bias voltage V_{FB} is applied, such that $eV_{FB} \geq E_g$, all levels at the n^+ side are raised in energy, all those at the p^+ side are lowered, the barrier height is considerably reduced from its equilibrium value V_B, and the concept of Fermi energy is strictly no longer valid but it is constructive to consider quasi Fermi level shown as E_{Fp} and E_{Fn}. Large number of carriers are injected across the junction to create an active region of population inversion in the vicinity of the junction as shown in figure 1.12

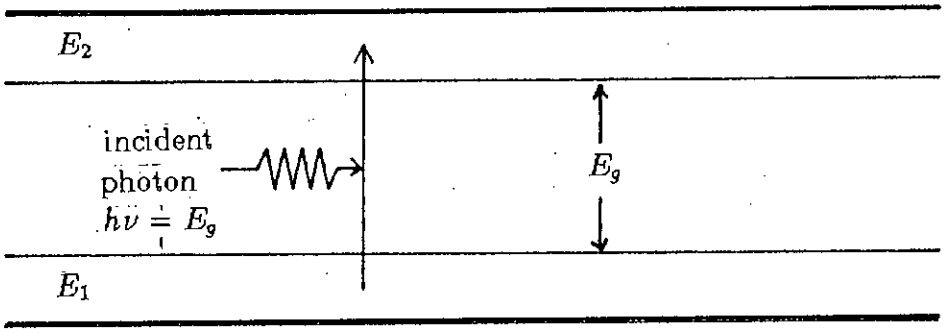

Figure 1.7: Interaction of photon and electron with no population inversion, photon is absorbed.

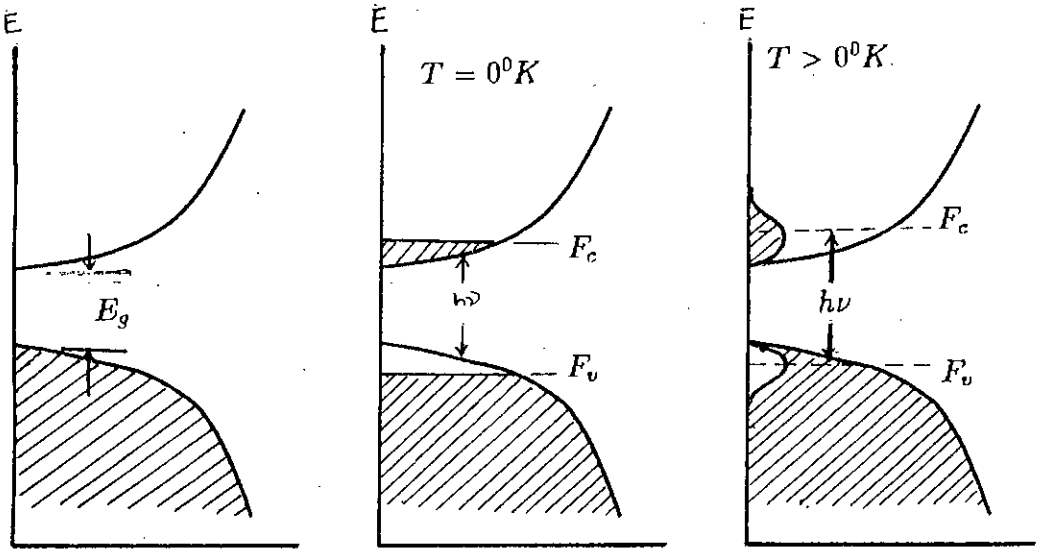

Figure 1.8: Energy vs. density of state for an intrinsic semiconductor.

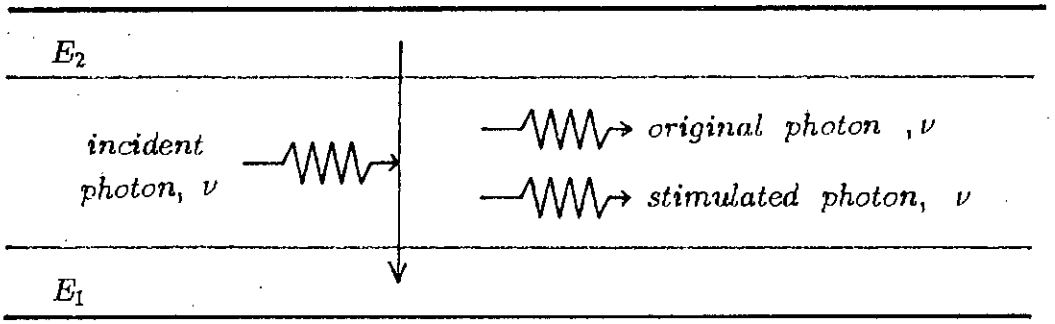

Figure 1.9: Interaction of photon and electron with population inversion, the original photon and a second stimulated photon is emerge.

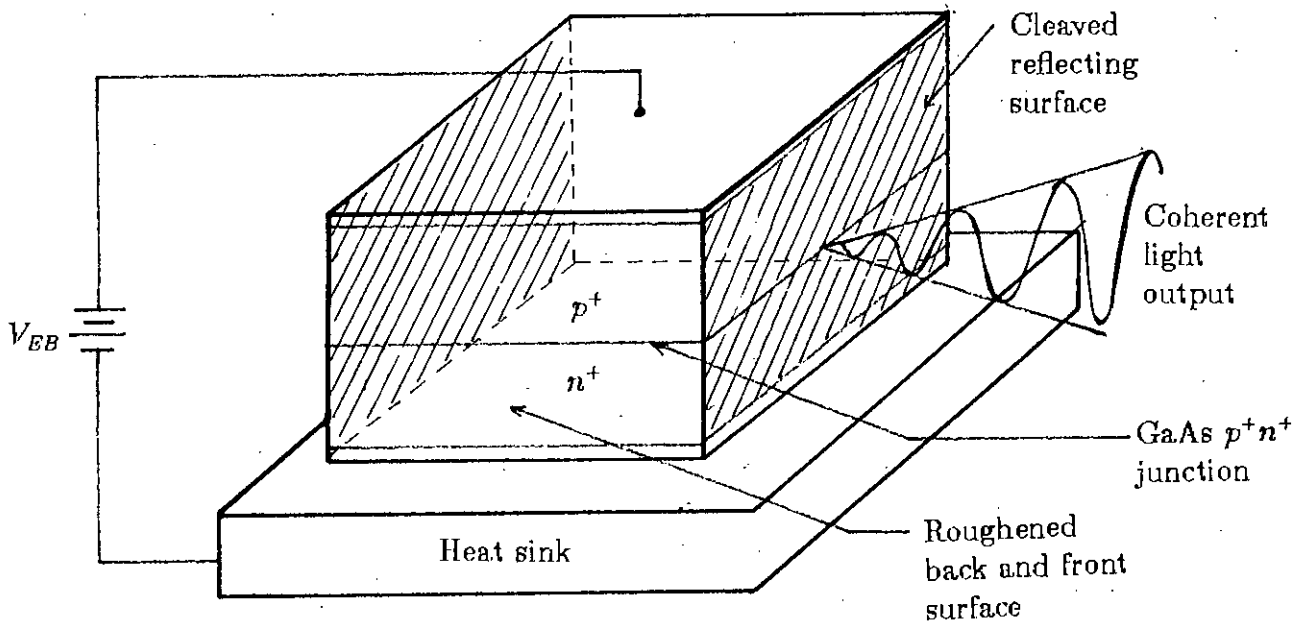

Figure1.10: Diagramatic representation of basic GaAs laser diode structure.

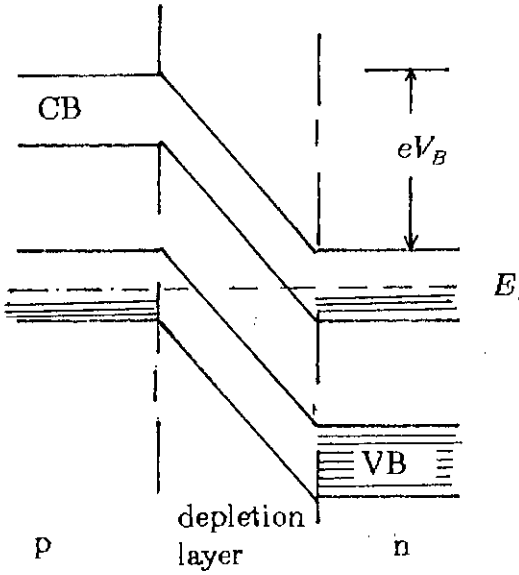

Figure 1.11: In equilibrium.

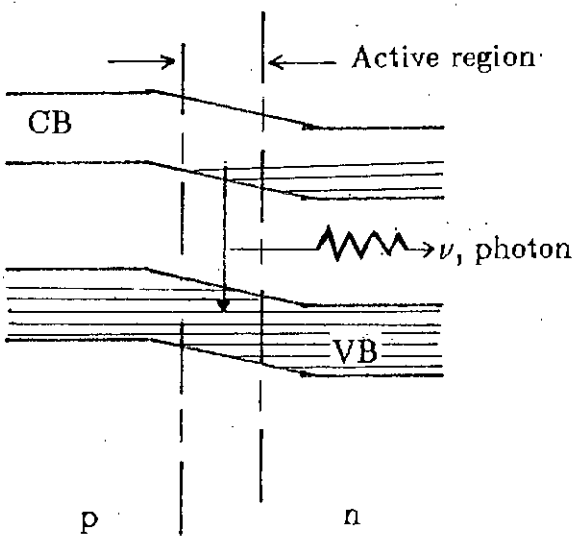

Figure 1.12: With forward bias eV>E
Energy band diagrams for a laser diode.

in which radiation transitions of electrons from the conduction band can occur. For this active region to exist, with consequential stimulated emission, the forward bias voltage must be $eV_{FB} > E_g$.

A schematic diagram of the structure of a laser diode is shown in figure 1.10. The GaAs crystal is very precisely cleaved on its end faces as shown to create smooth, parallel, semitransparent, reflecting surfaces, which are essential for lasing action. When small forward bias voltage, V_{FB} is applied, no population inversion occurs and there is only weak incoherent light output due to spontaneous emission as shown in figure 1.13. As soon as eV_{FB} becomes $> E_g$ and a critical current flows, an inverted population of carriers is produced, which is first responsible for spontaneous emission of photon. These photons reach the cleaved surfaces, internally reflected due to the high reflective index of the medium (around 3.6) and back into the active region. The photons then make a pass through the active region, stimulating additional coherent photon emissions as they traverse it. On reaching the far cleaved surface photons are again reflected and pass the active region and release more photons, all coherent with each other.

1.4 Distributed feedback (DFB) semiconductor lasers

A theoretical analysis of distributed feedback (DFB) laser was proposed by Kogelnik and Shank [17][18]. They proposed that the conventional resonator consisting of two (or more) end mirrors terminating the laser medium, can be made mirrorless by providing the feedback mechanism distributed throughout and integrated with the gain (lasing) medium. In particular, the feedback mechanism is provided by Bragg scattering from a periodic spatial variation of the gain medium or of the gain itself [17].

A DFB laser can be made in double-heterostructure (DH). At the beginning, optical feedback in such a DFB laser used to be provided by a corrugated surface between the active layer and the outer p-GaAlAs layer. The fabrication of the grating in such an active layer caused the interface recombination centers which increases the threshold current density substantially at higher temperatures. For this reason it was impossible to operate such lasers at around 300°K at low current

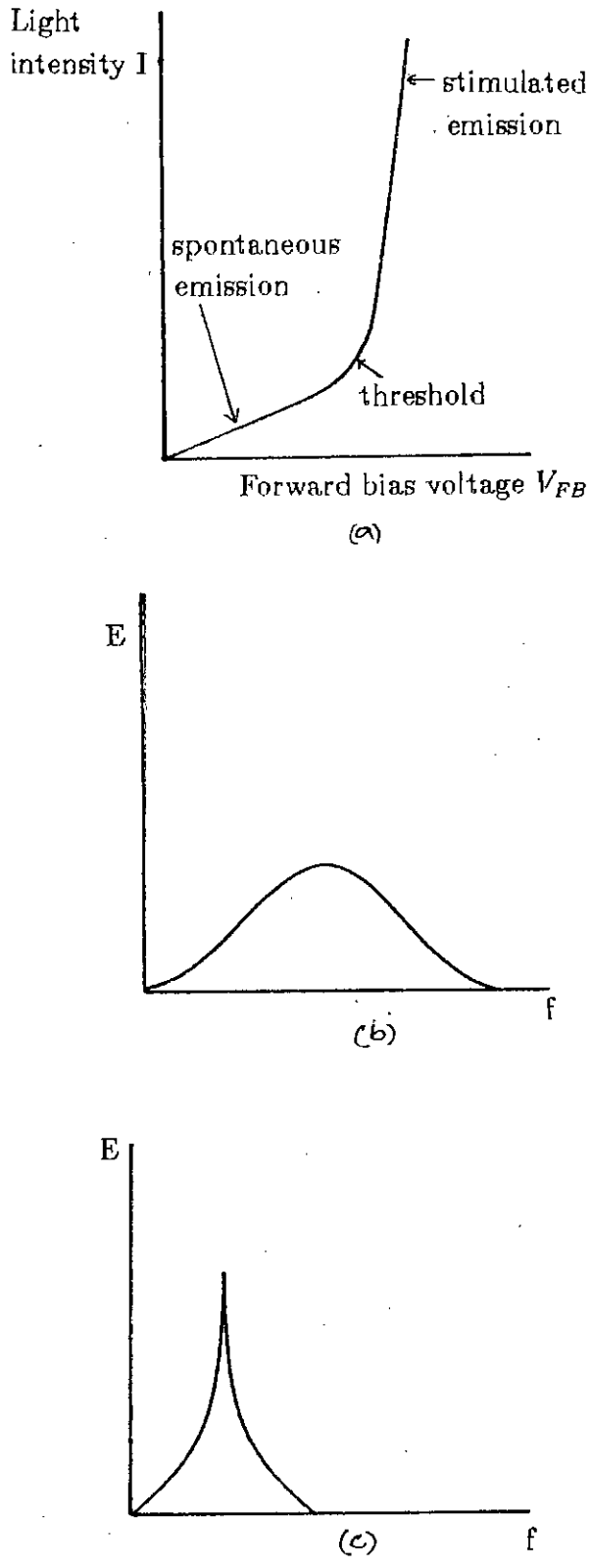

Figure 1.13: Schematic diagram representing (a) Output from forward-biased laser diode, (b) The radiation spectra for the spontaneous emission below the lasing threshold, (c) The radiation spectra for stimulated emission above threshold.

densities. This problem has been overcome by separate optical and carrier confinement heterostructure (SCH) jointly proposed by Aiki, Nakamura, Umeda from Central Research Laboratories, Hitachi Ltd. Japan and Yariv, Katzir and Yen at California Institute Of Technology, Pasadena, Calif. USA [19]. Here, the carriers are confined to the p-GaAlAs active layer while it extend to the $p - Ga_{1-y}Al_yAs$ ($y \sim 0.17$) layer and the $p - Ga_{1-z}Al_zAs$ ($z \sim 0.07$) layer grown successively on the active layer. The grating is made on the $p - Ga_{1-z}Al_zAs$ layer to obtain the optical feedback. Since the active layer is separated from the corrugated interface, the threshold current density has been found to be low enough to operate the diode at higher temperature. Numerous other realizations of DFB lasers have been reported in literatures [20]-[23]. DFB structures have the advantage of providing better frequency stability of mode of oscillation than cavities formed by partially transmitting mirrors at the ends of the structures.

Periodic structures with DFB have other applications. Bandpass transmission and reflection filters may be constructed using passive structures that utilize Bragg reflection [24] [25]. The reflection filter formed by such a structure is the equivalent of a mirror reflecting a band of frequencies . In surface acoustic applications [26] [27], such mirrors are utilized to build high-Q cavities.

1.5 Objective of this research

The technique of distributed feedback semiconductor lasers is now known [17][18][19][32][33][35]. Some theoretical analysis of index and gain coupling have been presented by Kogelnik and Shank [17] in 1972, Islam et. al. [32] in 1991 and Suhara et. al. [33] in 1992. Detailed analysis of pure gain coupled and 'gain plus index' coupled [32] semiconductor lasers are yet to be done. Recently, some techniques of fabrication of gain coupled lasers have been reported in [39]. After this, it seems to be worthwhile in working on developing analytical expressions for the design of gain and 'gain plus index' coupled DFB semiconductor lasers.

In this work, three types distributed feedback corrugation in semiconductor lasers will be studied. These corrugations are: (i) pure index coupling type, (ii) pure gain coupling type, (iii) 'gain plus index' coupling type. The equations repre-

senting the oscillation condition will be derived following recent researches [32]-[34]. For each case numerical computations will be performed using microcomputers to obtain threshold gain, the frequency at which threshold gain occurs for various combinations of DFB semiconductor laser parameters. The above computation work will then be done for different amount of external reflections. The proposed research work thus will be an investigation of some new structures of semiconductor lasers to deal with applications having external reflections.

1.6 A brief introduction to the chapters of this thesis

The main objective of this work is to study the bahaviours of a semiconductor injection laser having distributed periodic corrugations. To explain the necessity of periodic corrugation in a semiconductor laser, it is necessary to briefly introduce the working principle of the conventional Fabry-Perot semiconductor laser. Such an introduction is provided in chapter 2.

In chapter 3, equations for pure index corrugated DFB semiconductor laser without any reflection from outside are presented. The derivation starts off with the Maxwell's equations for Electric and Magnetic fields. The equation representing the oscillation condition for such a laser is presented in this chapter.

Chapter 4 deals with pure index corrugated DFB semiconductor laser with external feedback. In this analysis it is assumed that a portion of the laser output entering into an Fibre optic cable or going towards an optical disk is reflected back and enters into the DFB laser. Under this condition the equations derived in chapter 3 are modified in this chapter.

In chapter 5, it is assumed that both index and gain corrugations are present in a DFB semiconductor laser. For such a complex coupling, necessary equations are derived following the procedures of chapter 3. Also, following the procedures of chapter 4, the effect of external feedback is taken into account and the equations are derived for such a case. The equations representing the oscillation condition, derived for a 'gain plus index' corrugated DFB semiconductor laser with external feedback, are general forms of equations.

A computer method is presented, in chapter 6, for obtaining the solutions of the

general complex equations representing the oscillation condition of a DFB semiconductor laser. Numerical solutions and graphical plots for various values of the parameters are presented in this chapter. Comments on the obtained results are also presented in this chapter.

Discussions on the total work are presented in chapter 7. Some suggestions for future work are also presented in this chapter.

CHAPTER 2

Fabry-Perot laser

2.1 Introduction

This work deals with distributed feedback type of semiconductor laser. In order to explain the operation of such a laser it is necessary to explain the operation of a basic Fabry-Perot laser first, since the theory of laser oscillation can be explained with the help of a Fabry-Perot laser. For this reason a simple treatment of Fabry-Perot laser is necessary at this stage. In this chapter, the physical construction of a simple Fabry-Perot laser and its mechanism of operation will be briefly discussed. The structure of a simple Fabry-Perot laser is briefly explained in section 2.2. Also, using a model of reflection and transmission of waves at the two cavity mirrors of a Fabry-Perot laser the equations representing the amplitude and phase conditions of oscillation in such a laser are deduced in section 2.2. The equation for obtaining the frequency of oscillation of a Fabry-Perot laser is presented in section 2.3.

2.2 Fabry-Perot Laser

From the very beginning of laser invention, it is known that for laser generation it is necessary to have population inversion in a laser medium i.e. the higher energy state of the material will contain more atoms than the lower energy state. If such a medium is placed inside an optical resonator containing two reflectors, then an electromagnetic wave bounces back and forth between the two reflectors and passes through the laser medium and gets amplified [14]. If the amplification exceeds the losses caused by the imperfect reflection in the mirrors and scattering in the laser medium, the field energy stored in the resonator increases with time. This causes the amplification constant to decreases as a result of gain saturation [14]. The

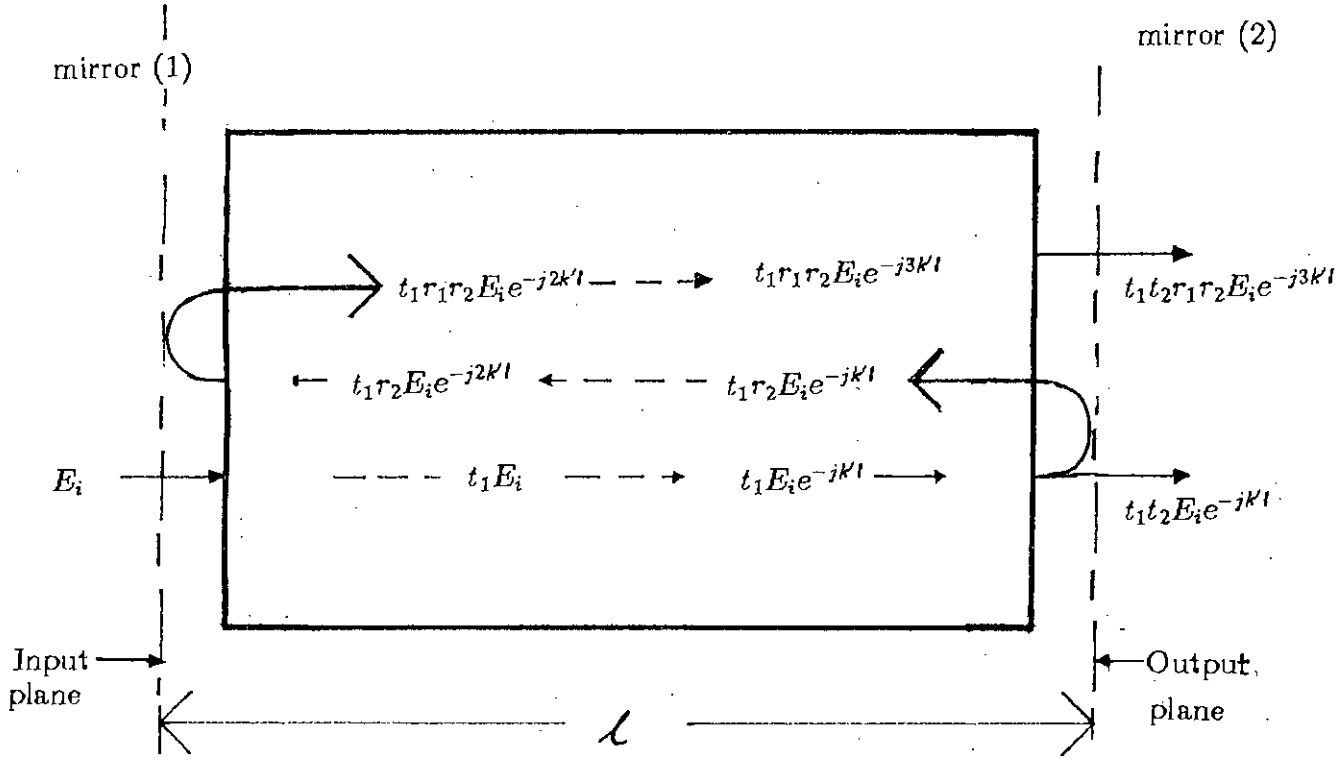

Figure 2.1: Schematic diagram of a Fabry-Perot laser.

oscillation level keeps on increasing until the saturated gain per pass just equals the losses. At this point the net gain per pass is unity and no further increase in the radiation intensity is possible; that is the steady-state oscillation is obtained. This type of laser is known as Fabry-Perot laser. A schematic representation of such a Fabry-Perot laser is shown in figure 2.1. In such a case an amplification medium with an inverted atomic population is placed between two mirrors as shown in figure 2.1.

Let us consider the model of figure 2.1 which is a Fabry-Perot laser containing two mirrors and the laser medium with an inverted atomic population in between. For such a case the complex propagation constant of the medium may be written [14] as

$$k'(\omega) = k + k\frac{\chi'(\omega)}{2n^2} - \jmath k\frac{\chi''(\omega)}{2n^2} - \jmath\alpha/2 \tag{2.1}$$

In this case, α accounts for the distributed passive losses of the medium. Thus, the intensity loss-factor per pass is $exp(-\jmath\alpha)$. In equation (2.1), $(k - \jmath\alpha/2)$ is the propagation constant of the medium at frequencies well removed from that of the laser transition, and $\chi(\omega) = \chi'(\omega) - \jmath\chi''(\omega)$ is the complex dielectric susceptibility due to the laser transition. The imaginary part of $\chi(\omega)$ is given [14] by

$$\chi'' = \frac{(N_1 - N_2)\lambda^3}{8\pi^3 t_{spont} + \Delta\nu_n} \quad \frac{1}{1 + [4(\nu - \nu_o)^2/(\Delta\nu)^2]} \tag{2.2}$$

where, $\nu = \omega/2\pi$ is the frequency of laser output light. The relation between $\chi'(\nu)$ and $\chi''(\nu)$ can be written [14] as

$$\chi'(\nu) = \frac{2(\nu_o - \nu)}{\Delta\nu}\chi''(\nu) \tag{2.3}$$

In the example of figure 2.1, a plane wave of amplitude E_i is incident on the left mirror of a Fabry-Perot etalon containing a laser medium. The ratio of transmitted to incident field at the left mirror is taken as t_1 (mirror transmission coefficient) and that at the right mirror is t_2. The ratios of reflected to incident field inside the laser medium at the left and right boundaries are r_1 and r_2 (facet reflection coefficient) respectively.

Here, the propagation factor corresponding to a single transition is $exp(-\jmath k' l)$ where, k' is given by equation (2.1) and l is the length of the etalon. Therefore, adding the partial waves at the output one can write [14] the total outgoing wave E_t as

$$\begin{aligned} E_t &= t_1 t_2 E_i e^{-\jmath k' l}[1 + r_1 r_2 e^{-\jmath k' l} + r_1^2 r_2^2 e^{-4\jmath k' l} + ...] \\ &= E_i[\frac{t_1 t_2 e^{-\jmath k' l}}{1 - r_1 r_2 e^{-\jmath 2k' l}}] \\ &= E_i[\frac{t_1 t_2 e^{-\jmath (k+\Delta k) l} e^{(\gamma-\alpha)l/2}}{1 - r_1 r_2 e^{-\jmath 2(k+\Delta k) l} e^{(\gamma-\alpha)l}}] \end{aligned} \tag{2.4}$$

In equation (2.4), the following relations have been used

$$k' = (k + \Delta k) + \jmath(\gamma - \alpha)/2, \tag{2.5}$$

$$\Delta k = \frac{k\chi'(\omega)}{2n^2} \tag{2.6}$$

$$\gamma = -k\frac{\chi''(\omega)}{n^2} \tag{2.7}$$

$$= (N_2 - N_1)\frac{\lambda^2}{8\pi n^2 t_{spont}} g(\nu) \tag{2.8}$$

If the atomic transition is inverted (*i.e.* $N_2 > N_1$), then $\gamma > 0$ and the denominator of equation (2.4) can become very small. The transmitted wave E_t can thus become larger than the incident wave E_i. The Fabry-Perot etalon (with laser medium) in this case acts as an amplifier with a power gain $|\frac{E_t}{E_i}|^2$.

If the denominator of equation (2.4) becomes zero, which happens when

$$r_1 r_2 e^{-\jmath 2[k+\Delta k(\omega)]l} e^{[\gamma(\omega)-\alpha]l} = 1 \tag{2.9}$$

then the ratio E_t/E_i becomes infinite. This corresponds to a finite transmitted wave E_t with a zero incident wave ($E_i = 0$)-that is to oscillation condition. Physically condition (2.9) represents the case in which a wave making a complete round trip inside the resonator returns to the starting plane with the same amplitude and with the same phase. It is possible to split the oscillation condition (2.9) into an equation for amplitude condition and an equation for the phase condition
Thus, for the threshold gain constant $\gamma_t(\omega)$ we get

$$r_1 r_2 e^{[\gamma_t(\omega)-\alpha]l} = 1 \tag{2.10}$$

Similarly, after separation, we get the following equation for the phase condition.

$$2[k + \Delta k(\omega)]l = 2\pi m \qquad m = 1, 2, 3..... \tag{2.11}$$

The amplitude condition (2.10) can be written as

$$\gamma_t(\omega) = \alpha - \frac{1}{l} \ln r_1 r_2 \tag{2.12}$$

Using equation (2.8) to replace $\gamma_t(\omega)$in the above equation we get

$$N_t \equiv (N_2 - N_1)_t = \frac{8\pi n^2 t_{spont}}{g(\nu)\lambda^2}(\alpha - \frac{1}{l} \ln r_1 r_2) \tag{2.13}$$

This is the population inversion density at threshold.

2.3 The frequency of oscillation

The phase condition (2.11) is satisfied at an infinite set of frequencies for different values of m. If in addition, the gain condition is satisfied at one or more of these frequencies, the laser actually will oscillate at this frequency.

In order, to solve for the oscillation frequency, we put the value of Δk from equation (2.6) in phase condition equation (2.11) and obtain the equation

$$kl[1 + \frac{\chi'(\nu)}{2n^2}] = m\pi \tag{2.14}$$

We now introduce

$$\nu_m = \frac{mc}{2ln} \tag{2.15}$$

so that it corresponds to the mth resonance frequency of the passive $[N_2 - N_1 = 0]$ resonator. It has been shown in [14] that the propagation constant $\gamma(\omega)$ can be written as

$$\gamma(\omega) = \frac{-k\chi''(\omega)}{n^2} \tag{2.16}$$

For this case we can write $\gamma(\nu)$ as

$$\gamma(\nu) = \frac{-k\chi''(\nu)}{n^2} \tag{2.17}$$

So, putting the value of $\chi''(\nu)$ from (2.17) in equation (2.3) and then using the value of $\chi'(\nu)$ of the resulting equation in equation (2.14) we get

$$\nu[1 - \frac{(\nu_o - \nu)}{\Delta\nu} \quad \frac{\gamma(\nu)}{k}] = \nu_m \tag{2.18}$$

In the above equation ν_o is the centre frequency of the atomic lineshape function. By adjusting the laser length such that one of its resonance frequencies ν_m is very near to ν_o which will result in a slowly varying gain constant $g(\nu)$ with respect to ν. Replacing $\gamma(\nu)$ in (2.14) by $\gamma(\nu_m)$ and $(\nu_o - \nu)$ by $(\nu_o - \nu_m)$ we get [14]

$$\nu = \nu_m - (\nu_m - \nu_o)\frac{\gamma(\nu_m)c}{2\pi n\Delta\nu} \tag{2.19}$$

2.4 Summary

A brief introduction to a simple Fabry-Perot laser has been presented. The equations for amplitude and phase conditions for obtaining oscillations in a Fabry-Perot laser have been presented. The equations for the frequency of oscillation for such a laser is also presented. The discussions of this chapter will help in explaining the operation of DFB lasers in the next 3 chapters.

CHAPTER 3

DFB semiconductor laser having pure index corrugation and without any reflection from outside

3.1 Introduction

The principles of a simple Fabry-Perot laser has been presented in the previous chapter. In this chapter, the equations for a DFB semiconductor laser is developed. Starting with the Maxwell's equations and considering the laser cavity as a resonant waveguide cavity the equation for a simple semiconductor laser is developed in section 3.2.

It is now well-known that three types of corrugations are possible in a DFB semiconductor laser. These are: (i) pure refractive index corrugation, (ii) pure gain corrugation and (iii) a combination of refractive index and gain corrugation. In the first case, the refractive index of the active layer of a semiconductor laser is periodically corrugated. In the second case, the gain of the medium of the active layer is varied periodically, and in the third case, both refractive index and gain are varied in the active layer.

In this work, at first, only index corrugation is considered and the equations for such a case are derived. This chapter deals with index corruagation only which is termed as pure index corrugation or pure index coupling. In section 3.3, the equations of a simple semiconductor laser of section 3.2 are then extended for a semiconductor laser with refractive index corrugation only. In section 3.4, the boundary conditions for a DFB laser are applied to the solutions obtained in section 3.3. Thus, the equations for forward and backward waves for a DFB semiconductor laser with refractive index corrugation and no optical feedback from outside are derived in

section 3.4. Using the equations of the two waves of section 3.4 the oscillation condition for a DFB semiconductor laser with refractive index corrugation is deduced in section 3.5.

3.2 Wave equation for a semiconductor laser

It is well-known that a semiconductor laser consists of a layered semiconductor structure placed inside an optical resonator. In such a resonator two opposite field waves propagate back and forth inside the cavity. In a distributed feedback (DFB) laser, reflection occurs from the backscattering of the periodic perturbation as shown in figure 3.1. As a result, such a laser does not need end reflectors. The propagation of electromagnetic waves in semiconductor material is given [32][14][31] by the Maxwell's equations.

$$\nabla \times \overline{E} = -\frac{\partial \overline{B}}{\partial t} \tag{3.1}$$

$$\nabla \times \overline{H} = \sigma \overline{E} + \frac{\partial \overline{D}}{\partial t} \tag{3.2}$$

$$\nabla . \overline{B} = 0 \tag{3.3}$$

$$\nabla . \overline{D} = 0 \tag{3.4}$$

Here, σ is the conductivity of the medium.

In the above equation $\overline{D}$ is the electric flux density which is related to the electric field intensity $\overline{E}$ by [32][14][31]

$$\overline{D} = \varepsilon_o n^2 \overline{E} + \overline{P} \tag{3.5}$$

In equation (3.5), ε_o is the free space permittivity, n is the refractive index. Here P(r,t) is electric polarization, which can be written [32][14][31] as

$$\overline{P} = \varepsilon_o \chi \overline{E} \tag{3.6}$$

Here, χ is the dielectric susceptibility of the medium. From equation (3.1) and (3.2)

$$\nabla \times \nabla \times \overline{E} = -\frac{\partial}{\partial t}(\nabla \times \overline{B}) = -\mu_o \frac{\partial}{\partial t}(\nabla \times \overline{H}) \tag{3.7}$$

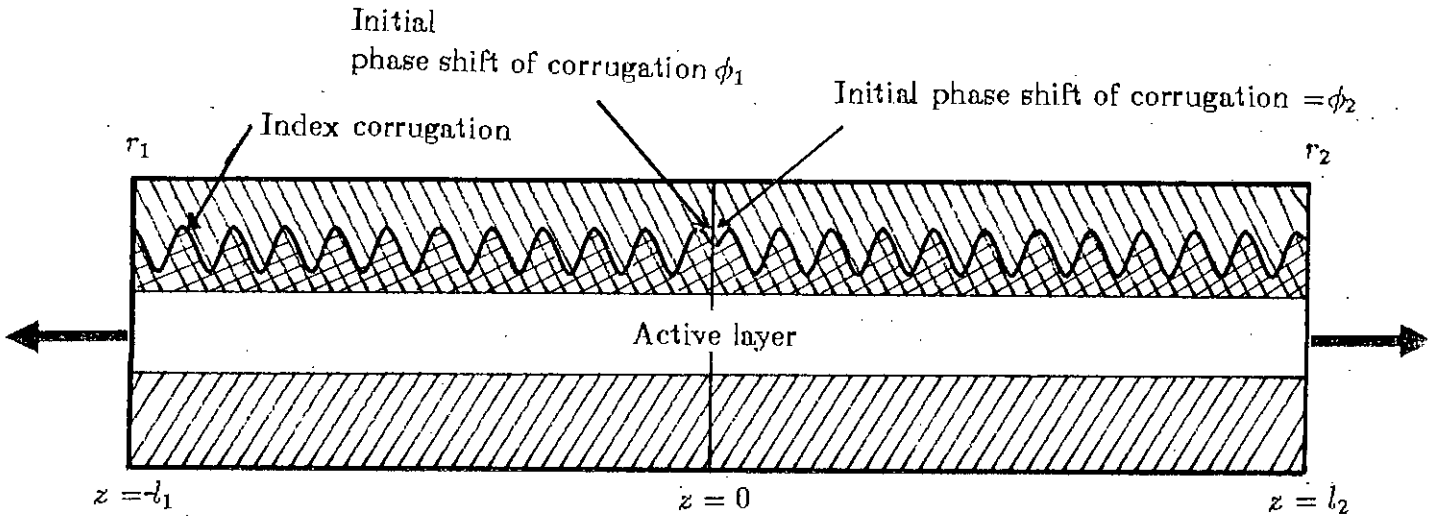

Figure 3.1: Scematic diagram of an index corrugated DFB semiconductor laser.

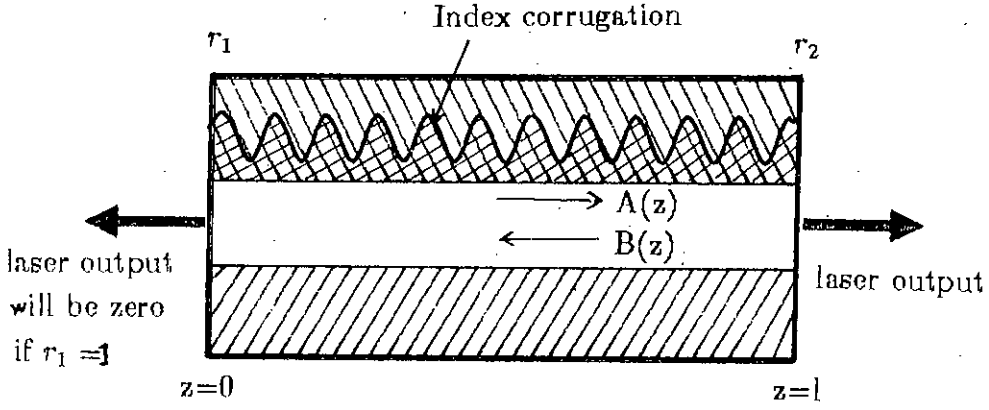

Figure 3.2: Schematic diagram of a simplified index corrugated DFB laser considering a length of l (from $z = 0$ to $z = l$).

In this case, $\nabla \times \nabla \times \overline{E} = \nabla(\nabla.\overline{E}) - \nabla^2\overline{E} = -\nabla^2\overline{E}$ (since $\nabla.\overline{D} = 0$ and thus$\overline{E} = 0$). Therefere, from equations (3.1)-(3.7)

$$-\nabla^2\overline{E} = -\mu_o\frac{\partial}{\partial t}(\sigma\overline{E} + \varepsilon_o n^2\frac{\partial\overline{E}}{\partial t} + \varepsilon_o\chi\frac{\partial\overline{E}}{\partial t}) \tag{3.8}$$

or,

$$-\nabla^2\overline{E} = -\mu_o\sigma\frac{\partial\overline{E}}{\partial t} - \mu_o\varepsilon_o n^2\frac{\partial^2\overline{E}}{\partial^2 t} - \jmath\omega\mu_o\varepsilon_o\chi\frac{\partial\overline{E}}{\partial t} \tag{3.9}$$

Now, by defining σ' as [32]

$$\sigma' = \sigma + \jmath\omega\varepsilon_o\chi \tag{3.10}$$

equation (3.9) can be written as [32]

$$\nabla^2\overline{E} - \mu_o\sigma'\frac{\partial\overline{E}}{\partial t} - \mu_o\varepsilon_o n^2\frac{\partial^2\overline{E}}{\partial^2 t} = 0 \tag{3.11}$$

This is the generalized wave equation of a semiconductor laser without any corrugation. The solution of equation (3.11) may be written in the form

$$\overline{E} = A(z)F(x,y)e^{\jmath\omega t - \jmath\beta z} + B(z)F(x,y)e^{\jmath\omega t + \jmath\beta z} + c.c. \tag{3.12}$$

Now, considering a semiconductor laser without any corrugation and also $\sigma' = 0$ equation (3.11) reduces to

$$\nabla^2\overline{E} - \mu_o\varepsilon_o n^2\frac{\partial^2\overline{E}}{\partial^2 t} = 0 \tag{3.13}$$

or,

$$(\nabla^2 + \mu_o\varepsilon_o n^2\omega^2)F(x,y)e^{\jmath\beta z} = 0 \tag{3.14}$$

or,

$$[\frac{\partial^2}{\partial x^2} + \frac{\partial^2}{\partial y^2} + \mu_o\varepsilon_o n^2\omega^2 - \beta^2]F(x,y)e^{\jmath\beta z} = 0 \tag{3.15}$$

In the above equation $F(x,y)$ is as defined in equation (3.12).

3.3 Wave equations for a semiconductor laser having refractive index corrugation only

In the previous section the effect of index corrugation has not been taken into consideration. Let us now consider that a refractive index corrugation of the form [32][33][34]

$$n = \overline{n} + (\frac{\Delta n}{2} e^{2j\beta_D z + j\phi} + c.c.) \tag{3.16}$$

is present in the semiconductor laser with periodic variation in the z direction. Here, we assume that ϕ is the initial phase of corrugation and $\Delta n \ll \overline{n}$. In this equation of corrugation, β_B is the propagation constant satisfying Bragg condition ($\beta_B = \pi/\Lambda$). The c.c. (complex conjugate) term is present because the physical terms are real. Figure 3.1 and figure 3.2 are two schematic representation of DFB lasers having such a corrugation. However, for this section we refer to figure 3.2

From equation (3.16) the square of n can be written as

$$n^2 = [\overline{n} + (\frac{\Delta n}{2} e^{2j\beta_D z + j\phi} + c.c.)]^2 \tag{3.17}$$

or,

$$\begin{aligned} n^2 &= \overline{n}^2 + \frac{(\Delta n)^2}{4} e^{4j\beta_D z + j2\phi} + \frac{(\Delta n)^2}{4} e^{-4j\beta_D z - j2\phi} \\ &\quad + \overline{n}\Delta n e^{2j\beta_D z + j\phi} + \overline{n}\Delta n e^{-2j\beta_D z - j\phi} + c.c. \end{aligned} \tag{3.18}$$

Here, the terms containing higher power of Δn may be neglected since $\Delta n \ll \overline{n}$. With this approximation equation (3.18) reduces to

$$n^2 \equiv \overline{n}^2 + \overline{n}\Delta n e^{2j\beta_D z + j\phi} + c.c. \tag{3.19}$$

It may be noted that after considering the index corrugation, βz is to be replaced by $\beta_D z$ and equation (3.12) may be written as

$$\overline{E} = A(z)F(x,y)e^{j\omega t - j\beta_D z} + B(z)F(x,y)e^{j\omega t + j\beta_D z} + c.c. \tag{3.20}$$

Using equation (3.19) and (3.20) we replace $\overline{n}$ and $\overline{E}$ in equation (3.11) and obtain the following equation.

$$\nabla^2[A(z)F(x,y)e^{\gamma\omega t-\jmath\beta_D z}+B(z)F(x,y)e^{\gamma\omega t+\jmath\beta_D z}+c.c.]$$
$$-\mu_o\sigma'\frac{\partial}{\partial t}[A(z)F(x,y)e^{\gamma\omega t-\jmath\beta_D z}+B(z)F(x,y)e^{\gamma\omega t+\jmath\beta_D z}+c.c.]$$
$$-\mu_o\varepsilon_o[\overline{n}^2+(\overline{n}\Delta ne^{2\jmath\beta_D z+j\phi}+c.c.)]\frac{\partial^2}{\partial t^2}[A(z)F(x,y)e^{\gamma\omega t-\jmath\beta_D z}$$
$$+B(z)F(x,y)e^{\gamma\omega t+\jmath\beta_D z}+c.c.]=0 \qquad (3.21)$$

Splitting into x, y and z direction variations we get

$$(\frac{\partial^2}{\partial x^2}+\frac{\partial^2}{\partial y^2})A(z)F(x,y)e^{\gamma\omega t-\jmath\beta_D z}$$
$$+\frac{\partial^2}{\partial z^2}[A(z)F(x,y)e^{\gamma\omega t-\jmath\beta_D z}]$$
$$+(\frac{\partial^2}{\partial x^2}+\frac{\partial^2}{\partial y^2})B(z)F(x,y)e^{\gamma\omega t+\jmath\beta_D z}$$
$$+\frac{\partial^2}{\partial z^2}[B(z)F(x,y)e^{\gamma\omega t+\jmath\beta_D z}]$$
$$-\jmath\omega\mu_o\sigma'A(z)F(x,y)e^{\gamma\omega t-\jmath\beta_D z}$$
$$-\jmath\omega\mu_o\sigma'B(z)F(x,y)e^{\gamma\omega t+\jmath\beta_D z}$$
$$+\mu_o\varepsilon_o\omega^2[\overline{n}^2A(z)F(x,y)e^{\gamma\omega t-\jmath\beta_D z}$$
$$+\overline{n}^2B(z)F(x,y)e^{\gamma\omega t+\jmath\beta_D z}$$
$$+\overline{n}\Delta nA(z)F(x,y)e^{\gamma\omega t+\jmath\beta_D z+j\phi}$$
$$+\overline{n}\Delta nB(z)F(x,y)e^{\gamma\omega t+\jmath 3\beta_D z+j\phi}$$
$$+\overline{n}\Delta nA(z)F(x,y)e^{\gamma\omega t-\jmath 3\beta_D z-j\phi}$$
$$+\overline{n}\Delta nB(z)F(x,y)e^{\gamma\omega t-\jmath\beta_D z-j\phi}]+c.c.=0 \qquad (3.22)$$

After further simplification the above equation can be written as

$$(\frac{\partial^2}{\partial x^2}+\frac{\partial^2}{\partial y^2})A(z)F(x,y)e^{\gamma\omega t-\jmath\beta_D z}$$
$$+\frac{\partial^2A(z)}{\partial z^2}F(x,y)e^{\gamma\omega t-\jmath\beta_D z}$$
$$-2\jmath\beta_B\frac{\partial A(z)}{\partial z}F(x,y)e^{\gamma\omega t-\jmath\beta_D z}$$
$$-\beta_B^2A(z)F(x,y)e^{\gamma\omega t-\jmath\beta_D z}$$
$$+(\frac{\partial^2}{\partial x^2}+\frac{\partial^2}{\partial y^2})B(z)F(x,y)e^{\gamma\omega t+\jmath\beta_D z}$$
$$+\frac{\partial^2B(z)}{\partial z^2}F(x,y)e^{\gamma\omega t+\jmath\beta_D z}$$

$$
\begin{aligned}
&+2\jmath\beta_B\frac{\partial B(z)}{\partial z}F(x,y)e^{\jmath\omega t+\jmath\beta_o z}\\
&-\beta_B^2 B(z)F(x,y)e^{\jmath\omega t+\jmath\beta_o z}\\
&-\jmath\omega\mu_o\sigma' A(z)F(x,y)e^{\jmath\omega t-\jmath\beta_o z}\\
&-\jmath\omega\mu_o\sigma' B(z)F(x,y)e^{\jmath\omega t+\jmath\beta_o z}\\
&+\mu_o\varepsilon_o\omega^2[\overline{n}^2 A(z)F(x,y)e^{\jmath\omega t-\jmath\beta_o z}\\
&+\overline{n}^2 B(z)F(x,y)e^{\jmath\omega t+\jmath\beta_o z}\\
&+\overline{n}\Delta n A(z)F(x,y)e^{\jmath\omega t+\jmath\beta_o z+j\phi}\\
&+\overline{n}\Delta n B(z)F(x,y)e^{\jmath\omega t+\jmath 3\beta_o z+j\phi}\\
&+\overline{n}\Delta n A(z)F(x,y)e^{\jmath\omega t-\jmath 3\beta_o z-j\phi}\\
&+\overline{n}\Delta n B(z)F(x,y)e^{\jmath\omega t-\jmath\beta_o z-j\phi}]+c.c.=0
\end{aligned}
\tag{3.23}
$$

In a semiconductor laser the lowest order mode can be obtained by the variations of x and y direction. Actually this can be obtained by controlling the thickness.

The variation of field amplitudes is usually very small in the z direction. As a result, in the above equation, the second order derivatives in the z direction may be neglected. Now to obtain spatial average, we multiply both sides by $F^*(x,y)e^{\jmath\beta_o z}e^{-\jmath\omega t}$ and perform integration for x, y and z within the limits -∞ to ∞, $-\infty$ to ∞, and $-2\pi/\beta_B$ to $+2\pi/\beta_B$ respectively. In addition the time average of both sides are also taken over a period of $\Delta T = 1/\omega$. Now, we choose $\int_{-\infty}^{\infty}\int_{-\infty}^{\infty}|F(x,y)|^2dxdy = 1$. After these operations the c.c. terms vanish because of the time averaging of the $e^{-2\jmath\omega t}$ terms.

Thus we get,

$$
\begin{aligned}
[\frac{\partial^2}{\partial x^2}+\frac{\partial^2}{\partial y^2}-\beta_B^2 \quad & -\jmath\omega\mu_o\int_{-\infty}^{\infty}\int_{-\infty}^{\infty}\sigma'|F(x,y)|^2dxdy+\mu_o\varepsilon_o\omega^2\overline{n}^2]A(z)\\
& -2\jmath\beta_B\frac{\partial A(z)}{\partial z}+\mu_o\varepsilon_o\omega^2\overline{n}\Delta n e^{-j\phi}B(z)=0
\end{aligned}
\tag{3.24}
$$

Substituting equation (3.15) into the above equation, we get

$$
\begin{aligned}
\frac{\partial A(z)}{\partial z} = \quad & \frac{1}{2\jmath\beta_B}[\beta^2-\beta_B^2-\jmath\omega\mu_o\int_{-\infty}^{\infty}\int_{-\infty}^{\infty}\sigma'|F(x,y)|^2dxdy+\mu_o\varepsilon_o\omega^2\overline{n}^2]A(z)\\
& +\frac{\mu_o\varepsilon_o\omega^2\overline{n}\Delta n e^{-j\phi}}{2\jmath\beta_B}B(z)=0
\end{aligned}
\tag{3.25}
$$

or,

$$\frac{\partial A(z)}{\partial z} = \frac{\beta^2-\beta_B^2}{2\jmath\beta_B}A(z) - \frac{\omega\mu_o}{2\beta_B}\int_{-\infty}^{\infty}\int_{-\infty}^{\infty}\sigma'|F(x,y)|^2dxdy + \mu_o\varepsilon_o\omega^2\overline{n}^2A(z) + \frac{\mu_o\varepsilon_o\omega^2\overline{n}\Delta ne^{-j\phi}}{2\jmath\beta_B}B(z) = 0 \tag{3.26}$$

The factor in the first term of the r.h.s of equation (3.26) may be approximated as follows

$$\frac{\beta^2-\beta_B^2}{2\jmath\beta_B} = \frac{(\beta+\beta_B)(\beta-\beta_B)}{2\jmath\beta_B} \cong -\jmath(\beta-\beta_B) \equiv -\jmath\Delta\beta \tag{3.27}$$

where [40],

$$\Delta\beta = (\beta-\beta_B) = \frac{2\pi\overline{n}}{\lambda} - \frac{\pi}{\Lambda} \tag{3.28}$$

Taking the factor in the second term of equation (3.26)

$$\begin{aligned}
&-\frac{\omega\mu_o}{2\beta_B}\int_{-\infty}^{\infty}\int_{-\infty}^{\infty}\sigma'|F(x,y)|^2dxdy \\
&= -\frac{\omega\mu_o}{2\omega\sqrt{\varepsilon\mu_o}}\int_{-\infty}^{\infty}\int_{-\infty}^{\infty}\sigma'|F(x,y)|^2dxdy \\
&= -\frac{1}{2\overline{n}}\sqrt{\frac{\mu_o}{\varepsilon_o}}\int_{-\infty}^{\infty}\int_{-\infty}^{\infty}\sigma'|F(x,y)|^2dxdy \\
&= -\frac{1}{2\varepsilon_o\overline{n}^2}\overline{n}\sqrt{\varepsilon_o\mu_o}\int_{-\infty}^{\infty}\int_{-\infty}^{\infty}\sigma'|F(x,y)|^2dxdy \\
&= -\frac{1}{2\varepsilon_o\overline{n}^2}\overline{n}\sqrt{\varepsilon_o\mu_o}\int_{-\infty}^{\infty}\int_{-\infty}^{\infty}\sigma|F(x,y)|^2dxdy \\
&+\frac{1}{2j\varepsilon_o\overline{n}^2}\overline{n}\sqrt{\varepsilon_o\mu_o}\int_{-\infty}^{\infty}\int_{-\infty}^{\infty}\omega\varepsilon_o\chi|F(x,y)|^2dxdy \\
&= \frac{1}{2}(\overline{g}-\alpha)
\end{aligned} \tag{3.29}$$

Here, $\sigma' = \sigma + j\omega\varepsilon_o\chi$, $\overline{g}$ = relative gain and α = loss, $\beta_B = \omega\sqrt{\mu_o\varepsilon} = \overline{n}\omega\sqrt{\mu_o\varepsilon_o}$ and $\overline{n} = \sqrt{\varepsilon_r}$ [32]. Next, taking the factor in the third term of equatin (3.26)

$$\begin{aligned}
\frac{\mu_o\varepsilon_o\omega^2\overline{n}\Delta ne^{-j\phi}}{2\jmath\beta_B} &= \frac{\mu_o\varepsilon_o\omega^2\overline{n}\Delta ne^{-j\phi}}{2\jmath\omega\overline{n}\sqrt{\varepsilon_o\mu_o}} \\
&= \frac{\omega\sqrt{\mu_o\varepsilon_o}\Delta ne^{-j\phi}}{2\jmath} \\
&= -\jmath\frac{k_o\Delta ne^{-j\phi}}{2} \\
&= -\jmath\kappa_n e^{-\jmath\phi}
\end{aligned} \tag{3.30}$$

Here, $n = \overline{n} + (\frac{\Delta n}{2} e^{2\jmath\beta_D z + j\phi} + \text{c.c.})$, $\kappa_n = \frac{k_o|\Delta n|}{2}$, and k_o = the wave number in free space.

From equations (3.26)-(3.30) we get

$$\frac{dA(z)}{dz} = [-\jmath\Delta\beta + \frac{1}{2}(\overline{g} - \alpha)]A(z) - \jmath\kappa_n e^{-\jmath\phi} B(z) \tag{3.31}$$

Here, the term $\Delta\beta$ appears due to the index corrugation. Following the above procedure, in a similar manner, the equation for B(z) is obtained as

$$\frac{dB(z)}{dz} = [\jmath\Delta\beta - \frac{1}{2}(\overline{g} - \alpha)]B(z) + \jmath\kappa_n e^{-\jmath\phi} A(z) \tag{3.32}$$

Since equation (3.31) contains both $A(z)$ and $B(z)$ terms and equation (3.32) also contains $A(z)$ and $B(z)$ terms therefore, the forward and backward waves are coupled.

Next, differentiating both sides of equation (3.31) the following equationis obtained

$$\frac{d^2A(z)}{dz^2} = [-\jmath\Delta\beta + \frac{1}{2}(\overline{g} - \alpha)]\frac{dA(z)}{dz} - \jmath\kappa_n e^{-\jmath\phi}\frac{dB(z)}{dz} \tag{3.33}$$

Substituting the expression of $\frac{dB(z)}{dz}$ from equation (3.32)

$$\begin{aligned}\frac{d^2A(z)}{dz^2} = \quad & [-\jmath\Delta\beta + \frac{1}{2}(\overline{g} - \alpha)]\frac{dA(z)}{dz} - \jmath\kappa_n e^{-\jmath\phi}[\jmath\Delta\beta - \frac{1}{2}(\overline{g} - \alpha)]B(z) \\ & + \jmath\kappa_n^2 A(z)\end{aligned} \tag{3.34}$$

Next, the expression of B(z) obtained from equation (3.31) is replaced in the above equation. The resulting equation is

$$\begin{aligned}\frac{d^2A(z)}{dz^2} = \quad & [-\jmath\Delta\beta + \frac{1}{2}(\overline{g} - \alpha)]\frac{dA(z)}{dz} \\ & + [\jmath\Delta\beta - \frac{1}{2}(\overline{g} - \alpha)][\frac{dA(z)}{dz} - \{-\jmath\Delta\beta + \frac{1}{2}(\overline{g} - \alpha)\}A(z)] \\ & + \kappa_n^2 A(z)\end{aligned} \tag{3.35}$$

Thus,

$$\frac{d^2A(z)}{dz^2} = [\{\jmath\Delta\beta - \frac{1}{2}(\overline{g} - \alpha)\}^2 + \kappa_n^2]A(z) \tag{3.36}$$

By writing the complex propagation constant γ as [32][38]

$$\gamma^2 = [\jmath\Delta\beta - \frac{1}{2}(\overline{g} - \alpha)]^2 + \kappa_n^2 \tag{3.37}$$

equation (3.36) may be written as

$$\frac{d^2A(z)}{dz^2} = \gamma^2 A(z) \tag{3.38}$$

The solution of this equation may be written as

$$A(z) = A_1 e^{\gamma z} + A_2 e^{-\gamma z} \tag{3.39}$$

where, γ is given by equation (3.37). Again equation (3.31) can be written as

$$B(z) = \frac{1}{\jmath\kappa e^{-\jmath\phi}}\{[-\jmath\Delta\beta + \frac{1}{2}(\overline{g} - \alpha)]A(z) - \frac{A(z)}{dz}\} \tag{3.40}$$

Replacing A(z) from equation (3.39) into the above equation we get

$$B(z) = \frac{e^{\jmath\phi}}{\jmath\kappa}\{[-\jmath\Delta\beta + \frac{1}{2}(\overline{g} - \alpha) - \gamma]A_1 e^{\gamma z} + [-\jmath\Delta\beta + \frac{1}{2}(\overline{g} - \alpha) + \gamma]A_2 e^{-\gamma z}\} \tag{3.41}$$

This equation is in the form of

$$B(z) = B_1 e^{\gamma z} + B_2 e^{-\gamma z} \tag{3.42}$$

Equation (3.39) and (3.42) are the two general wave equations for a semiconductor laser having refractive index corrugation only.

3.4 Wave equations for DFB semiconductor lasers having refractive index corrugation only and no reflection from outside

The wave equations of a particular type of laser may be obtained by applying the boundary conditions of that laser to equations (3.39) and (3.42). For this section let us consider the DFB laser of figure 3.2 with refractive index corrugation only. Here, $z = 0$ plane is chosen to coincide with the left facet and $z = l$ plane with the right facet.

Putting z=0 in equation (3.39)

$$A(0) = A_1 + A_2 \tag{3.43}$$

Writing equation (3.39) in terms of A(0)

$$A(z) = A(0)\frac{A_1 e^{\gamma z} + A_2 e^{-\gamma z}}{A_1 + A_2} = A(0)\frac{e^{\gamma z} + (A_2/A_1)e^{-\gamma z}}{1 + A_2/A_1} \tag{3.44}$$

The reverse travelling wave B(z) of electric field at z=l plane is equal to the product of the forward wave A(z) and the relfection coefficient at z=l plane (plane 2). So,

$$r_2(A(l)e^{-\jmath\beta_0 l}) = B(l)e^{\jmath\beta_0 l} \tag{3.45}$$

Here, r_2 is the reflection co-efficient at $z = l$ plane.

Putting the values of $A(l)$ from equation (3.39) and $B(l)$ from equation (3.41) in the above equation

$$\begin{aligned} r_2[A_1 e^{\gamma l} + A_2 e^{-\gamma l}]e^{-\gamma\beta_0 l} = \frac{e^{\jmath\phi}}{\jmath\kappa}\{&[-\jmath\Delta\beta + \frac{1}{2}(\overline{g} - \alpha) - \gamma]A_1 e^{\gamma l} \\ &+[-\jmath\Delta\beta + \frac{1}{2}(\overline{g} - \alpha) + \gamma]A_2 e^{-\gamma l}\}e^{\jmath\beta_0 l} \end{aligned} \tag{3.46}$$

Dividing both sides by A_1 and $e^{-\jmath\beta_0 l}$ and multiplying by $\jmath\kappa$

$$\begin{aligned} \jmath\kappa r_2(e^{\gamma l} + \frac{A_2}{A_1}e^{-\gamma l}) = e^{2\jmath\beta_0 l + \jmath\phi}\{&[-\jmath\Delta\beta + \frac{1}{2}(\overline{g} - \alpha) - \gamma]e^{\gamma l} \\ &+[-\jmath\Delta\beta + \frac{1}{2}(\overline{g} - \alpha) + \gamma]\frac{A_2}{A_1}e^{-\gamma l}\} \end{aligned} \tag{3.47}$$

$$\begin{aligned} &\{\jmath\kappa r_2 e^{-\gamma l} - [-\jmath\Delta\beta + \frac{1}{2}(\overline{g} - \alpha) + \gamma]e^{\jmath 2\beta_0 l + \jmath\phi}e^{-\gamma l}\}\frac{A_2}{A_1} \\ &= -\jmath\kappa r_2 e^{\gamma l} + [-\jmath\Delta\beta + \frac{1}{2}(\overline{g} - \alpha) - \gamma]e^{\jmath 2\beta_0 l + \jmath\phi}e^{\gamma l} \end{aligned} \tag{3.48}$$

$$\frac{A_2}{A_1} = \frac{-\jmath\kappa r_2 e^{\gamma l} + [-\jmath\Delta\beta + \frac{1}{2}(\overline{g} - \alpha) - \gamma]e^{\jmath 2\beta_0 l + \jmath\phi}e^{\gamma l}}{\jmath\kappa r_2 e^{-\gamma l} - [-\jmath\Delta\beta + \frac{1}{2}(\overline{g} - \alpha) + \gamma]e^{\jmath 2\beta_0 l + \jmath\phi}e^{-\gamma l}} \tag{3.49}$$

Putting the value of $\frac{A_2}{A_1}$ in equation (3.44) the numerator of A(z) can be written as

$$
\begin{aligned}
Num. = \quad & A(0) \times \\
& \{\jmath\kappa r_2 e^{-\gamma l} - [-\jmath\Delta\beta + \frac{1}{2}(\overline{g} - \alpha) + \gamma] e^{\jmath 2\beta_0 l + \jmath\phi} e^{-\gamma l}\} e^{\gamma z} \\
& + \{-\jmath\kappa r_2 e^{\gamma l} + [-\jmath\Delta\beta + \frac{1}{2}(\overline{g} - \alpha) - \gamma] e^{\jmath 2\beta_0 l + \jmath\phi} e^{\gamma l}\} e^{-\gamma z} \qquad (3.50) \\
& = A(0) \times \gamma [e^{\gamma(z-l)} + e^{-\gamma(z-l)}] e^{\jmath 2\beta_0 l - \jmath\phi} \\
& + \{\jmath\kappa r_2 - [-\jmath\Delta\beta + \frac{1}{2}(\overline{g} - \alpha)]\} [e^{\gamma(z-l)} - e^{-\gamma(z-l)}] e^{-\jmath 2\beta_0 l - \jmath\phi} \qquad (3.51)
\end{aligned}
$$

and the denominator of A(z) as

$$
\begin{aligned}
Denom. = \quad & \{\jmath\kappa r_2 e^{-\gamma l} - [-\jmath\Delta\beta + \frac{1}{2}(\overline{g} - \alpha) + \gamma] e^{\jmath 2\beta_0 l + \jmath\phi} e^{-\gamma l}\} \\
& + \{-\jmath\kappa r_2 e^{\gamma l} + [-\jmath\Delta\beta + \frac{1}{2}(\overline{g} - \alpha) - \gamma] e^{\jmath 2\beta_0 l + \jmath\phi} e^{\gamma l}\} \qquad (3.52) \\
& = -\gamma [e^{-\gamma l} + e^{\gamma l}] e^{\jmath 2\beta_0 l + \jmath\phi} \\
& + \{-\jmath\kappa r_2 + [-\jmath\Delta\beta + \frac{1}{2}(\overline{g} - \alpha)]\} [e^{\gamma l} - e^{-\gamma l}] e^{-\jmath 2\beta_0 l + \jmath\phi} \qquad (3.53)
\end{aligned}
$$

Eliminating $e^{-\jmath 2\beta_0 l + \jmath\phi}$ from both numerator and denominator the equation of A(z) is

$$
\begin{aligned}
A(z) = \quad & A(0) \times \\
& \frac{-\gamma \cosh[\gamma(z-l)] + \{\jmath\kappa r_2 e^{-\jmath 2\beta_0 l - \jmath\phi} - [-\jmath\Delta\beta + \frac{1}{2}(\overline{g} - \alpha)]\} \sinh[\gamma(z-l)]}{-\gamma \cosh[\gamma l] + \{-\jmath\kappa r_2 e^{-\jmath 2\beta_0 l - \jmath\phi} + [-\jmath\Delta\beta + \frac{1}{2}(\overline{g} - \alpha)]\} \sinh[\gamma l]}
\end{aligned} \qquad (3.54)
$$

Since, $\sinh x = \frac{e^x - e^{-x}}{2}$ and $\cosh x = \frac{e^x + e^{-x}}{2}$

Now after multiplying the numerator by A(0) and the denominator by $A_1 + A_2$ of the R.H.S of (3.41)

$$
\begin{aligned}
& B(z) = A(0) \times \\
& \frac{\frac{e^{\jmath\phi}}{\jmath\kappa}\{[-\jmath\Delta\beta + \frac{1}{2}(\overline{g} - \alpha) - \gamma] e^{\jmath z} + [-\jmath\Delta\beta + \frac{1}{2}(\overline{g} - \alpha) + \gamma] \frac{A_2}{A_1} e^{-\gamma z}\}}{1 + \frac{A_2}{A_1}}
\end{aligned} \qquad (3.55)
$$

Putting the value of $\frac{A_2}{A_1}$ from equation (3.49), replacing $[-\jmath\Delta\beta + \frac{1}{2}(\overline{g} - \alpha)]^2 - \gamma^2$ by $-\kappa^2$ and after simplifying, we get

$$
\begin{aligned}
& B(z) = A(0) \times \\
& \frac{-\gamma r_2 e^{\jmath\phi} \cosh[\gamma(z-l)] + \{r_2 e^{\jmath\phi}[-\jmath\Delta\beta + \frac{1}{2}(\overline{g} - \alpha)] - \jmath\kappa e^{-\jmath 2\beta_0 l + \jmath 2\phi}\} \sinh[\gamma(z-l)]}{-\gamma e^{2\jmath\beta_0 l + \jmath\phi} \cosh[\gamma l] + \{-\jmath\kappa r_2 + [-\jmath\Delta\beta + \frac{1}{2}(\overline{g} - \alpha)] e^{2\jmath\beta_0 l + \jmath\phi}\} \sinh[\gamma l]}
\end{aligned} \qquad (3.56)
$$

Dividing both numerator and denominator by $e^{2\jmath\beta_D l+\jmath\phi}$ the equation of B(z) becomes

$$B(z) = A(0) \times \frac{-\gamma r_2 e^{-2\jmath\beta_D l}\cosh[\gamma(z-l)] + \{r_2 e^{-2\jmath\beta_D l}[-\jmath\Delta\beta + \frac{1}{2}(\overline{g}-\alpha)] - \jmath\kappa e^{\jmath\phi}\}\sinh[\gamma(z-l)]}{-\gamma\cosh[\gamma l] + \{-\jmath\kappa r_2 + e^{-2\jmath\beta_D l-\jmath\phi} + [-\jmath\Delta\beta + \frac{1}{2}(\overline{g}-\alpha)]\}\sinh[\gamma l]} \tag{3.57}$$

Equations (3.54) and (3.57) are the two wave equations which contain the information of the location of the facets, reflection coefficient r_2, relative gain $\overline{g}$ and loss α. These equations may be equally applied to DFB and DBR lasers. In a DBR laser $\overline{g}$=0 i.e., zero gain in the corrugation area, but in a DFB laser both gain and loss are present.

3.5 The equation representing the oscillation condition of a pure index corrugated DFB semiconductor laser with no reflection from outside

Consider a DFB semiconductor laser with its left facet at z=-l_1 and the right facet at $z = l_2$ having reflection coefficients of r_1 at the left facet (plane 1) and r_2 at the right facet (plane 2) as shown in figure 3.3. It may be recalled that the solution of wave equation is of the form

$$E = A(z)F(x,y)e^{\jmath\omega t-\jmath\beta z} + B(z)F(x,y)e^{\jmath\omega t+\jmath\beta z} + c.c. \tag{3.58}$$

Consider the section 0 to l_2 of the laser where $0 \leq z \leq l_2$ named as region 2. Following equations (3.54) and (3.57) the expressions for the forward and reverse wave amplitudes for this section may be written as

$$A_2(z) = A_2(0) \times \frac{-\gamma\cosh[\gamma(z-l_2)] + \{\jmath\kappa r_2 e^{-\jmath 2\beta_D l_2-\jmath\phi_2} - [-\jmath\Delta\beta + \frac{1}{2}(\overline{g}-\alpha)]\}\sinh[\gamma(z-l_2)]}{-\gamma\cosh[\gamma l_2] + \{-\jmath\kappa r_2 e^{-\jmath 2\beta_D l_2-\jmath\phi_2} + [-\jmath\Delta\beta + \frac{1}{2}(\overline{g}-\alpha)]\}\sinh[\gamma l_2]} \tag{3.59}$$

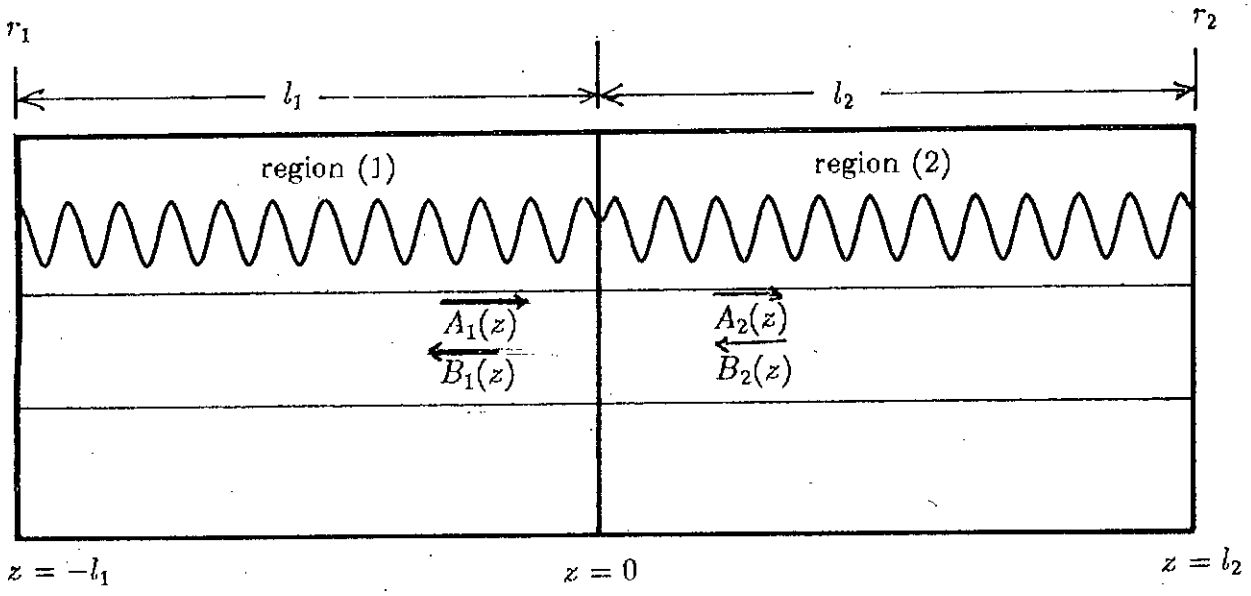

Figura 3.3: Forward and reverse travelling waves in a DFB semiconductor laser with longitudinal dimensions extending from $z = -l_1$ to l_2.

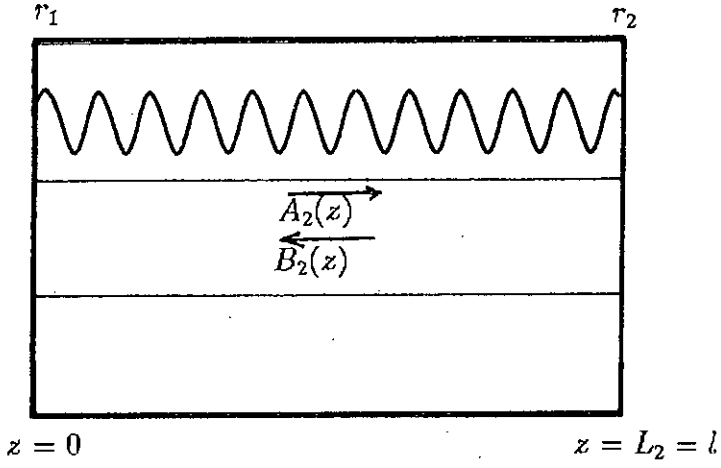

Figura 3.4: Forward and reverse travelling waves in a DFB semiconductor laser with longitudinal dimensions extending from $z = 0$ to l.

$$B_2(z) = A_2(0) \times$$
$$\frac{-\gamma r_2 e^{-2\jmath\beta_D l_2}\cosh[\gamma(z-l_2)] + \{r_2 e^{-2\jmath\beta_D l_2}[-\jmath\Delta\beta + \frac{1}{2}(\overline{g}-\alpha)] - \jmath\kappa e^{\jmath\phi_2}\}}{-\gamma\cosh[\gamma l_2] + \{-\jmath\kappa r_2 + e^{-2\jmath\beta_D l_2 - \jmath\phi_2} + [-\jmath\Delta\beta + \frac{1}{2}(\overline{g}-\alpha)]\}}$$
$$\times\frac{\sinh[\gamma(z-l_2)]}{\sinh[\gamma l_2]} \tag{3.60}$$

where,

$$\gamma^2 = [\jmath\Delta\beta - \frac{1}{2}(\overline{g}-\alpha)]^2 + \kappa^2 \tag{3.61}$$

and ϕ_2 is the phase shift of index corrugation at the z=0 plane. Equation (3.16) is the same equation as (3.37).

For convenience equations (3.59) and (3.60) may be written as follows

$$A_2(z) = A_2(0)P(z) \tag{3.62}$$

$$B_2(z) = A_2(0)Q(z) \tag{3.63}$$

For the other section of the laser the value of z is $-l_1 \leq z \leq 0$. We call this section as region 1. The expressions for $A_1(z)$ and $B_1(z)$ of this section may be obtained by replacing $A_2(0)$ with $A_1(0)$, z with -z, ϕ_2 with ϕ_1, l_2 with l_1 and r_2 with r_1 in the above equations of $A_2(z)$ and $B_2(z)$.

So,

$$A_1(z) = A_1(0) \times$$
$$\frac{-\gamma\cosh[\gamma(-z-l_1)] + \{\jmath\kappa r_1 e^{\jmath 2\beta_D l_1 - \jmath\phi_1} - [-\jmath\Delta\beta + \frac{1}{2}(\overline{g}-\alpha)]\}\sinh[\gamma(-z-l_1)]}{-\gamma\cosh[\gamma l_1] + \{-\jmath\kappa r_1 e^{-\jmath 2\beta_D l_1 - \jmath\phi_1} + [-\jmath\Delta\beta + \frac{1}{2}(\overline{g}-\alpha)]\}\sinh[\gamma l_1]} \tag{3.64}$$

and

$$B_1(z) = A_1(0) \times$$
$$\frac{-\gamma r_1 e^{-2\jmath\beta_D l_1}\cosh[\gamma(-z-l_1)] + \{r_1 e^{-\jmath 2\beta_D l_1}[-\jmath\Delta\beta + \frac{1}{2}(\overline{g}-\alpha)] - \jmath\kappa e^{\jmath\phi_1}\}}{-\gamma\cosh[\gamma l_1] + \{-\jmath\kappa r_1 e^{-\jmath 2\beta_D l_1 - \jmath\phi_1} + [-\jmath\Delta\beta + \frac{1}{2}(\overline{g}-\alpha)]\}}$$
$$\times\frac{\sinh[\gamma(-z-l_1)]}{\sinh[\gamma l_1]} \tag{3.65}$$

In the above equations, $A_2(z)$ and $B_2(z)$ are the expressions for waves $A(z)$ and $B(z)$ in region 2 (figure 3.3) and $A_1(z)$ and $B_1(z)$ are the expressions for waves

$A(z)$ and $B(z)$ in region 1 (figure 3.3). For convenience, equations (3.64) and (3.65) may be written as follows

$$A_1(z) = A_1(0)R(z) \tag{3.66}$$

$$B_1(z) = A_1(0)S(z) \tag{3.67}$$

At z=0 the boundary conditions are

$$A_2(0) = B_1(0) \tag{3.68}$$

$$A_1(0) = B_2(0) \tag{3.69}$$

Now, putting the value of $B_1(0)$ from equation (3.67) in equation (3.68) results in

$$A_2(0) = A_1(0)S(0) \tag{3.70}$$

Next, putting the value of $A_1(0)$ from equation (3.65) in the above equation

$$A_2(0) = B_2(0)S(0) \tag{3.71}$$

Substituting $B_2(0)$ from equation (3.59) in the above equation results in

$$\begin{aligned} A_2(0) &= A_2(0)Q(0)S(0) \\ i.e., Q(0)S(0) &= 1 \end{aligned} \tag{3.72}$$

Replacing Q(0) and S(0) by their expressions in the above equation the following equation is obtained

$$\begin{aligned} &[-\gamma r_1 e^{-2\jmath\beta_D l_1}\cosh(-\gamma l_1) - \{r_1 e^{-\jmath 2\beta_D l_1}[-\jmath\Delta\beta + \frac{1}{2}(\overline{g}-\alpha)] - \jmath\kappa e^{\jmath\phi_1}\}\sinh(\gamma l_1)] \\ &\times[-\gamma r_2 e^{-2\jmath\beta_D l_2}\cosh(-\gamma l_2) + \{r_2 e^{-\jmath 2\beta_D l_2}[-\jmath\Delta\beta + \frac{1}{2}(\overline{g}-\alpha)] - \jmath\kappa e^{\jmath\phi_2}\}\sinh(-\gamma l_2)] \\ &= [-\gamma\cosh(\gamma l_1) + \{-\jmath\kappa\ r_1 e^{-\jmath\beta_D l_1 - \jmath\phi_1} + [-\jmath\Delta\beta + \frac{1}{2}(\overline{g}-\alpha)]\}\sinh(\gamma l_1)] \\ &\times[-\gamma\cosh(\gamma l_2) + \{-\jmath\kappa\ r_2 e^{-\jmath 2\beta_D l_2 - \jmath\phi_2} + [-\jmath\Delta\beta + \frac{1}{2}(\overline{g}-\alpha)]\}\sinh(\gamma l_2)] \end{aligned} \tag{3.73}$$

This equation represents the oscillation condition for a DFB semiconductor laser. In this equation index corrugation is considered. It will be shown later that for considering index as well as gain corrugation this equation is to be modified by replacing κ by $\kappa_n + \jmath\kappa_g$ [17][40].

3.6 Summary

Starting with the Maxwell's equations the wave equations of a simple semiconductor laser have been derived. Using a sinusoidal index corrugation the equations for the forward and reverse waves in an index corrugated DFB semiconductor laser have been derived. The equation representing the resonance condition of an index corrugated DFB semiconductor laser has been derived.

CHAPTER 4

DFB semiconductor laser having pure index corrugation with external feedback

4.1 Introduction

The wave equations and the oscillation condition for a DFB type semiconductor laser with refractive index corrugation and without external feedback has been presented in chapter 3. In this chapter, the effect of external feedback in a DFB semiconductor laser is considered. It has been observed that the behaviour of a semiconductor laser could be significantely affected by external optical feedback i.e., feedback of a portion of the laser output back into the laser cavity from a reflecting surface external to it [30]. Such feedback appears from the surface of a connecting device such as a collimate lens, optical disk or optical fibre [31]. The effect of external feedback depends on the distance of the reflecting surface from the laser cavity, the phase change of the reflected wave at the reflecting surface and the value of the power reflection coefficient at the reflecting surface.

In section 4.2, the effect of external feedback in terms of wave reflection is explained. An expression for the effective reflection coefficient at the right facet (output facet) of a DFB semiconductor laser is derived with the help of a simple model following previous researches [30][32][34].

In section 4.3, the equation of an index coupled DFB semiconductor laser are modified by taking into account of the effect of the external feedback. The equations representing the oscillation condition have been presented for four combinations of left facet reflection coefficient, right facet reflection coefficient and the lengths of the right and left halves of the generalized DFB laser model.

4.2 The effect of external feedback in a DFB semiconductor laser

In the previous chapter, equations have been developed without taking into account of the effect of external feedback. Here, external feedback refers to the portion of the laser output entering back into the laser after facing a reflection from the surface of a device external to the laser. A schematic diagram illustrating such a reflection is presented in figure 4.1 [30][32][33][34]. In this model it is assumed that output of the laser is taken out through the right facet. Thus the left facet is the back port and the right facet is the front port of the laser.

Here, it is considered that a laser output wave of amplitude 1 is incident on the right facet (figure 4.1) and a portion $\sqrt{R_2}$ of this wave is reflected back into the laser. Therefore, $\sqrt{1-R_2}$ of the incident wave is transmitted through the facet. A portion ($\sqrt{\Gamma}$) of this transmitted wave then faces reflection at the surface of another device at B. The reflected wave after travelling backward over the distance of length l_{ext} meter ($\theta/2$ radians) then enters into the laser through the right facet. At this time, $\sqrt{1-R_2}$ portion of the reflected wave enters into the laser. Thus, ultimately $\sqrt{1-R_2}\sqrt{\Gamma}e^{-j\theta}\sqrt{1-R_2}\sqrt{\eta} = (1-R_2)\sqrt{\eta\Gamma}e^{-j\theta}$ fraction of the unity amplitude incident wave is now entering into the laser. We now have $\sqrt{R_2}$ fraction of the incident wave due to the reflection at the right facet plus $(1-R_2)\sqrt{\eta\Gamma}e^{-j\theta}$ fraction of the incident wave through the process of reflection from the surface of an external device. Thus, the effective reflection coefficient is changed from r_2 to r_2' where,

$$r_2' = \sqrt{R_2} + (1-R_2)\sqrt{\eta\Gamma}e^{-j\theta} \tag{4.1}$$

This expression for the effective reflection coefficient has also been used by Suhara et. al [33][34]. Therefore, for taking into account of the effects of the external cavity reflection entering into the laser cavity i.e., external feedback the reflection coefficient r_2 at the right facet of a DFB semiconductor laser will be replaced by the expression of r_2' of equation (4.1).

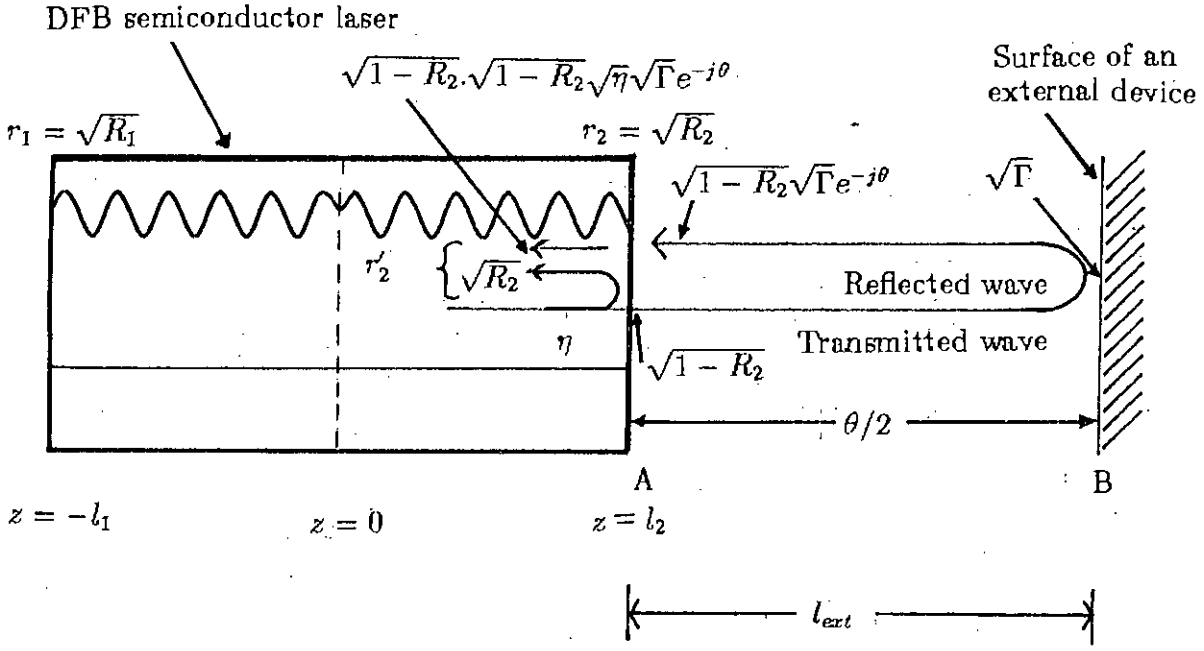

Figure 4.1: A schematic diagram of a DFB laser illustrating the effect of external feedback. An wave having an amplitude of 1 is incident at the right facet of the laser experiances reflection. $\sqrt{R_2}$ portion of this wave is reflected back into the laser and $\sqrt{1-R_2}$ portion passes outward and later experiances reflection at the surface of another external device, ultimatemately $(1-R_2)\sqrt{\eta\Gamma}e^{-j\theta}$ portion of the wave comes back into the laser. Thus the effective reflection coefficient is $r_2' = \sqrt{R_2} + (1-R_2)\sqrt{\eta\Gamma}e^{-j\theta}$.

4.3 The equation representing the oscillation condition for an index coupled DFB laser taking into account of the effect of external feedback

The schematic diagram of a DFB semiconductor laser extending from $z = -l_1$ to $z = l_2$ is shown in figure 4.2. In this section, one half of the DFB semiconductor laser of figure 4.2 will be considered for analysis. This will simplify the equations significantly. The modified DFB semiconductor laser is shown in figure 4.3.

Since, the left half of the laser is absent, we may write

$$l_1 = 0, \quad A_1(z) = 0, \quad B_1(z) = 0 \tag{4.2}$$

Also, we assume $r_1 = 1$ i.e., 100% reflection from the left facet. The boundary conditions for this DFB semiconductor laser is

$$A_2(0) = B_2(0) \tag{4.3}$$

Putting the values of $A_2(0)$ and $B_2(0)$ from equations (3.59) and (3.60) in the above equation the following equation is obtained

$$\begin{aligned} &-\gamma \cosh[-\gamma l_2] + \{\jmath\kappa r_2 e^{-2\jmath\beta_D l_2 - \jmath\phi_2} - [-\jmath\Delta\beta + \frac{1}{2}(\overline{g} - \alpha)]\} \sinh[-\gamma l_2] \\ &= -\gamma r_2 e^{-2\jmath\beta_D l_2} \cosh[-\gamma l_2] + \{r_2 e^{-2\jmath\beta_D l_2}[-\jmath\Delta\beta + \frac{1}{2}(\overline{g} - \alpha)] - \jmath\kappa e^{\jmath\phi_2}\} \sinh[-\gamma l_2] \end{aligned} \tag{4.4}$$

Dividing both sides of equation (4.3) by $\sinh(\gamma - l_2)$ we can write

$$\begin{aligned} &-\gamma \coth[-\gamma l_2] + \{\jmath\kappa r_2 e^{-2\jmath\beta_D l_2 - \jmath\phi_2} - [-\jmath\Delta\beta + \frac{1}{2}(g - \alpha)]\} \\ &\quad = -\gamma r_2 e^{-2\jmath\beta_D l_2} \coth[-\gamma l_2] + \{r_2 e^{-2\jmath\beta_D l_2}[-\jmath\Delta\beta + \frac{1}{2}(g - \alpha)] - \jmath\kappa e^{\jmath\phi_2}\} \end{aligned} \tag{4.5}$$

After rearranging the above equation, we can write

$$\begin{aligned} &-[-\jmath\Delta\beta + \frac{1}{2}(g - \alpha)] - [-\jmath\Delta\beta + \frac{1}{2}(g - \alpha)] r_2 e^{-2\jmath\beta_D l_2} + \jmath\kappa r_2 e^{-2\jmath\beta_D l_2 - \jmath\phi_2} + \jmath\kappa e^{\jmath\phi_2} \\ &\quad = \{-\gamma r_2 e^{-2\jmath\beta_D l_2} + \gamma\} \coth[-\gamma l_2] \end{aligned} \tag{4.6}$$

Here, r_2 is the reflection coefficient on the right facet of the semiconductor laser medium.

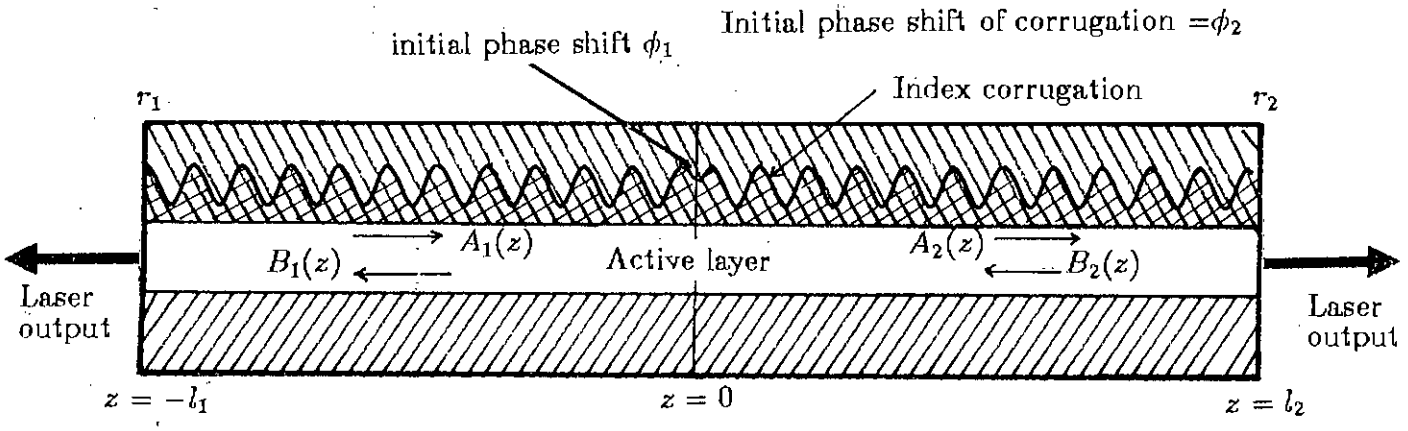

Figure 4.2: Schematic diagram of a pure index corrugated DFB semiconductor laser.

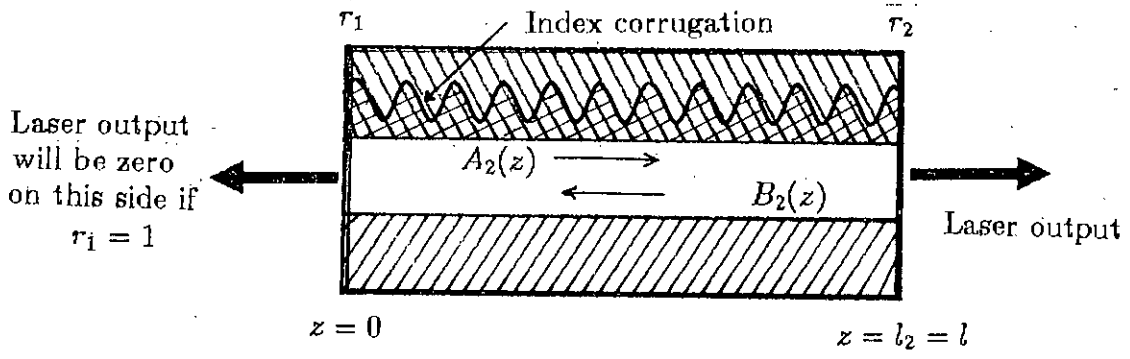

Figure 4.3: Schematic diagram of a simplified pure index corrugated DFB semiconductor laser considering a length of l (from $z = 0$ to $z = l$).

We now consider reflection of the laser output from the surface of an external device as shown in figure 4.4. In order to consider the effect of this reflection or feedback from the external cavity we replace r_2 by r_2' where

$$r_2' = \sqrt{R_2} + (1 - R_2)\sqrt{\eta\Gamma}e^{-\jmath\theta} \tag{4.7}$$

and $\sqrt{R_2} = r_2$.

4.4 The oscillation condition for a pure index coupled DFB laser considering four combinations of r_1, r_2, l_1 and l_2 and considering external reflection

Let us now consider the DFB laser of figure 4.2 which is the same as figure 3.1 of chapter 3 consisting of two halves extending from $-l_1$ to l_2. It has already been shown in chapter 3 that equation (3.73) represents the oscillation condition for such a laser in the absence of any external feedback. Here, we see that we can have a combination of values of r_1, r_2, l_1 and l_2. In this section we shall derive a DFB semiconductor laser for four cases taking into account of external feedback.

First of all, let us assume the simple case i.e., $r_1 = r_2 = 0$ but $l_1 \neq 0$, $l_2 \neq 0$. Putting this value in equation (3.73) we get

$$\begin{aligned} &-\jmath\kappa e^{\jmath\phi_1}\sinh(\gamma l_1) \times \{-\jmath\kappa e^{\jmath\phi_1}\sinh(\gamma l_1)\} \\ &= [-\gamma\cosh(-\gamma l_1) + [-\jmath\Delta\beta + \frac{1}{2}(g-\alpha)]\sinh(-\gamma l_1)] \\ &\times [-\gamma\cosh(\gamma l_2) + [-\jmath\Delta\beta + \frac{1}{2}(g-\alpha)]\sinh(-\gamma l_1)] \end{aligned} \tag{4.8}$$

Secondly, we consider $r_1 = 0$, $r_2 = 0$, $l_1 = 0$ and $l_2 \neq 0$. Equation (3.73) then becomes

$$(-\gamma) \times \{-\gamma\cosh(\gamma l_2) + [-\jmath\Delta\beta + \frac{1}{2}(g-\alpha)]\sinh(\gamma l_2)\} = 0 \tag{4.9}$$

Since $\gamma \neq 0$, the above equation reduces to

$$\gamma\cosh(\gamma l_2) + [\jmath\Delta\beta - \frac{1}{2}(g-\alpha)]\sinh(\gamma l_2) = 0 \tag{4.10}$$

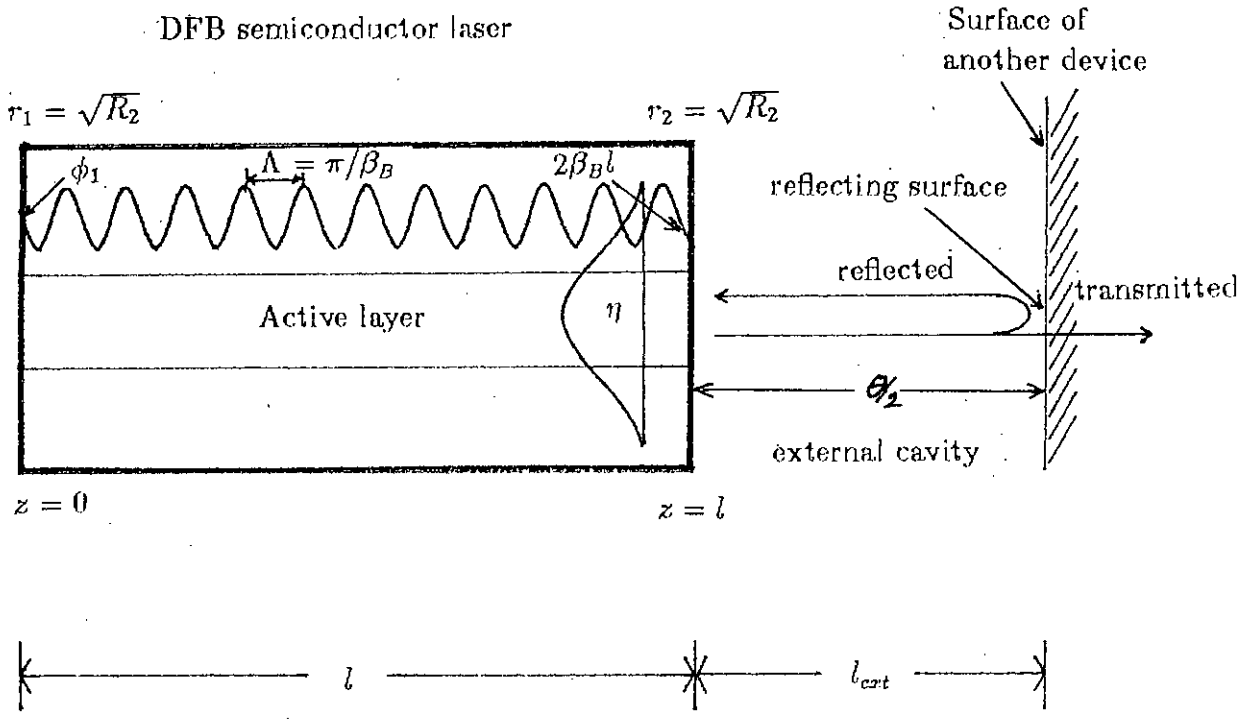

Figure 4.4: The index corrugated DFB semiconductor with laser light reflected from the surface of another external device and entering into the laser (i.e., in preesnce of external reflection). The total phase shift during the travel is $\theta = 2k_0 l_{ext}$.

In the third case, let us consider $r_1 = 0$, $l_1 = 0$, $r_2 \neq 0$ and $l_2 \neq 0$. In this case, equation (3.73) becomes

$$(-\gamma) \times \{-\cosh(\gamma l_2)\} + \{-\jmath\kappa r_2 e^{-2\jmath\beta_D l_2 - \jmath\phi_2} + [-\jmath\Delta\beta + \frac{1}{2}(g-\alpha)]\} \sinh(\gamma l_2) = 0 \tag{4.11}$$

Again, since $\gamma \neq 0$ then the above equation results in

$$\gamma \cosh(\gamma l_2) + \{\jmath\kappa r_2 e^{-2\jmath\beta_D l_2 - \jmath\phi_2} + [-\jmath\Delta\beta + \frac{1}{2}(g-\alpha)]\} \sinh(\gamma l_2) = 0 \tag{4.12}$$

In the fourth case, let us assume $l_1 = 0$, $r_1 \neq 0$, $l_2 \neq 0$ *and* $r_2 \neq 0$. For these values of parameters the equation representing the oscillation condition may be obtained from equation (3.73) by putting the above mentioned values. Thus this equation may be written as

$$\begin{aligned}&[-\gamma r_1 r_2 e^{-2\jmath\beta_D l_2} \cosh(\gamma l_2) + r_1\{r_2 e^{-\jmath 2\beta_D l_2}[\frac{1}{2}(\overline{g}-\alpha) - \jmath\Delta\beta] - \jmath\kappa e^{\jmath\phi_2}\} \sinh(\gamma l_2)] \\ &= [-\gamma \cosh(\gamma l_2) - \{-\jmath\kappa r_2 e^{-\jmath\beta_D l_2 - \jmath\phi_2} + [\frac{1}{2}(\overline{g}-\alpha) - \jmath\Delta\beta] \sinh(\gamma l_2)\end{aligned} \tag{4.13}$$

After simplification of this equation we can write

$$\begin{aligned}&\gamma(1 - r_1 r_2 e^{-2\jmath\beta_D l_2}) \cosh(\gamma l_2) + (r_1 r_2 e^{-\jmath 2\beta_D l_2} + 1)\{\frac{1}{2}(\overline{g}-\alpha) - \jmath\Delta\beta\} \sinh(\gamma l_2) \\ &-\jmath(r_1 + r_2 e^{-\jmath 2\beta_D l_2 - \jmath\phi_2})\kappa \sinh(\gamma l_2) = 0\end{aligned} \tag{4.14}$$

This is a practical case, since in this model reflection terms for both left and right facets are present.

Here, we recall that for taking into account of the effect of reflection from the surface of another device external to the laser we have to replace r_2 in equations (4.7), (4.9), (4.11) and (4.13) by r_2' where

$$r_2' = \sqrt{R_2} + (1 - R_2)\sqrt{\eta\Gamma} e^{-\jmath\theta} \tag{4.15}$$

Here, the phase term is

$$\theta = 2k_o l_{ext} = \frac{2\beta l_{ext}}{\overline{n}} = \frac{2(\Delta\beta + \beta_D) l_{ext}}{\overline{n}} \tag{4.16}$$

and l_{ext} is the length of the external cavity. In the above equation ϕ_1 is the initial phase shift of the index grating at $z = 0$ for region 1 and ϕ_2 is the initial phase shift of the index grating for region 2.

In equations (4.7)-(4.13) κ is the coupling term for pure index coupling DFB laser (i.e., $\kappa = \kappa_n$). It will be shown in the next section that while considering both index and gain coupling the coupling coefficient κ can be written as

$$\kappa = \kappa_n + j\kappa_g e^{-j\psi} \tag{4.17}$$

4.5 Summary

The phenomena of external feedback in a DFB semiconductor laser has been explained by considering a simple model. An expression for the effective reflection coefficient at the right facet has been presented by this model. By considering the effect of external feedback the equation representing the oscillation condition of an index corrugated DFB semiconductor laser has been derived.

CHAPTER 5

DFB semiconductor laser having 'gain plus index' corrugation and pure gain corrugation with external feedback

5.1 Introduction

In the previous two chapters, wave equations and the equation representing the oscillation condition have been presented for a pure index coupled DFB semiconductor laser. In this chapter, equations are derived for a DFB laser having refractive index corrugation as well as gain corrugation. Such a DFB semiconductor laser having both index and gain corrugations will be termed as 'gain plus index' corrugated DFB laser [32].

In section 5.2, generalized wave equations for a 'gain plus index' corrugated DFB semiconductor laser are derived. This derivation is similar to the deductions presented in the previous chapters.

In section 5.3, the equation representing the oscillation condition for the above mentioned 'gain plus index' corrugated type of laser is deduced by assuming the generalized type of DFB laser model extending from $z = -l_1$ to l_2. The equation is then simplified for the simplified model of a DFB semiconductor laser extending from $z = 0$ to $z = l_2$.

5.2 Generalized wave equations for a 'gain plus index' coupled semiconductor DFB laser

We now consider a DFB semiconductor laser in which, both gain and refractive index corrugations are present which is termed here as 'gain plus index' coupled DFB semiconductor laser [32]. We recall the general wave equation for a semiconductor

laser deduced from Maxwell's equations in section 3.2. From equation (3.9), this wave equation can be rewritten as [32]

$$\nabla^2\overline{E} - \mu_o\sigma\frac{\partial\overline{E}}{\partial t} - \mu_o\varepsilon_o n^2\frac{\partial^2\overline{E}}{\partial t^2} - \mu_o\varepsilon_o\chi\frac{\partial^2\overline{E}}{\partial t^2} = 0 \tag{5.1}$$

This equation will be used for a gain plus index corrugated DFB semiconductor laser. We consider the index corrugation represented by equation (3.11). Thus the refractive index can be written as

$$\begin{aligned} n &= \overline{n} + (\frac{\Delta n}{2}e^{2\jmath\beta_D z + \jmath\phi} + c.c.) \\ &= \overline{n} + (\frac{\Delta n}{2}e^{2\jmath\pi z/\Lambda + \jmath\phi} + c.c.) \end{aligned} \tag{5.2}$$

Here, ϕ is the initial phase at z=0 and $\beta_B = \pi/\Lambda$ is the propagation constant corresponding to the Bragg wavelength and Λ is the spatial period of the index corrugation. Here, $\overline{n}$ is the average refractive index and Δn is the maximum amplitude variation. A DFB laser having the $\lambda/4$ shifted region is equivalent to $\phi = 0.5\pi$ in the present model. This model is shown in figure 5.1. However, for the analysis of this section the model of figure 5.2 is also acceptable.

Assuming a similar variation of dielectric susceptibility for gain corrugation we can write [32][34]

$$\begin{aligned} \chi &= \overline{\chi} + (\frac{\Delta\chi}{2}e^{2\jmath\beta_D z + \jmath\phi + \jmath\psi} + c.c.) \\ &= \overline{\chi} + (\frac{\Delta\chi}{2}e^{2\jmath\pi z/\Lambda + \jmath\phi + \jmath\psi} + c.c.) \end{aligned} \tag{5.3}$$

Here, χ is the average dielectric susceptibility and $\Delta\chi$ is the maximum amplitude variation, ψ is the phase difference between the index and gain corrugation. Consider $\Delta n << \overline{n}$ equation (5.2) can be written as

$$n^2 \simeq \overline{n}^2 + (\overline{n}\Delta n e^{2\jmath\beta_D z + \jmath\phi} + c.c.) \tag{5.4}$$

A solution of equation (5.1) may be written as

$$E = A(z)F(x,y)e^{\jmath\omega t - \jmath\beta z} + B(z)F(x,y)e^{\jmath\omega t + \jmath\beta z} + c.c. \tag{5.5}$$

Putting the value of $\overline{E}$ from equation (5.5) in equation (5.1) and replacing n^2 and χ in equation (5.1) by (5.4) and (5.3) we get

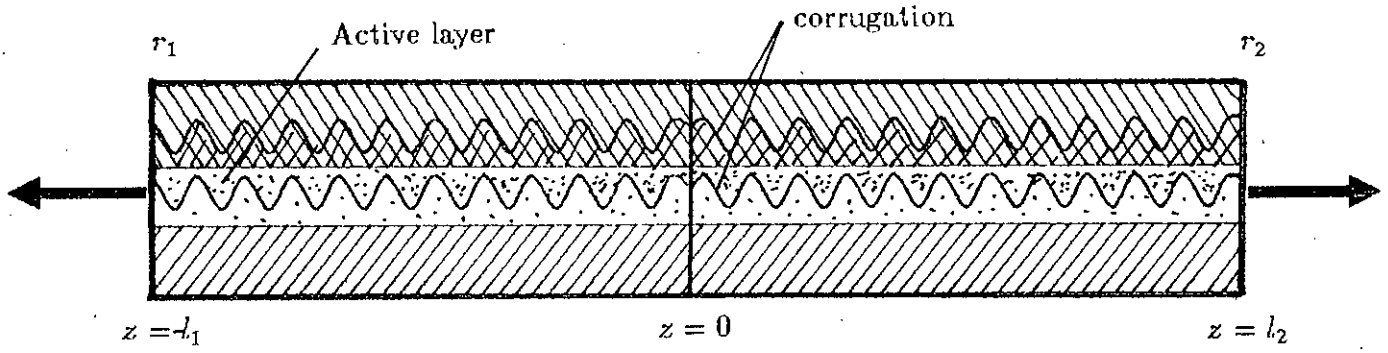

Figure 5.1: Schematic diagram of a 'gain plus index' corrugated DFB semiconductor laser.

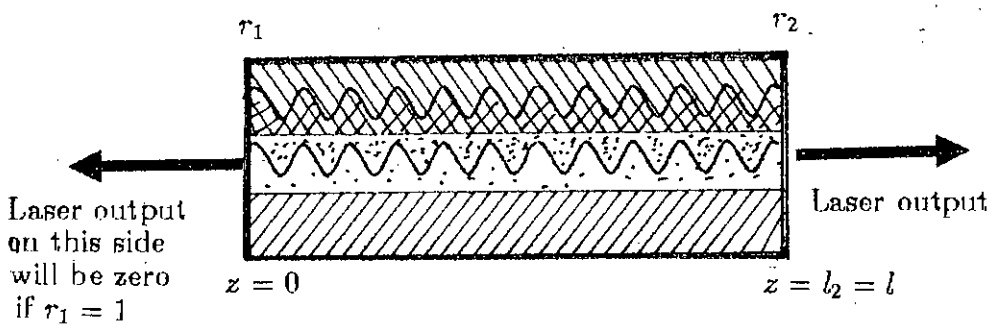

Figure 5.2: Schematic diagram of a simplified 'gain plus index' DFB semiconductor laser considering a length of l (from $z = 0$ to $z = l$).

$$
\begin{aligned}
&\nabla^2[A(z)F(x,y)e^{\jmath\omega t-\jmath\beta z}+B(z)F(x,y)e^{\jmath\omega t+\jmath\beta z}+c.c.]\\
&-\mu_o\sigma[\jmath\omega A(z)F(x,y)e^{\jmath\omega t-\jmath\beta z}+\jmath\omega B(z)F(x,y)e^{\jmath\omega t+\jmath\beta z}+c.c.]\\
&-\mu_o\varepsilon_o[n^2+(\overline{n}\Delta n e^{2\jmath\beta_D z+\jmath\phi}+c.c.)][-\omega^2 A(z)F(x,y)e^{\jmath\omega t-\jmath\beta_D z}\\
&-\omega^2 B(z)F(x,y)e^{\jmath\omega t+\jmath\beta_D z}+c.c.]\\
&-\mu_o\varepsilon_o[\overline{\chi}+(\frac{\Delta\chi}{2}e^{2\jmath\beta_D z+\jmath\phi+\jmath\psi}+c.c.)][-\omega^2 A(z)F(x,y)e^{\jmath\omega t-\jmath\beta_D z}\\
&-\omega^2 B(z)F(x,y)e^{\jmath\omega t+\jmath\beta_D z}+c.c.]=0
\end{aligned}
\tag{5.6}
$$

or,

$$
\begin{aligned}
&(\frac{\partial^2}{\partial x^2}+\frac{\partial^2}{\partial y^2})A(z)F(x,y)e^{\jmath\omega t-\jmath\beta_D z}+\frac{\partial^2 A(z)}{\partial z^2}F(x,y)e^{\jmath\omega t-\jmath\beta_D z}\\
&-2\jmath\beta_B\frac{\partial A(z)}{\partial z}F(x,y)e^{\jmath\omega t-\jmath\beta_D z}-\beta_B A(z)F(x,y)e^{\jmath\omega t-\jmath\beta_D z}\\
&+(\frac{\partial^2}{\partial x^2}+\frac{\partial^2}{\partial y^2})B(z)F(x,y)e^{\jmath\omega t+\jmath\beta_D z}+\frac{\partial^2 B(z)}{\partial z^2}F(x,y)e^{\jmath\omega t+\jmath\beta_D z}\\
&+2\jmath\beta_B\frac{\partial B(z)}{\partial z}F(x,y)e^{\jmath\omega t+\jmath\beta_D z}-\beta_B^2 B(z)F(x,y)e^{\jmath\omega t+\jmath\beta_D z}\\
&-\jmath\omega\mu_o\sigma A(z)F(x,y)e^{\jmath\omega t-\jmath\beta_D z}-\jmath\omega\mu_o\sigma B(z)F(x,y)e^{\jmath\omega t+\jmath\beta_D z}\\
&+\mu_o\varepsilon_o\omega^2[\overline{n}^2 A(z)F(x,y)e^{\jmath\omega t-\jmath\beta_D z}+\overline{n}^2 B(z)F(x,y)e^{\jmath\omega t+\jmath\beta_D z}\\
&+\overline{n}\Delta n A(z)F(x,y)e^{\jmath\omega t+\jmath\beta_D z+\jmath\phi}+\overline{n}\Delta n B(z)F(x,y)e^{\jmath\omega t+\jmath 3\beta_D z+\jmath\phi}\\
&+\overline{n}\Delta n A(z)F(x,y)e^{\jmath\omega t-3\jmath\beta_D z-\jmath\phi}+\overline{n}\Delta n B(z)F(x,y)e^{\jmath\omega t-\jmath\beta_D z-\jmath\phi}]\\
&+\mu_o\varepsilon_o\omega^2[\overline{\chi}A(z)F(x,y)e^{\jmath\omega t-\jmath\beta_D z}+\overline{\chi}B(z)F(x,y)e^{\jmath\omega t+\jmath\beta_D z}\\
&+\frac{\Delta\chi}{2}A(z)F(x,y)e^{\jmath\omega t+\jmath\beta_D z+\jmath\phi+\jmath\psi}+\frac{\Delta\chi}{2}B(z)F(x,y)e^{\jmath\omega t+3\jmath\beta_D z+\jmath\phi+\jmath\psi}\\
&+\frac{\Delta\chi}{2}A(z)F(x,y)e^{\jmath\omega t-\jmath 3\beta_D z-\jmath\phi-\jmath\psi}+\frac{\Delta\chi}{2}B(z)F(x,y)e^{\jmath\omega t-\jmath\beta_D z-\jmath\phi-\jmath\psi}]+c.c.=0
\end{aligned}
\tag{5.7}
$$

In the above equation, the variation of field amplitudes is very small in the z direction. As a result, the second order derivatives in the z direction may be neglected. Now, multiplying both sides by $F^*(x,y)e^{\jmath\beta_D z}e^{-\jmath\omega t}$ and perform integration for x, y and z within the limits $-\infty$ to ∞, $-\infty$ to ∞ and $-2\pi/\beta_B$ to $+2\pi/\beta_B$ respectively to obtain spatial average. In addition the time average of both sides are also taken over a period of $\Delta T = 1/\omega$. Choosing $\int_{-\infty}^{\infty}\int_{-\infty}^{\infty}|F(x,y)|^2 dxdy = 1$.

After this operations the c.c. terms vanish because of the time averaging of the $e^{-\jmath 3\omega t}$ terms.

It may be recalled that equation (3.13) represents a semiconductor laser having no corrugation. The same equation is also valid for the present case if we consider no corrugation. Thus

$$(\nabla^2 + \mu_o \varepsilon_o n^2 \omega^2) F(x,y) e^{\jmath \beta z} = 0 \tag{5.8}$$

Separating the z direction variation and the transvers plane variations we get

$$[\frac{\partial^2}{\partial x^2} + \frac{\partial^2}{\partial y^2} + \mu_o \varepsilon_o n^2 \omega^2] F(x,y) = \beta^2 F(x,y) \tag{5.9}$$

In this equation, n may be replaced by $\overline{n}$ since $\overline{n} >> \Delta n$.

Now, utilizing equation (5.9) in the equation resulting after averaging of equation (5.7) mentioned above we get

$$\begin{aligned}[\beta^2 - \beta_B^2 - \quad & \jmath\omega\mu_o \int_{-\infty}^{\infty}\int_{-\infty}^{\infty} \sigma |F(x,y)|^2 dxdy + \mu_o\varepsilon_o\omega^2 \int_{-\infty}^{\infty}\int_{-\infty}^{\infty} \overline{\chi} |F(x,y)|^2 dxdy] A(z) \\ & -2\jmath\beta_B \frac{\partial A(z)}{\partial z} + [\mu_o\varepsilon_o\omega^2 e^{-\jmath\phi} \int_{-\infty}^{\infty}\int_{-\infty}^{\infty} \overline{n}\Delta n |F(x,y)|^2 dxdy \\ & +\mu_o\varepsilon_o\omega^2 e^{-\jmath\phi-\jmath\psi} \int_{-\infty}^{\infty}\int_{-\infty}^{\infty} \frac{\Delta\chi}{2} |F(x,y)|^2 dxdy] B(z) = 0 \end{aligned} \tag{5.10}$$

Next, dividing both sides by $2\jmath\beta_B$ and after rearranging we get

$$\begin{aligned} & \frac{\partial A(z)}{\partial z} = \\ & [\frac{\beta^2 - \beta_B^2}{2\jmath\beta_B} - \frac{\omega\mu_o}{2\beta_B} \int_{-\infty}^{\infty}\int_{-\infty}^{\infty} \sigma |F(x,y)|^2 dxdy + \frac{\mu_o\varepsilon_o\omega^2}{2\jmath\beta_B} \int_{-\infty}^{\infty}\int_{-\infty}^{\infty} \overline{\chi} |F(x,y)|^2 dxdy] A(z) \\ & +[\frac{\mu_o\varepsilon_o\omega^2 e^{-\jmath\phi}}{2\jmath\beta_B} \int_{-\infty}^{\infty}\int_{-\infty}^{\infty} \overline{n}\Delta n |F(x,y)|^2 dxdy \\ & +\frac{+\mu_o\varepsilon_o\omega^2 e^{-\jmath\phi-\jmath\psi}}{2\jmath\beta_B} \int_{-\infty}^{\infty}\int_{-\infty}^{\infty} \frac{\Delta\chi}{2} |F(x,y)|^2 dxdy] B(z) \end{aligned} \tag{5.11}$$

After further rearrangement of this equation, we get

$$\begin{aligned} & \frac{\partial A(z)}{\partial z} = \\ & [\frac{\beta^2 - \beta_B^2}{2\jmath\beta_B} + \frac{\mu_o\varepsilon_o\omega^2}{2\jmath\beta_B} \int_{-\infty}^{\infty}\int_{-\infty}^{\infty} \overline{\chi} |F(x,y)|^2 dxdy - \frac{\omega\mu_o}{2\beta_B} \int_{-\infty}^{\infty}\int_{-\infty}^{\infty} \sigma |F(x,y)|^2 dxdy] A(z) \end{aligned}$$

$$-\jmath[\frac{\mu_o\varepsilon_o\omega^2}{2\jmath\beta_B}\int_{-\infty}^{\infty}\int_{-\infty}^{\infty}\overline{n}\Delta n|F(x,y)|^2dxdy$$
$$+\jmath\frac{\mu_o\varepsilon_o\omega^2e^{-\jmath\psi}}{2\jmath\beta_B}\int_{-\infty}^{\infty}\int_{-\infty}^{\infty}\frac{\Delta\chi}{2}|F(x,y)|^2dxdy]B(z)=0 \tag{5.12}$$

The first term of equation (5.12) may be simplified to define $\jmath\Delta\beta$ as

$$\frac{\beta^2-\beta_B^2}{2\jmath\beta_B}=\frac{(\beta+\beta_B)(\beta-\beta_B)}{2\jmath\beta_B}\simeq-\jmath(\beta-\beta_B)\equiv-\jmath\Delta\beta \tag{5.13}$$

Next, a quantity $\frac{1}{2}(\overline{g}-\alpha)$ may be defined as follows

$$\frac{\mu_o\varepsilon_o\omega^2}{2\beta_B}\int_{-\infty}^{\infty}\int_{-\infty}^{\infty}Im(\overline{\chi})|F(x,y)|^2dxdy$$
$$-\frac{\omega\mu_o}{2\beta_B}\int_{-\infty}^{\infty}\int_{-\infty}^{\infty}\sigma|F(x,y)|^2dxdy\equiv\frac{\overline{g}-\alpha}{2} \tag{5.14}$$

At this stage coupling for index corrugation will be denoted by κ_n and defined as [32]

$$\kappa_n\equiv\frac{\mu_o\varepsilon_o\omega^2}{2\beta_B}\int_{-\infty}^{\infty}\int_{-\infty}^{\infty}\overline{n}\Delta n|F(x,y)|^2dxdy \tag{5.15}$$

Similarly, coupling for gain corrugation will be denoted by κ_g and defined as

$$\kappa_g\equiv\frac{\mu_o\varepsilon_o\omega^2}{2\beta_B}\int_{-\infty}^{\infty}\int_{-\infty}^{\infty}\frac{Im(\Delta\chi)}{2}|F(x,y)|^2dxdy \tag{5.16}$$

Using equations (5.11)-(5.14) in equation (5.10) we get

$$\frac{dA(z)}{dz}=[-\jmath\Delta\beta+\frac{1}{2}(\overline{g}-\alpha)]A(z)-\jmath[\kappa_n+\jmath\kappa_ge^{-\jmath\psi}]e^{-\jmath\phi}B(z) \tag{5.17}$$

In a similar manner, it is possible to obtain the equation for $B(z)$ as

$$\frac{dB(z)}{dz}=[\jmath\Delta\beta-\frac{1}{2}(\overline{g}-\alpha)]B(z)+\jmath[\kappa_n+\jmath\kappa_ge^{+\jmath\psi}]e^{+\jmath\phi}A(z) \tag{5.18}$$

From these two coupled wave equations the following wave equations may be obtained

$$\frac{d^2A(z)}{dz^2}=[\{\jmath\Delta\beta-\frac{1}{2}(\overline{g}-\alpha)\}^2+\{\kappa_n+\jmath\kappa_ge^{+\jmath\psi}\}\{\kappa_n+\jmath\kappa_ge^{-\jmath\psi}\}]A(z) \tag{5.19}$$

and,

$$\frac{d^2B(z)}{dz^2}=[\{\jmath\Delta\beta-\frac{1}{2}(\overline{g}-\alpha)\}^2+\{\kappa_n+\jmath\kappa_ge^{+\jmath\psi}\}\{\kappa_n+\jmath\kappa_ge^{-\jmath\psi}\}]B(z) \tag{5.20}$$

The solutions of these equations are in the form of

$$A(z) = A_1 e^{\gamma z} + A_2 e^{-\gamma z} \tag{5.21}$$

$$B(z) = B_1 e^{\gamma z} + B_2 e^{-\gamma z} \tag{5.22}$$

From equations (5.19) and (5.20) it may be pointout that γ is the complex propagation constant which may be written as

$$\gamma^2 = [\jmath\Delta\beta - \frac{1}{2}(\overline{g} - \alpha)]^2 + [\kappa_n + \jmath\kappa_g e^{-\jmath\psi}][\kappa_n + \jmath\kappa_g e^{\jmath\psi}] \tag{5.23}$$

The dispersion curves for a gain plus index corrugated DFB laser may be obtained from this expression. By comparing equation (5.21) with equation (3.37) it may be observed that, if the gain corrugation is absent then κ_g =0 then equation (5.21) reduces to (3.37).

5.3 Oscillation condition of a 'gain plus index' corrugated DFB laser taking the effect of reflection from an external device surface

Let us first consider the model of the DFB laser shown in figure 5.1. We now compare equation (5.19) with equation (3.38) and find that equation (5.19) can be obtained from equation (3.38) if we replace κ_n by $\kappa_n + j\kappa e^{-j\psi}$ and κ_n^2 by $(\kappa_n + j\kappa e^{-j\psi})(\kappa_n + j\kappa e^{+j\psi})$. We also note that equations (5.21) and (5.22) are same as equations (3.39) and (3.42). Bearing these in mind we can accept equation (3.73) as the equation representing the oscillation condition for a 'gain plus index' corrugated DFB laser of the geometry shown in figure 5.1. Thus following equation (3.73), we can write the equation representing the oscillation condition for a 'gain plus index' corrugated DFB laser as

$$\begin{aligned}
&[-\gamma r_1 e^{-2\jmath\beta_D l_1}\cosh[\gamma l_1] - \{r_1 e^{-\jmath 2\beta_D l_1}[-\jmath\Delta\beta + \frac{1}{2}(\overline{g} - \alpha)] - \jmath\kappa e^{\jmath\phi_1}\}\sinh[\gamma l_1]] \\
&\times[-\gamma r_2 e^{-2\jmath\beta_D l_2}\cosh[\gamma l_2] - \{r_2 e^{-\jmath 2\beta_D l_2}[-\jmath\Delta\beta + \frac{1}{2}(\overline{g} - \alpha)] - \jmath\kappa e^{\jmath\phi_2}\}\sinh[\gamma l_2]] \\
&= [-\gamma\cosh[\gamma l_1] + \{-\jmath\kappa\, r_1 e^{-2\jmath\beta_D l_1 - \jmath\phi_1} + [-\jmath\Delta\beta + \frac{1}{2}(\overline{g} - \alpha)]\}\sinh[\gamma l_1]] \\
&\times[-\gamma\cosh[\gamma l_2] + \{-\jmath\kappa\, r_2 e^{-\jmath 2\beta_D l_2 - \jmath\phi_2} + [-\jmath\Delta\beta + \frac{1}{2}(\overline{g} - \alpha)]\}\sinh[\gamma l_2]]
\end{aligned} \tag{5.24}$$

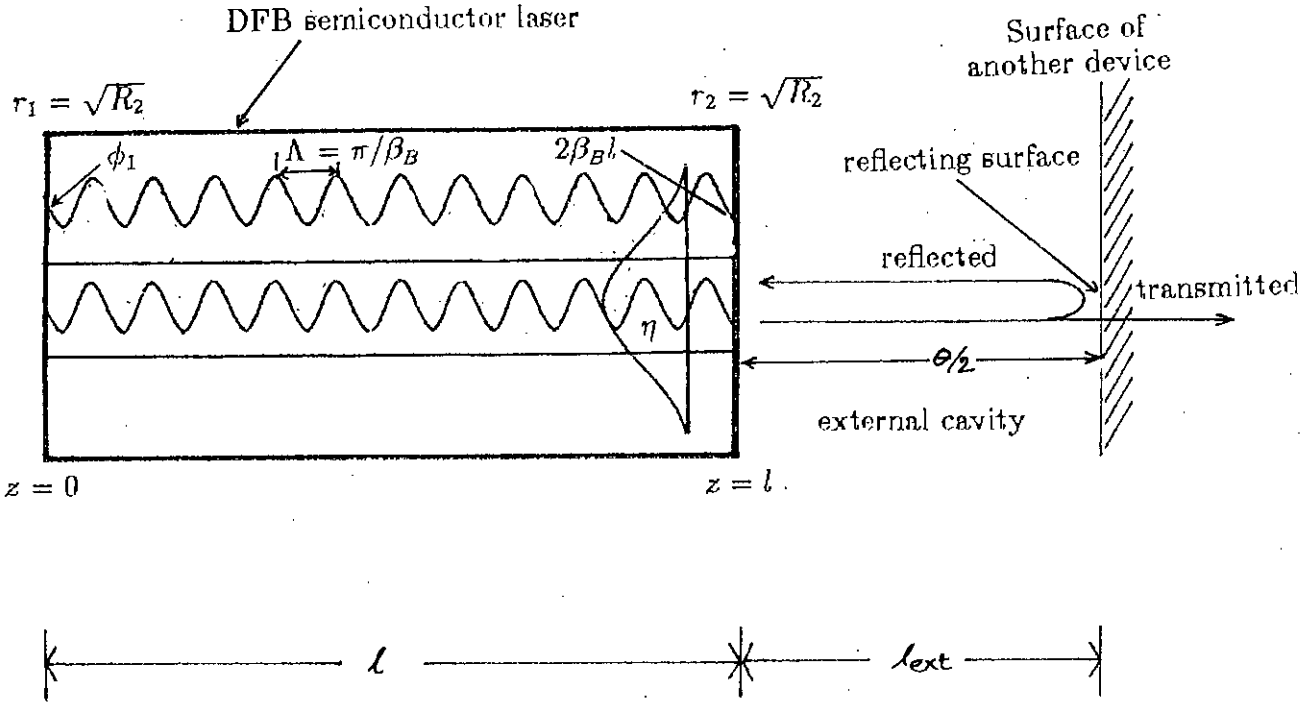

Figure 5.3: A 'gain plus index' DFB semiconductor laser with laser light in presence of external reflection. Here, $\theta = 2k_0 l_{ext}$.

where,

$$\kappa = \kappa_n + j\kappa_g e^{-j\psi} \tag{5.25}$$

Let us now consider the 'gain plus index' laser of figure 5.2 extending from z=0 to l. For this model we take $\phi_2 = \phi$, $l_2 = l$, $l_1 = 0$ in the above equation. The left facet has now moved to $z = 0$, so r_1 will remain in the equation. With these values the equation representing the oscillation condition of a 'gain plus index' corrugated DFB semiconductor laser becomes

$$\begin{aligned} -\gamma r_1[-\gamma r_2 e^{-j2\beta_D l}\cosh(\gamma l) - \{r_2 e^{-j2\beta_D l}[-j\Delta\beta + \frac{1}{2}(\overline{g} - \alpha)] - j\kappa e^{j\phi}\}\sinh(\gamma l)] \\ = -\gamma[-\gamma\cosh(\gamma l) + \{-j\kappa r_2 e^{-j2\beta_D l - j\phi} + [-j\Delta\beta + \frac{1}{2}(\overline{g} - \alpha)]\}\sinh(\gamma l)] \end{aligned} \tag{5.26}$$

After simplification this equation becomes

$$\begin{aligned} \gamma^2 r_1 r_2 e^{-j2\beta_D l}\cosh(\gamma l) + \gamma r_1 r_2 e^{-j2\beta_D l}[-j\Delta\beta + \frac{1}{2}(\overline{g} - \alpha)]\sinh(\gamma l) - j\gamma r_1\kappa e^{j\phi}\sinh(\gamma l) \\ = \gamma^2\cosh(\gamma l) + j\gamma\kappa r_2 e^{-j2\beta_s l - j\phi}\sinh(\gamma l) - \gamma[-j\Delta\beta + \frac{1}{2}(\overline{g} - \alpha)]\sinh(\gamma l) \end{aligned} \tag{5.27}$$

After further simplification we get

$$\begin{aligned} (1 - r_1 r_2 e^{-j2\beta_D l})\gamma^2\cosh(\gamma l) - \gamma[-j\Delta\beta + \frac{1}{2}(\overline{g} - \alpha)](1 + r_1 r_2 e^{-j2\beta_D l})\sinh(\gamma l) \\ + j\gamma[\kappa r_2 e^{-j2\beta_D l - j\phi} + \kappa r_1 e^{j\phi}]\sinh(\gamma l) = 0 \end{aligned} \tag{5.28}$$

For a 'gain plus index' corrugated DFB semiconductor laser κ in the above equation is to be replaced by $\kappa_n + j\kappa_g e^{-j\psi}$. With this change equation (5.26) becomes

$$\begin{aligned} (1 - r_1 r_2 e^{-j2\beta_D l})\gamma\cosh(\gamma l) - [\frac{1}{2}(\overline{g} - \alpha) - j\Delta\beta](1 + r_1 r_2 e^{-j2\beta_D l})\sinh(\gamma l) \\ + j\{(\kappa_n + j\kappa_g e^{j\psi})r_1 e^{j\phi} + (\kappa_n + j\kappa_g e^{j\psi})r_2 e^{-j2\beta_D l - j\phi}\}\sinh(\gamma l) = 0 \end{aligned} \tag{5.29}$$

Due to reflection from the surface of another device entering into the laser cavity, as shown in figure 5.3 r_2 is to be replaced by r_2' in the above equation so that

$$r_2' = \sqrt{R_2} + (1 - R_2)\sqrt{\eta}\Gamma e^{-j\theta} \tag{5.30}$$

$$\tag{5.31}$$

where,

$$\sqrt{R_2} = r_2 \tag{5.32}$$

5.4 Summary

The generalized wave equations for a 'gain plus index' coupled DFB semiconductor laser have been deduced. Using this similarity between these wave equations and the wave equation of chapter 3 the equation representing the oscillating condition of a 'gain plus index' corrugated DFB laser has been obtained for a laser cavity extending from $z = -l_1$ to l_2. This equation has been modified for a simplified model of the DFB laser extending from $z = 0$ to l assuming the reflection of r_1 at the left facet and r_2 at the right facet and a power reflection coefficient of Γ from the external surface.

CHAPTER 6

Numerical solutions of the general equation representing oscillation in a DFB laser

6.1 Introduction

In this chapter, a computer method is presented for obtaining the solutions of the general complex equation representing the oscillation in a DFB semiconductor laser. The computer programme can be used for (i) pure index coupled (ii) for pure gain coupled and (iii) for 'gain plus index' coupled DFB semiconductor laser. Numerical solutions for various values of parameters without external feedback are presented in section 6.3. Considering external feedback solutions for critical feedback are presented in section 6.4 and the effect of right facet reflection on critical feedback are discussed in section 6.5.

6.2 A computer method for solving the general equation representing the oscillation

In chapter 3, an equation has been developed which represents the oscillation condition of a pure index corrugated DFB semiconductor laser. In this section, the effect of external feedback has not been considered. This equation has been developed for a generalized DFB semiconductor laser model extending from $z = -l_1$ to l_2 and having reflection coefficient r_1 at the left facet and r_2 at the right facet. In chapter 4, the effect of external feedback is included in this equation. Besides this, a simplified model of a pure index coupled DFB semiconductor laser extended from $z = 0$ to l having a reflection coefficient r_1 at the left facet and r_2 at the right facet is considered in this chapter. In chapter 5, the presence of mixed type of coupling termed as 'gain plus index' coupling in a DFB semiconductor laser has

been considered. It now appears that the equation for 'gain plus index' coupled DFB semiconductor laser i.e., equation (5.24) can be treated as a general equation. From this equation (equation 5.24) one can obtain the equation (i) for pure index coupled laser, (ii) for pure gain coupled laser and (iii) for 'gain plus index' coupled laser. For computation purpose it is necessary to use equation (5.25) and (5.30) along with equation (5.24).

It may be noted that this equation is a complex one containing both real and imaginary terms. After replacing r_2 of equation (5.24) by the expression of r_2' of equation (5.30) the resulting equation is still a complex equation. This equation can be split into (i) an equation containing real terms and (ii) another equation containing imaginary terms. In order to get total solutions we have to get solutions of the real equation and also the solutions of the imaginary equation within a specific range of both +ve and -ve $\Delta\beta$ values. The two solutions will then be plotted on the same graph. The intersections of the two curves will give us the final solutions. This is demonstrated in figure 6.1.

The solutions of the real equation and the imaginary equations are obtained by iterative interval halving method of polynomial solution. A computer program has been developed for this purpose using Quick Basic in a personal computer. The flowchart of the program is presented in figure 6.2. In this program, arrangements have been made to obtain graphical plot of the solution while the computation process goes on. This enables us to look into the plots while the computation process is on. As a result it is possible to interrupt the computation and start a new cycle if it is found that the input parameters are to be changed. Such a process of computing and plotting simultaneously has been found to be essential for this case. A listing of the computer programme is presented in Appendix A. For obtaining the solutions of the complex equation representing the oscillation condition (equation 5.24) we provide input values for a number of parameters and then specify the +ve and -ve ranges of $\Delta\beta$ values. At the same time it is necessary to limit the +ve range of $(\overline{g}_{th} - \alpha)$ so that the computer does not waste time in obtaining solutions beyond this range. The reason for doing so is that we can not view the solutions beyond the above mentioned range because the plot window is fixed by the programme.

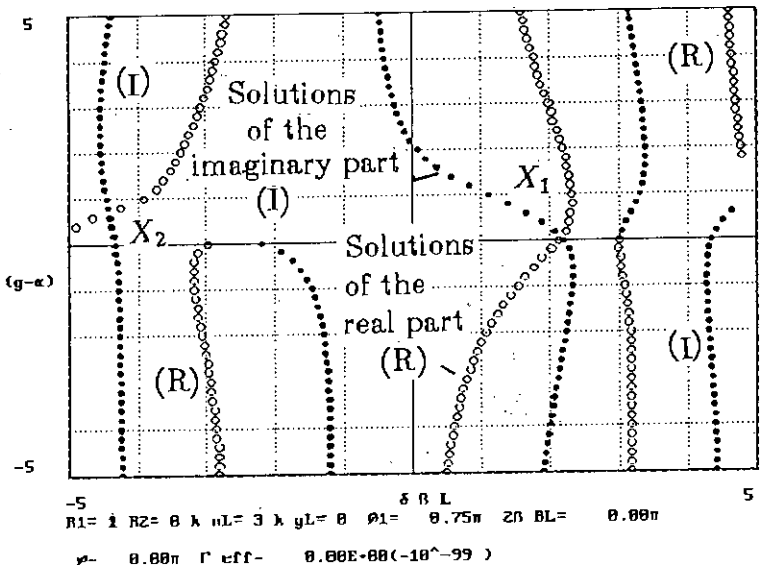

(a)

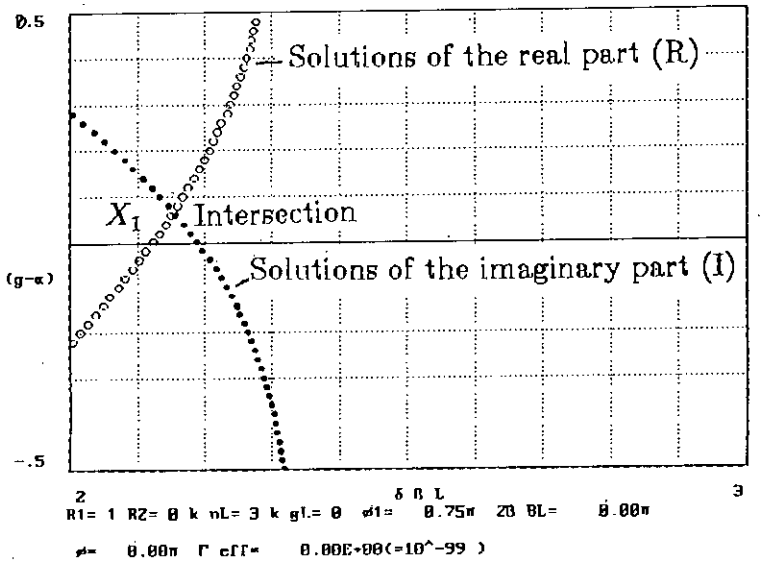

(b)

Figure 6.1: Solutions of real plot of equation (5.24) and imaginary part of equation (5.24) plotted on the same graph. (a) The crossing point X_1 and X_2 are the final solutions representing oscillation. (b) Expanded scale plots around X_1 to observe the crossing closely. The value of $(\overline{g} - \alpha)$ at X_1 is the relative threshold gain value and the $\Delta\beta_B l$ is the deviation from the Bragg frequency.

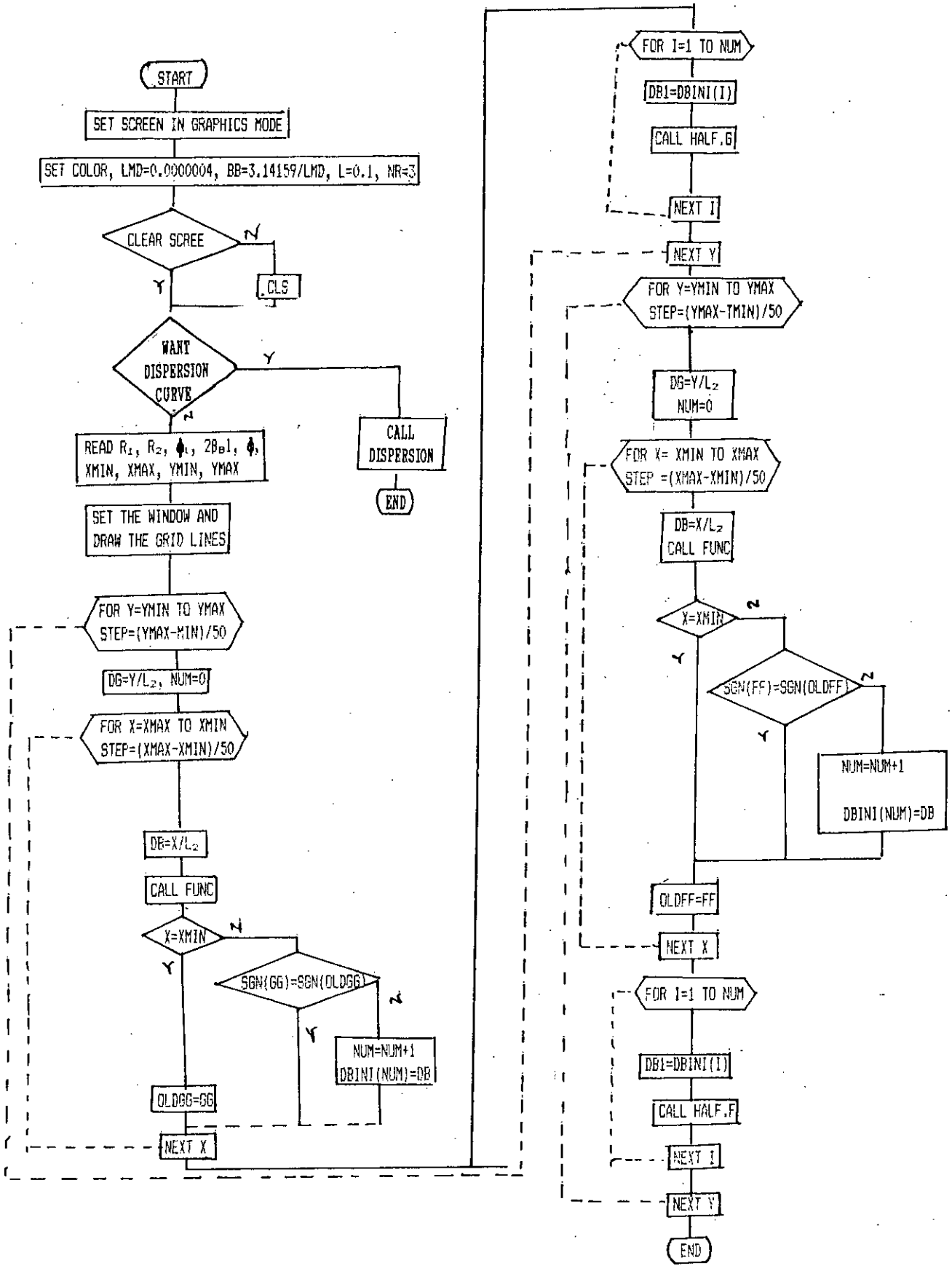

Figure 6.2(a): Flowchart of the programme for computing and plotting.

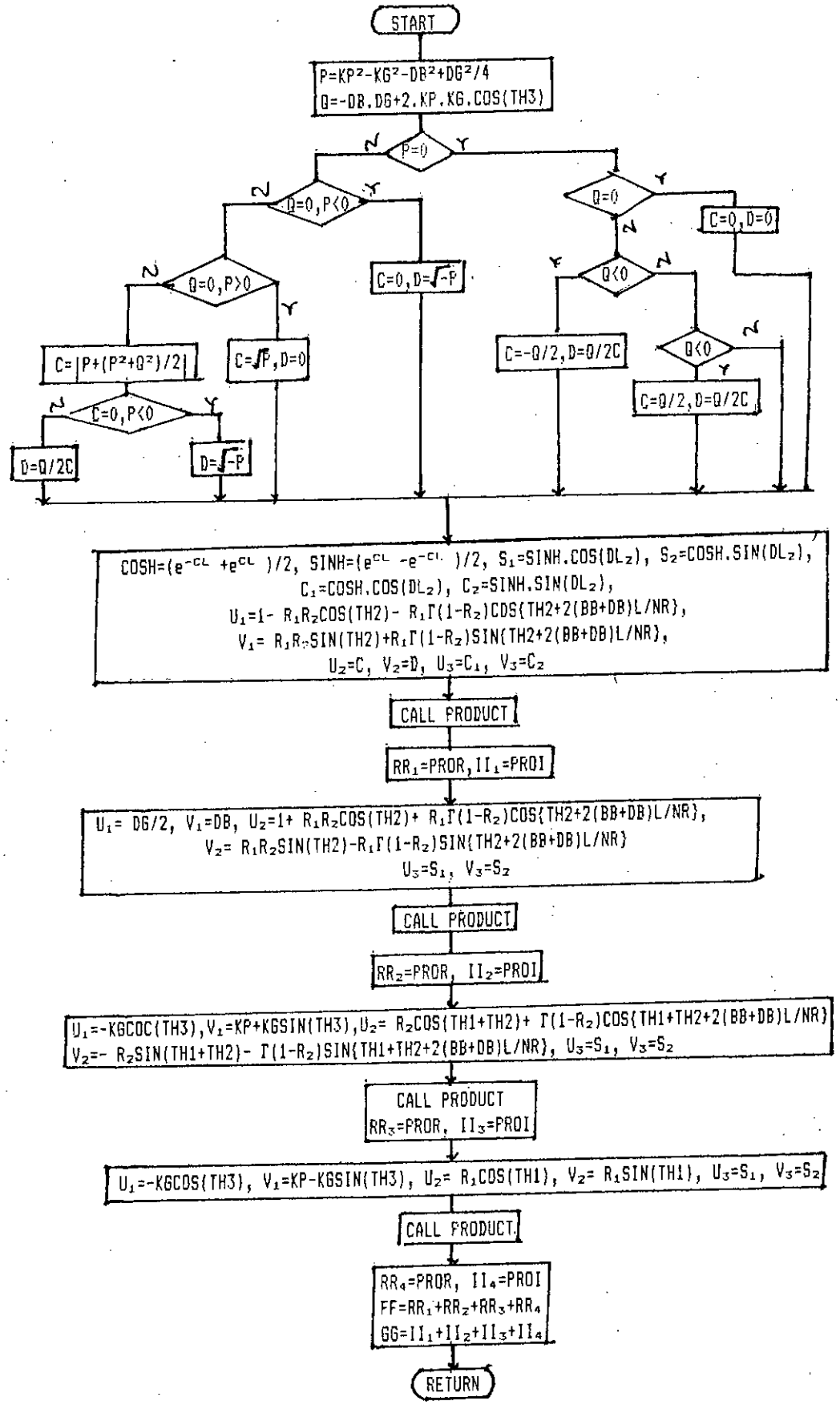

Figure 6.2(b): Flowchart of the subroutine FUNC.

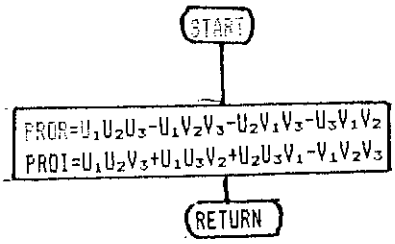

Figure 6.2(c): Flowchart of the subroutine PRODUCT.

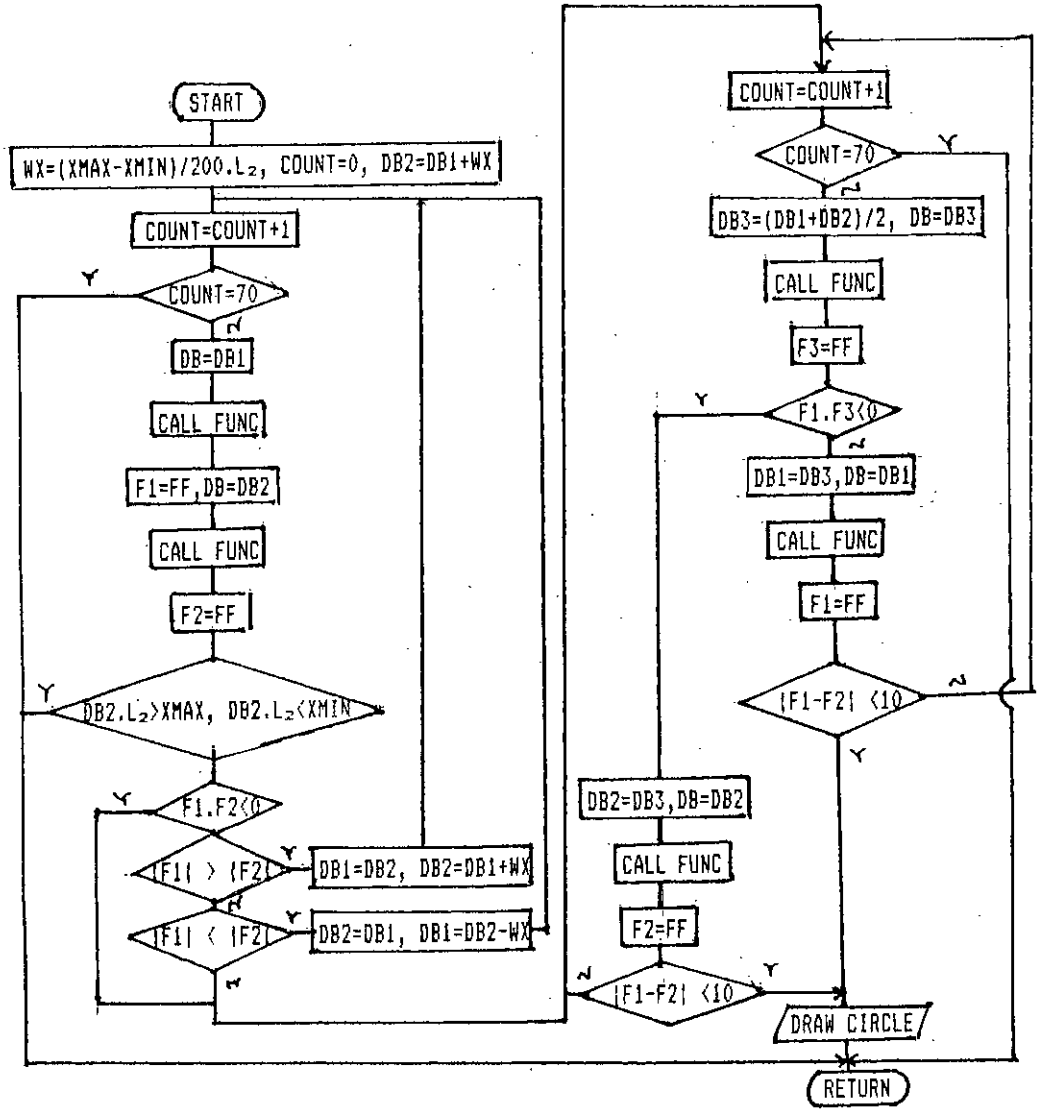

Figure 6.2(d): Flowchart of the subroutine HALF.F.

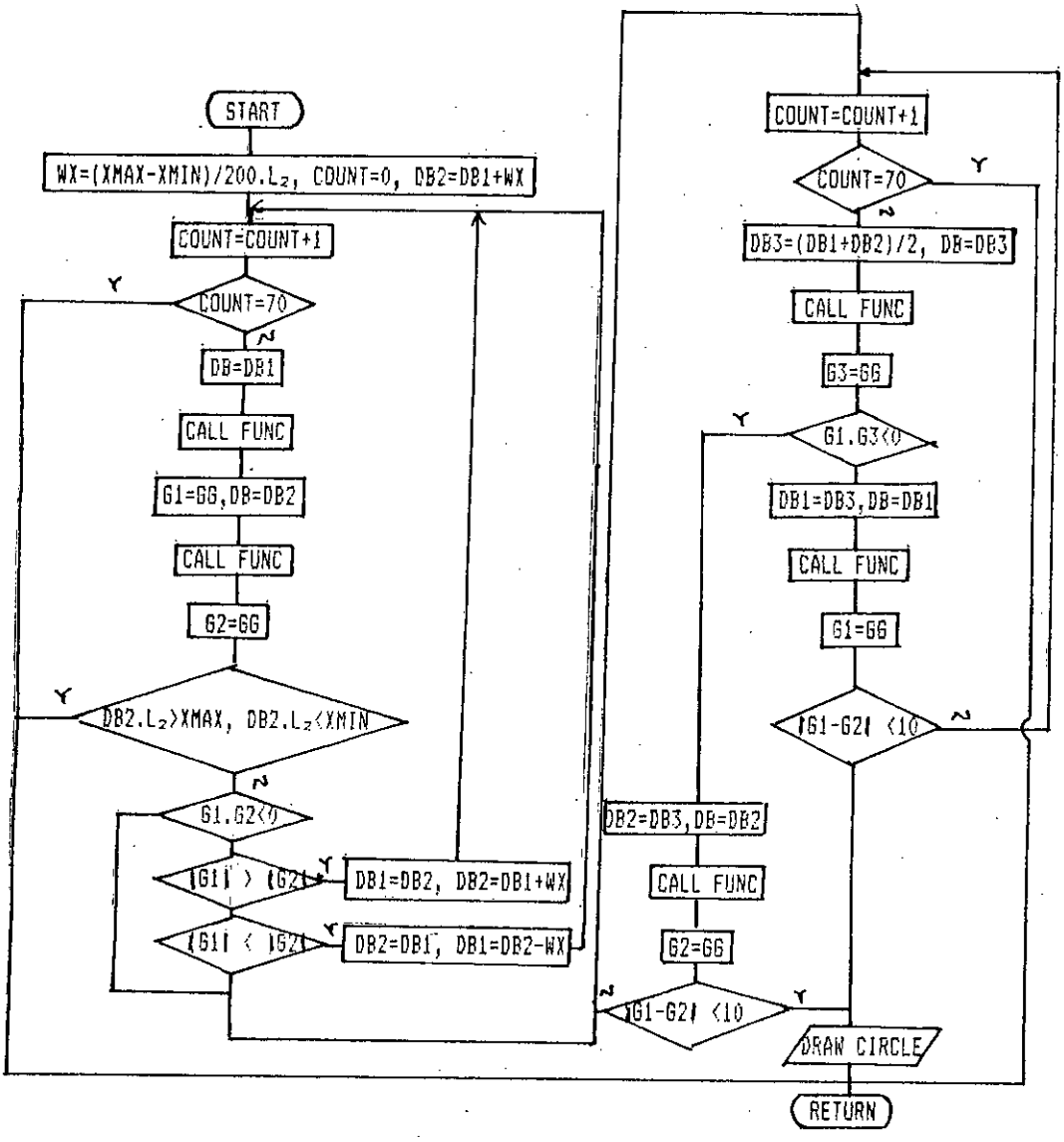

Figure 6.2(e): Flowchart of the subroutine HALF.G.

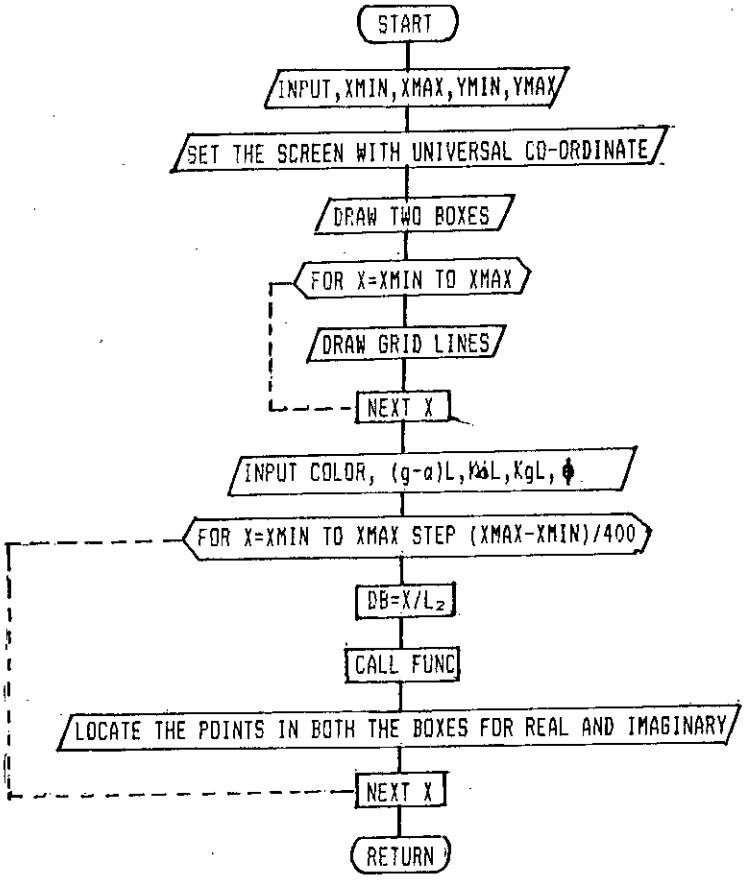

Figure 6.2(f): Flowchart of the subroutine DISPERSION.

6.3 Numerical solutions for various combinations of coupling coefficients to observe the effect of grating phase angle

For obtaining the solutions of a DFB semiconductor laser, various combinations of the values of the parameters $\kappa_n l$, $\kappa_g l$, ϕ_1, r_1, r_2, θ, $\beta_B l$, $\eta\Gamma$ are used. Actually, the programme has been prepared for providing inputs for κ_n, κ_g, $R_1 = r_1{}^2$ $R_2 = r_2{}^2$, ϕ_1 in radians, $2\beta_B l$ in even multiples of π i.e., $2p\pi$ (where, p is an integer). In this program, the value of l is taken as 0.0005 meter and the values of l_{ext} is chosen as 0.1 meter.

In order to obtain solutions of a pure index coupled DFB laser it is necessary to make $\kappa_g l$=0 and for pure gain coupling it is necessary to make $\kappa_n l$=0. For a 'gain plus index' coupling both κ_n and κ_g have finite values i.e., $\kappa_n l \neq 0$, $\kappa_g l \neq 0$. Thus we consider three cases of coupling i.e., (i) pure index coupled DFB laser, (ii) pure gain coupled DFB laser and (iii) 'gain plus index' coupled DFB laser. In this section we shall not consider the effect of external feedback.

i) Pure index coupled DFB semiconductor laser without external feedback:

For this case, we set $\kappa_g l$=0 and take four values of κ_n i.e., $\kappa_n l$=1, 2, 3, 4. For each of these cases, we take $R_1 = 1$, $R_2 = 0$, $l = 0.0005\ meter$, $2\beta_B l = 0$, $\psi = 0\pi$ and $\eta\Gamma = 0$. This means that reflection from external cavity i.e., external feedback is absent.

The solutions of the oscillation condition are then obtained using the above mentioned computer programme by varying the grating phase shift angle ϕ_1. The threshold gain values obtained from the solutions are then plotted against grating phase angle values. Thus, four curves are obtained as shown in figure 6.3. From this figure, it may be observed that for $\kappa_n l = 3$, the minimum threshold gain occurs at $\phi_1 = 0.75\pi$ radians and the maximum value occurs at $\phi_1 = 1.5\pi$ radians. The difference between the minimum and maximum gain is around 0.3 which is not large. In the same figure (figure 6.3) it is found that for $\kappa_n l = 2$ this difference is around 1.5 which is significant. For low values of threshold gain within the range

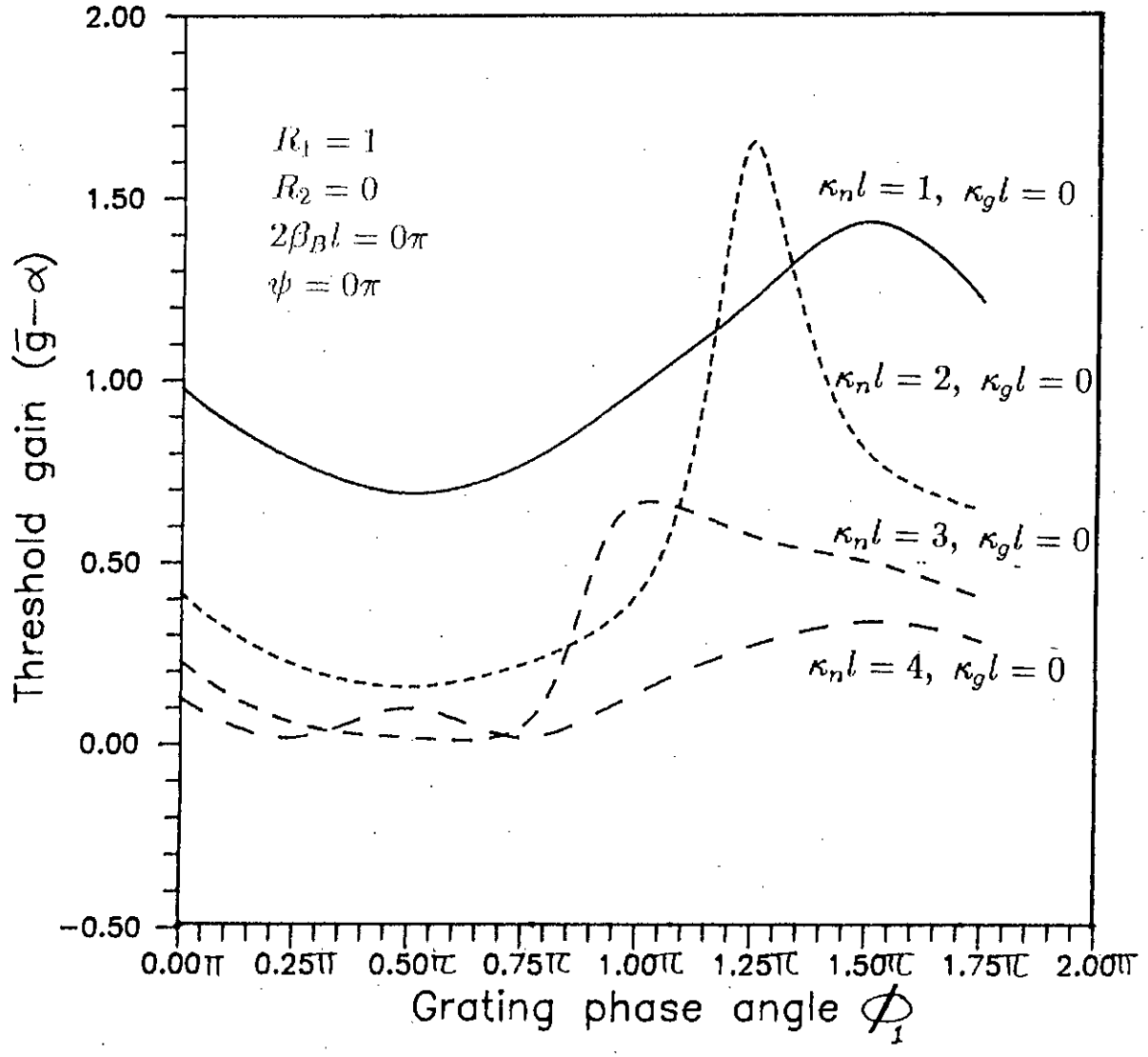

Figure 6.3: Gain vs. grating phase angle for a pure index coupled ($\kappa_n l \neq 0,\ \kappa_g l = 0$) DFB semiconductor laser for the values of index coupling coefficient $\kappa_n l$=1, 2, 3 and 4. Here $R_1 = 1,\ R_2 = 0$ and $\eta\Gamma = 0$.

of $\phi_1 = 0.2\pi$ to $\phi_1 = 0.6\pi$ $\kappa_n l$=4, 3 and 2 are good choices.

ii) Pure gain coupled DFB semiconductor laser without external feedback:

For this case, we set $\kappa_n l = 0$ and take four values of $\kappa_g l$ i.e., $\kappa_g l$=1, 2, 3, 4. For each of these cases we take $R_1 = 1$, $R_2 = 0$ and $\eta\Gamma = 0$. This means that external cavity reflection i.e., external feedback is absent.

The solutions of the oscillation condition are then obtained using the generalized computer programme by varying the phase shift angle ϕ_1. The threshold gain values obtained from the solutions are then plotted against grating phase angle values. Here also, four curves are obtained as shown in figure 6.4. It is very difficult to say which of these four coupling is the best. However, it may be observe that the curve for $\kappa_g l = 3$ has high threshold gain values for the whole range of vales of ϕ_1 between 0 to 2π. It appears that for $\phi_1 = 0\pi$ to 0.65π the curve for $\kappa_g l = 2$ shows lowest threshold gain value. Also for ϕ_1 =0.25π to 0.65π the curve for $\kappa_g l = 4$ shows low value of threshold gain but these values are higher than those of the curve for $\kappa_g l = 2$.

ii) 'Gain plus index' coupled DFB semiconductor laser without external feedback:

For a 'gain plus index' coupled DFB semiconductor laser, at first, we consider $\kappa_n l = 1$ and take four values of κ_g i.e., $\kappa_g l$=1, 2, 3, 4. For each of these four combinations we take $R_1 = 1$, $R_2 = 0$ and $\eta\Gamma = 0$. Thus, here also we do not take into account of the effect of external feedback.

As before, the solutions of the oscillation conditions are obtained using the generalized computer programme by varying the grating phase shift angle ϕ_1. For each case the threshold gain values are plotted against grating phase angle values. The curves obtained in this way are shown in figure 6.5. The curves indicate that the combination of $\kappa_n l = 1$ and $\kappa_g l = 3$ provides minimum threshold gain values over the range of $\phi_1 = 0.1\pi$ to 2π.

Next, we assume $\kappa_g l = 1$ and take four values of κ_n i.e., $\kappa_n l$ =1, 2, 3 and 4. For these cases the other parameter values are chosen as before and the effect of external

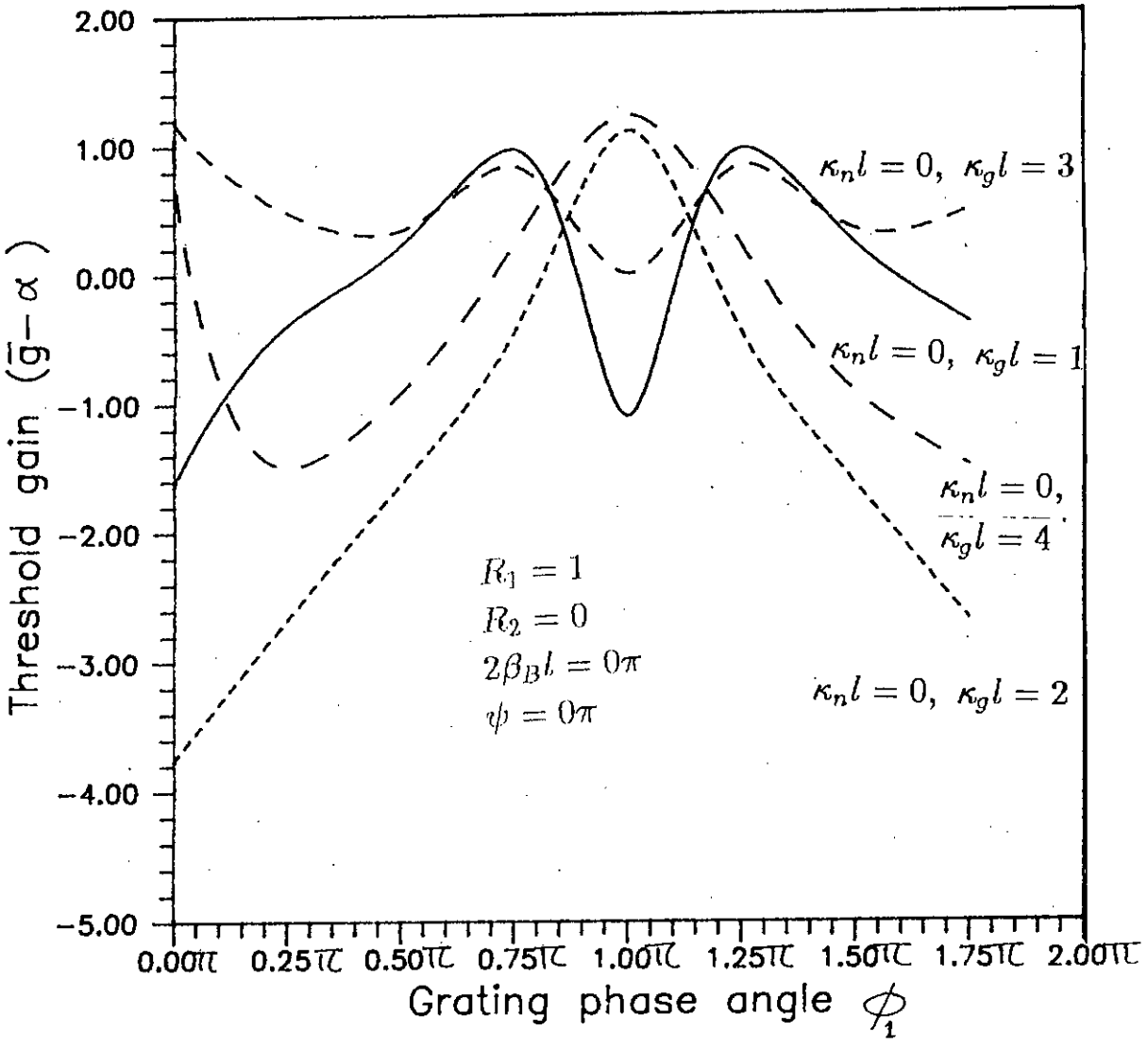

Figure 6.4: Gain vs. grating phase angle for a pure gain coupled ($\kappa_n l = 0,\ \kappa_g l \neq 0$) DFB semiconductor laser for gain coupling coefficient. Values of $\kappa_g l$=1, 2, 3 and 4. Here $R_1 = 1,\ R_2 = 0$ and $\eta\Gamma = 0$.

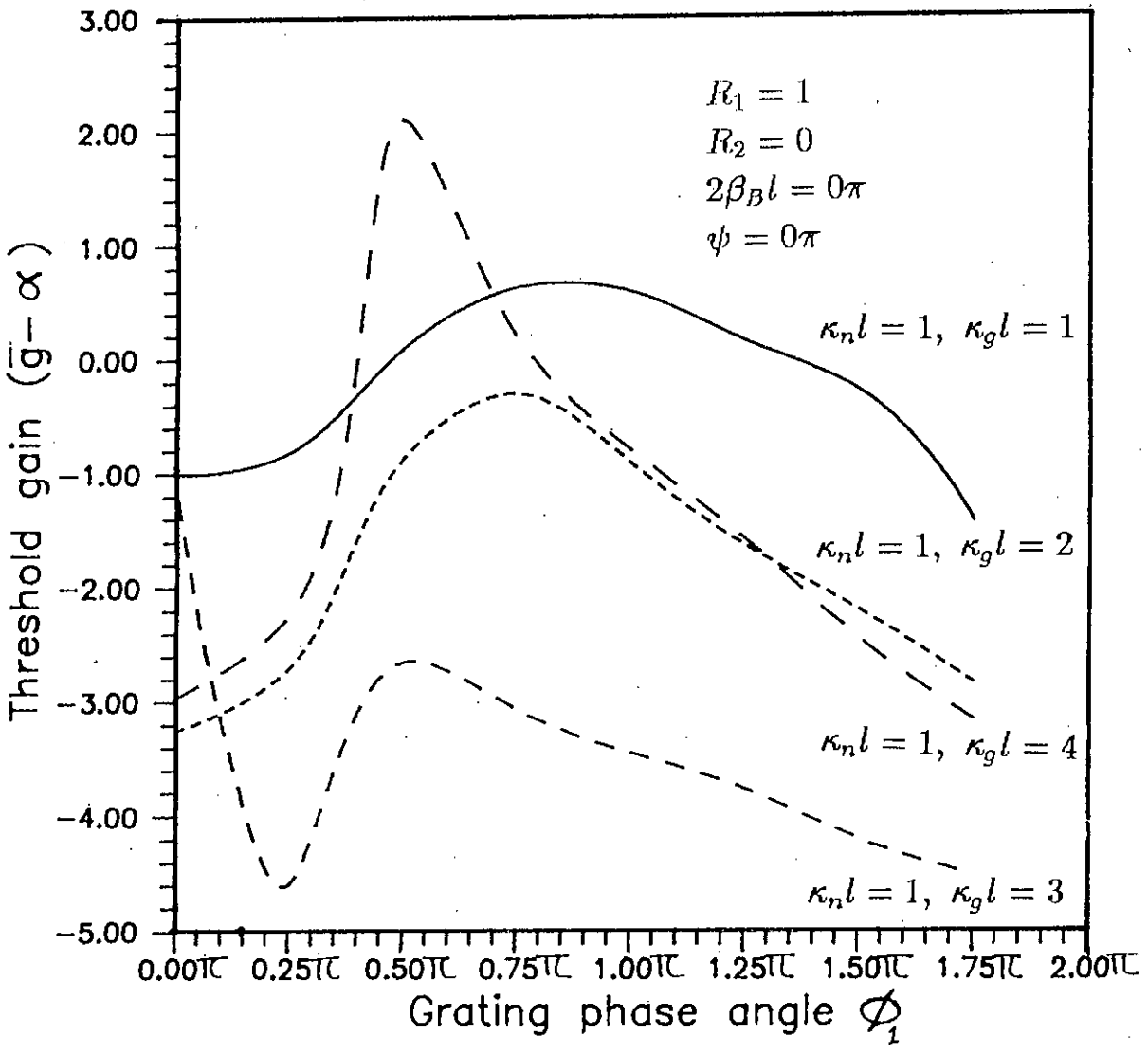

Figure 6.5: Plots of threshold gain vs. grating phase angle for 'gain plus index' coupled ($\kappa_n l \neq 0,\ \kappa_g l \neq 0$) DFB semiconductor laser for index coupling coefficient $\kappa_n l$=1 and gain coupling coefficient of $\kappa_g l$=1, 2, 3 and 4. Here $R_1 = 1$, $R_2 = 0$ and $\eta\Gamma = 0$.

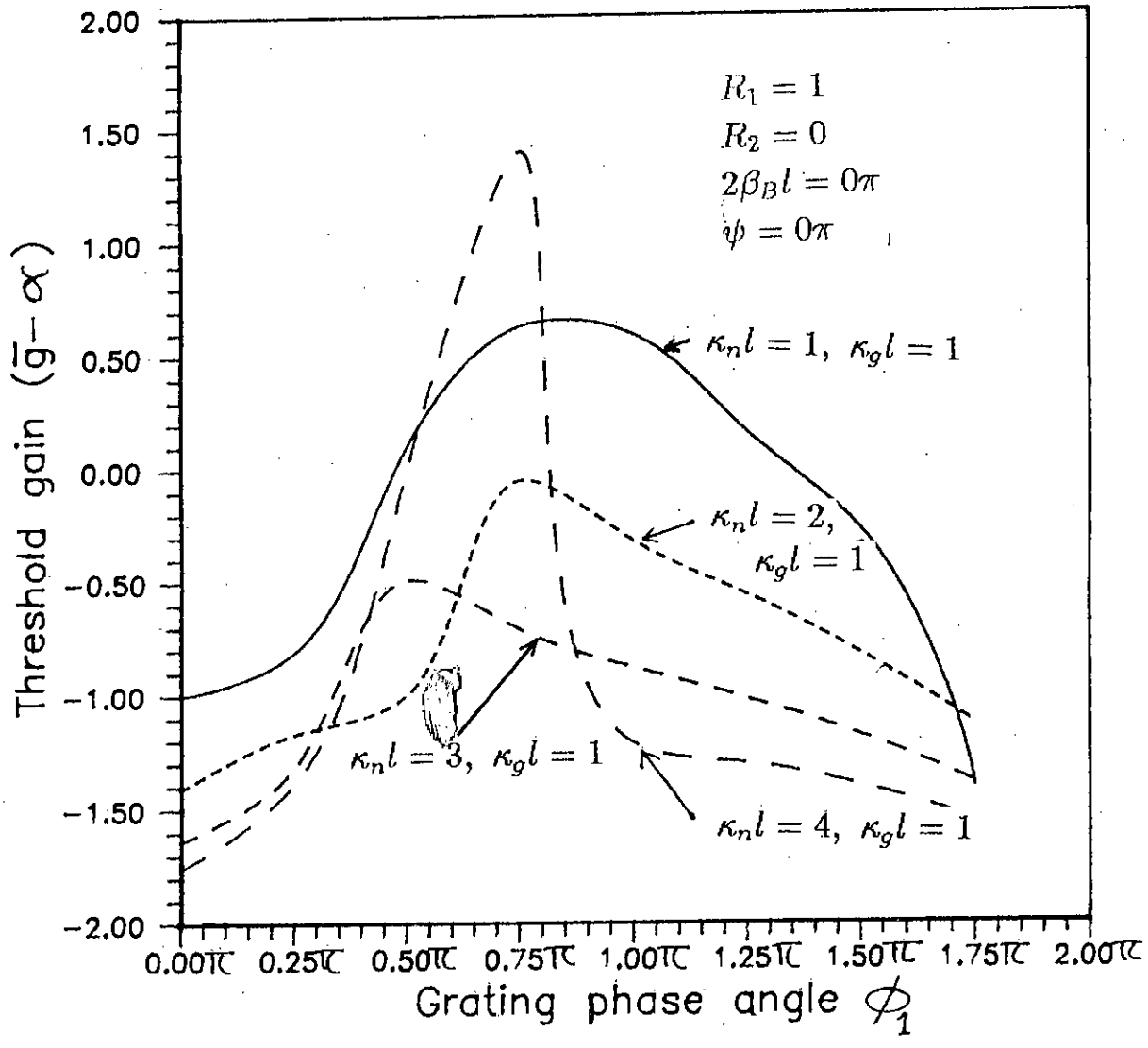

Figure 6.6: Plots of threshold gain vs. grating phase angle for 'gain plus index' coupled ($\kappa_n l \neq 0,\ \kappa_g l \neq 0$) DFB semiconductor laser for gain coupling coefficient $\kappa_g l$=1 and index coupling coefficient of $\kappa_g l$=1, 2, 3 and 4. Here $R_1 = 1$, $R_2 = 0$ and $\eta\Gamma = 0$.

feedback is neglected. Solutions of the oscillation conditions are then obtained for the four cases. The resulting four curves are shown in figure 6.6. From these curves it may be observed that the average value of the threshold gain over the range of $\phi_1 = 0\pi$ to 2π is lowest for $\kappa_n l = 4$ and $\kappa_g l = 1$ at $\phi_1 = 0\pi$.

6.4 Numerical solutions considering external feedback

It is now considered that external feedback is present. Due to the presence of external feedback, external cavity modes will appear in addition to the main lasing mode. To demonstrate this let us take a particular example of pure index coupled DFB laser having $\kappa_n l$=3, $\kappa_g l$=0, R_1=1, $R_2 = 0$, $\phi_1 = 0.75\pi$, $2\beta_B l = 0\pi$ and $\psi = 0\pi$. For this case three different curves are plotted in figure 6.7 for three different values of feedback ratio (Γ_{eff}). The first one is plotted for $\Gamma_{eff} = 0.0398$. In this curve we found that the plots of the real and imaginary solutions cross each other at one point i.e., the laser has only one mode, the main mode (figure 6.7(a)). The next one is plotted for $\Gamma_{eff} = 0.0603$. In this plot we find that the plots of real and imaginary solutions cross each other at one point and they touch at a second point (figure 6.7(b)). The touching point indicates the appearance of a second lasing mode in addition to the main lasing mode. This second lasing mode is the external cavity mode. Since this mode appears when the feedback ratio has been increased from 0.0398 to 0.0603 so $\Gamma_{eff} = 0.0603$ is the critical feedback ratio (Γ_c). Next, we increase the value of Γ_{eff} to $\Gamma_{eff} = 0.1$ which is grater than the critical feedback ratio Γ_c. Plots of the solutions for this case is shown in figure 6.7(c). In this plot we find that the touching point in the previous plot now appears as crossing point i.e., the plots of the real and imaginary solutions intersect each other at two places in addition to the intersection corresponding to the main mode. The two intersections appeared as a result of increasing the feedback ratio will correspond to two external cavity modes. The mode with the lowest relative gain (0.03) is the main mode ($p - mode$) [30][33][34], the next mode with next higher gain (0.04) is the external cavity mode ($m - mode$) [30][33][34] and the mode with highest gain is the second external cavity mode ($m' - mode$) [33][34]. Following this procedure we obtain the critical feedback ratios, the values of $\Delta\beta_B l$ at which the external cavity

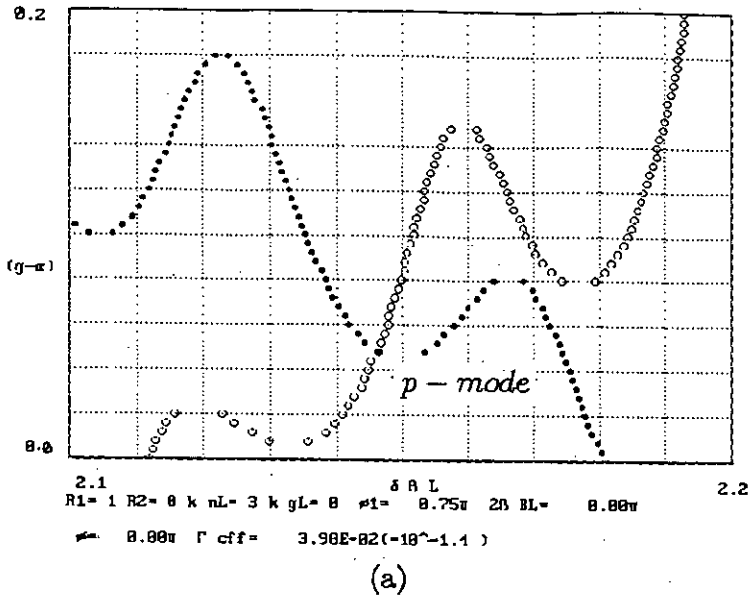

(a)

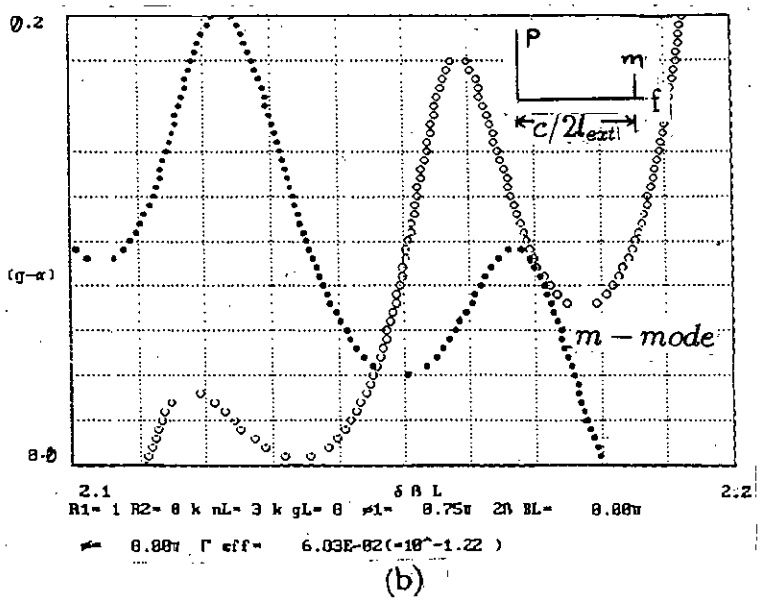

(b)

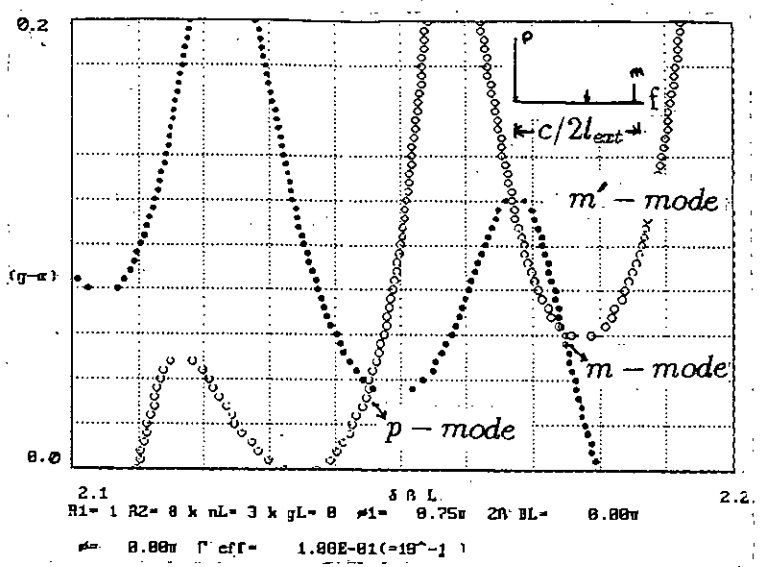

(c)

Figure 6.7: Plots of real and imaginary solutions for three values of external feedback ratio and for a particular set of parameters. (a) here, external feedback ratio Γ_{eff}=0.0396. Only the main mode (p-mode) is seen to appear. There is no external cavity mode (b) The external feedback ratio Γ_{eff} is raised to 0.0603. At this value of Γ_{eff} the external cavity mode (m-mode) is just seen to appear (c) The external feedback ratio is further increased to 0.1. At this value two external cavity modes (m-mode) and (m'-mode) are seen to appear.

modes appear and also the relative values of gains for main mode plus the external cavity modes for different combinations of parameter values.

Similar to the examples considered in the last section, here also three cases i.e., (i) pure index coupling with external feedback, (ii) pure gain coupling with external feedback and (iii) 'gain plus index coupled' with external feedback are considered.

i) Pure index coupled DFB semiconductor laser with external feedback:

Four values of pure index coupling are taken as example and computations are performed for different values of grating phase shift angle ϕ_1. The values of index coupling are $\kappa_n l$ =1, 2, 3 and 4 (with $\kappa_g l = 0$). For these cases the remaining parameter values are $R_1 = 1$, $R_2 = 0$, $l = 0.0005$ meter, and $2\beta_B l = 0\pi$, $\eta\Gamma = 0$ (i.e., no external reflection). The obtained threshold gain values for each of these cases are plotted against ϕ_1 and the plots are shown in figure 6.3. From these plots we find that the lowest gain occurs for the laser with index coupling coefficient $\kappa_n l$=3 at $\phi_1 = 0.75\pi$.

With this finding (i.e., taking $\phi_1 = 0.75\pi$ and $\kappa_n l = 3$) we continue computations to find the external cavity modes by considering the external reflection and assuming l_{ext}=0.1 meter. To do so, the effective feedback coefficient ($\eta\Gamma$) is increased gradually from 0. For this case, the values of relative gain are plotted against feedback ratio. These plots are shown in figure 6.8. From this figure we see that the critical feedback ratio for this type of laser is 0.60 i.e., $\Gamma_{eff} = 0.60$ since, within the range of $\eta\Gamma$=0 to 0.60 external cavity modes do not exist. The mode with the lowest relative gain is the main mode ($p - mode$) and the external cavity mode with the lower relative gain is the $m - mode$ and the higher relative gain is for $m' - mode$. From the plot it is found that the main mode has nearly constant gain for the range of feedback ratio values of 0.045 to 0.2. However the variation of gain at the begining is also not significantly large. After the critical feedback ratio value the gain for the $m - mode$ decreases while for the $m' - mode$ increases with the feedback ratio.

For the same parameter values of κ_n, κ_g, ϕ_1, $2\beta_B l$, ψ the deviation from the Bragg frequency (i.e., $\Delta\beta_B l$) is plotted against feedback ratio. This plot is shown in figure 6.9. In this plot it is also found that the frequency of the main mode is nearly

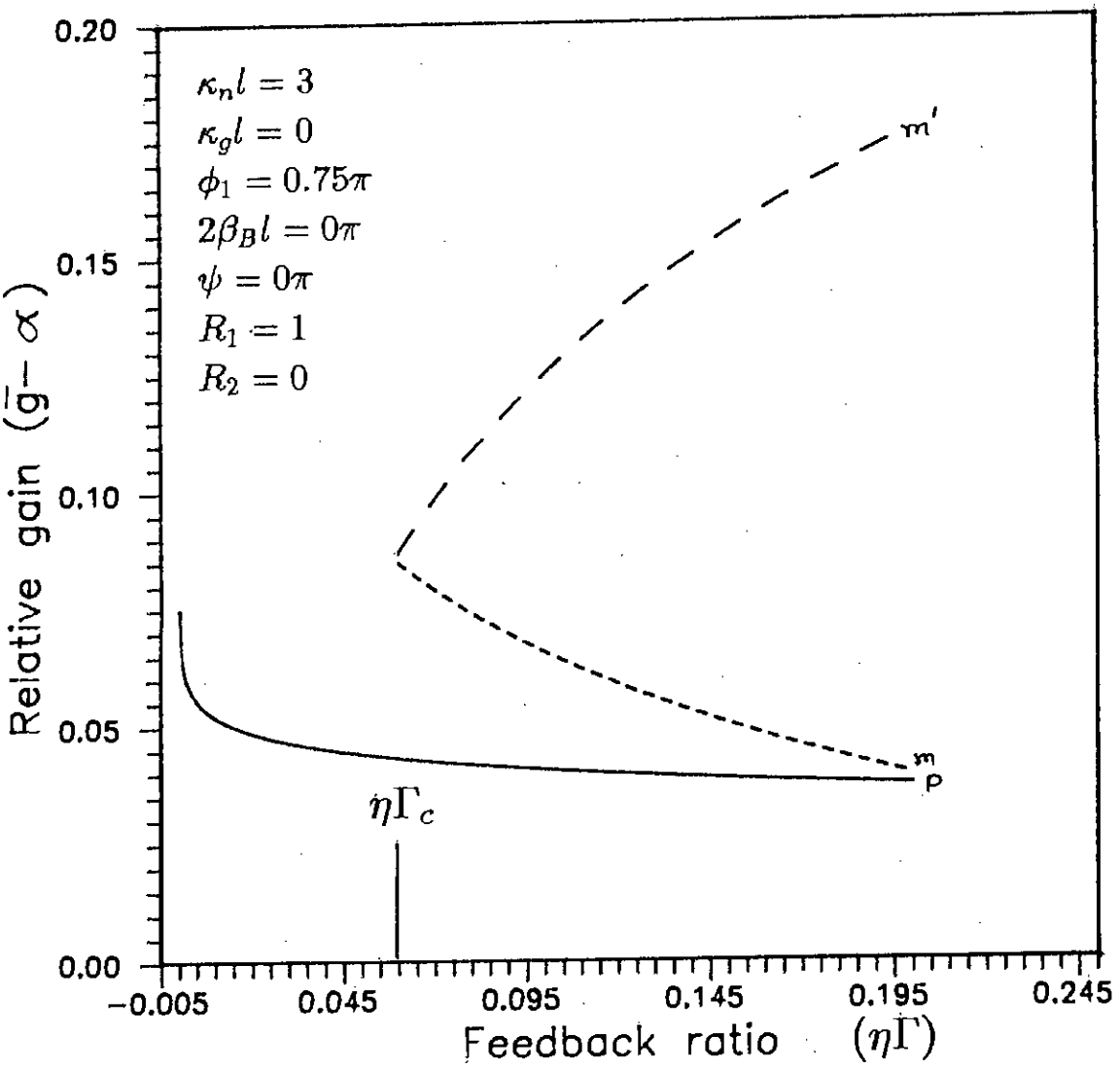

Figure 6.8: Plots of relative gain vs. feedback ratio for pure index coupled' DFB semiconductor laser indicating the point of critical feedback ratio. Here, $\kappa_n l = 3$, $\kappa_g l = 0$, $\phi_1 = 0.75\pi$, $R_1 = 1$, $R_2 = 0$, $l = 0.0005$ *meter*, $l_{ext} = 0.1$ *meter*, $\psi = 0\pi$.

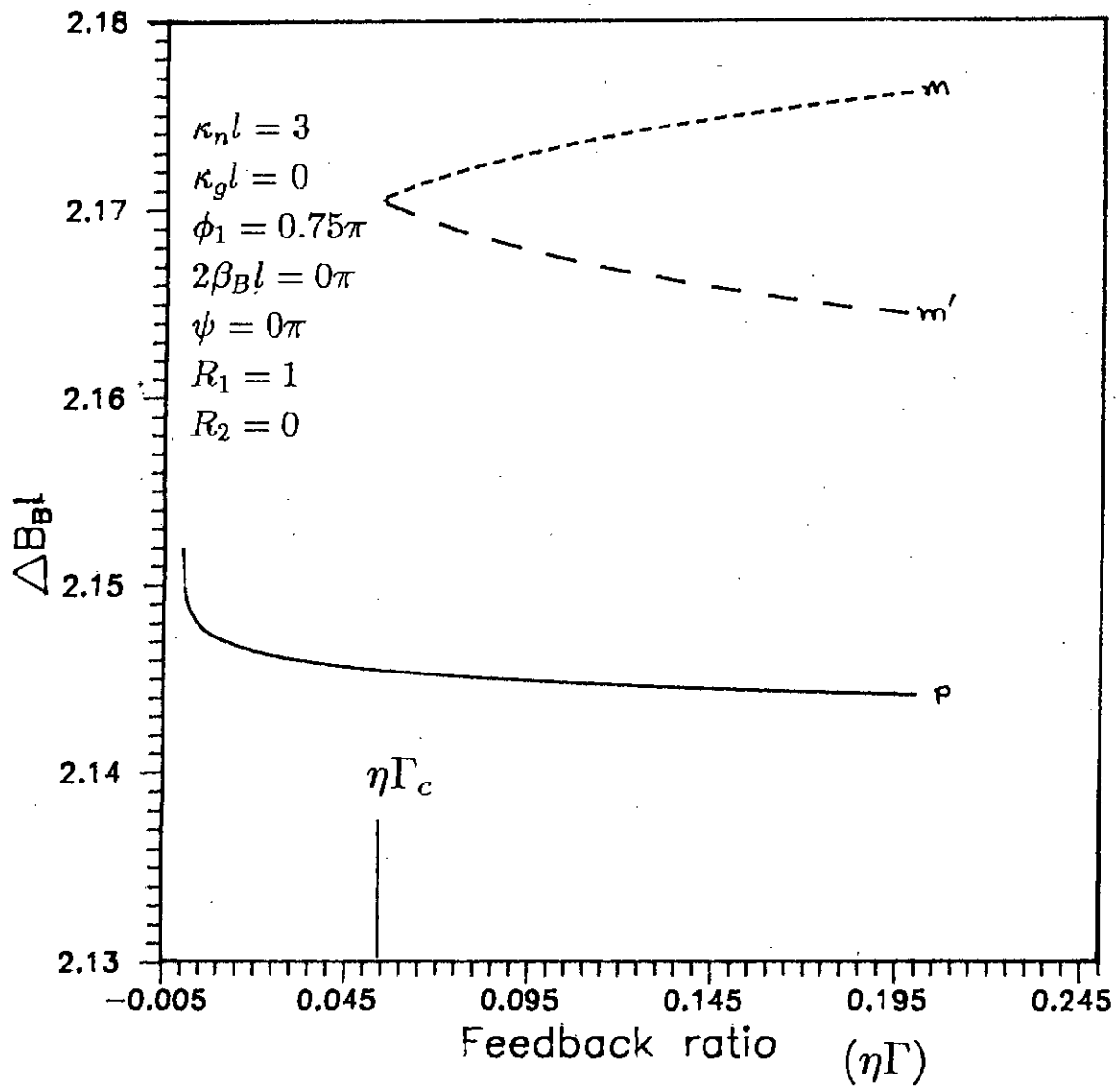

Figure 6.9: Plots of deviation from Bragg condition $\Delta\beta_B l$ vs. feedback ratio for pure index coupled DFB semiconductor laser indicating the point of critical feedback ratio. Here, $\kappa_n l = 3$, $\kappa_g l = 0$, $\phi_1 = 0.75\pi$, $R_1 = 1$, $R_2 = 0$, $l = 0.0005$ *meter*, $l_{ext} = 0.1$ *meter*, $\psi = 0\pi$.

constant over the considered values of $\eta\Gamma$ except for a very small range of values at the begining. Figure 6.9 shows that one of the external cavity mode ($m - mode$) has a values of of $\Delta\beta_B l$. Figure 6.9 shows that the ($m' - mode$) has a lower values of $\Delta\beta_B l$.

ii) Pure gain coupled DFB semiconductor laser with external feedback:

For pure gain coupled DFB semiconductor laser also four values of gain coupling are taken as example. These values are $\kappa_g l$=1, 2, 3 and 4 (with $\kappa_n l = 0$). Here also, the remaining parameter values are choosen to be $R_1 = 1$, $R_2 = 0$, $l = 0.0005\ meter$, $2\beta_B l = 0\pi, \eta\Gamma = 0$ (i.e., no external feedback) as in the pure index coupling examples. The obtained threshold gain values for each of these cases are plotted against ϕ_1 in figure 6.4. From these plots, we find that the lowest threshold gain occurs for the laser with $\kappa_n l = 0$, $\kappa_g l = 2$ at grating phase shift of $\phi_1 = 0.0\pi$. To find the critical feedback ratio and external cavity modes for this particular type of laser, taking $\kappa_n l = 0$, $\kappa_g l = 2$, $\phi_1 = 0.0\pi$, $l = 0.0005$ meter, l_{ext}=0.1 meter, $2\beta_B l = 0\pi$, $\psi = 0\pi$, $R_1 = 1$, $R_2 = 0$ the oscillation condition is solved for different values of feedback ratio. The resulting curves are shown in figure 6.10 and 6.11. In figure 6.10, the relative gain values are plotted against feedback ratio (Γ_{eff}) values. From the plots we find that the external cavity modes appear after the value of $\Gamma_{eff} = .0023$. Therefore, the critical feedback ratio for the present combination is 0.0023. The main mode ($p - mode$) has the lowest relative gain. The external cavity mode with the lower relative gain is $m - mode$ and the mode with higher gain is $m' - mode$. Figure 6.11 shows the plots of the deviation from the Bragg frequency (i.e., $\Delta\beta_B l$). against Γ_{eff}. From this figure it may be obtained that the critical feedback ratio is 0.002 (i.e., $\Gamma_c = 0.002$). The external cavity mode with lower relative gain ($m - mode$) has higher values of $\Delta\beta_B l$ and the mode with higher relative gain ($m' - mode$) has lower values of $\Delta\beta_B l$.

iii) 'Gain plus index coupled DFB semiconductor laser with external feedback:

For 'gain plus index' coupled DFB laser at first we take four combinations of index and gain coupling values. The values are (i) $\kappa_n l = 1$, $\kappa_g l = 1$, (ii) $\kappa_n l =$

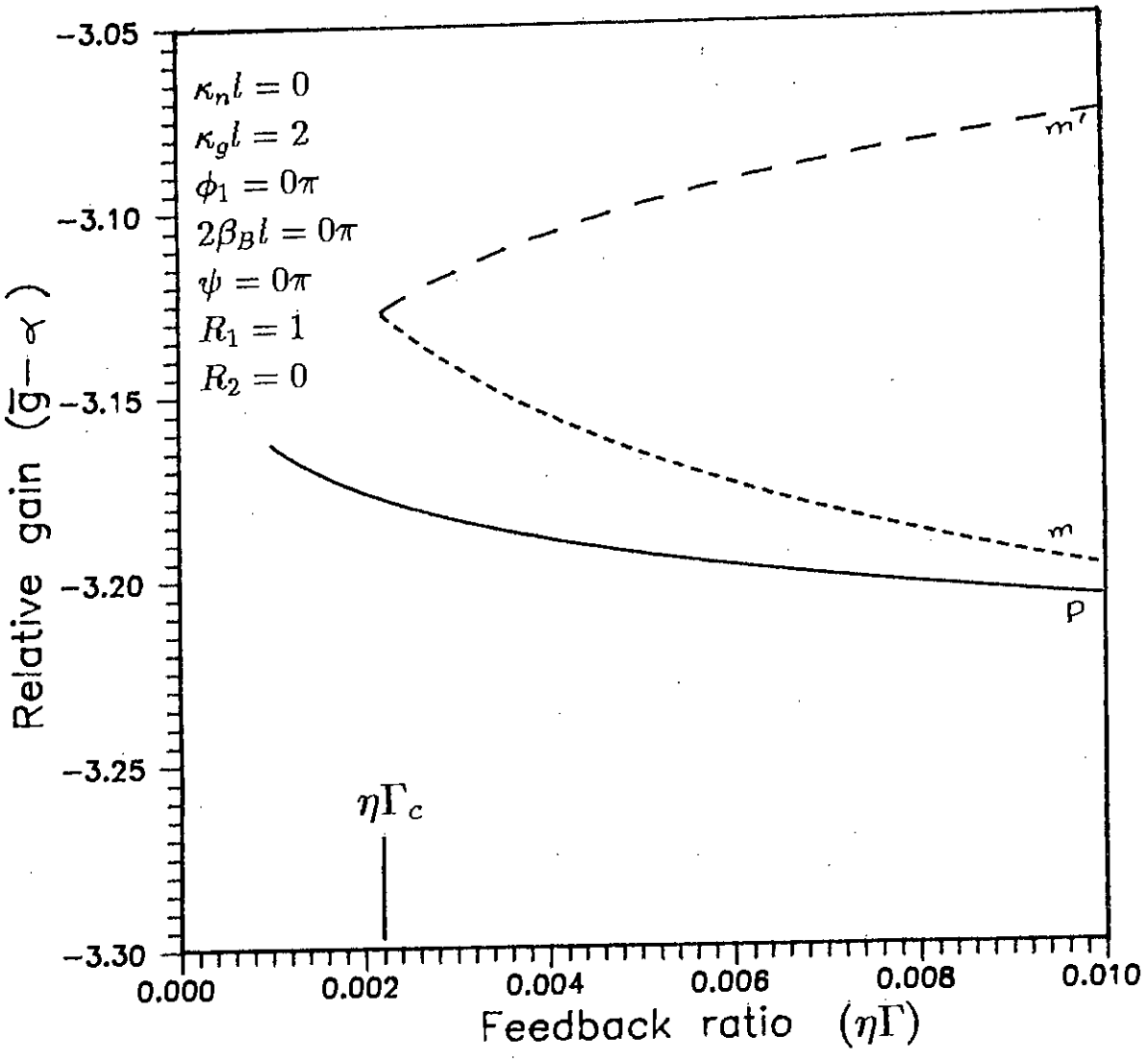

Figure 6.10: Plots of relative gain vs. feedback ratio for pure gain coupled' DFB semiconductor laser indicating the point of critical feedback ratio. Here, $\kappa_n l = 0$, $\kappa_g l = 2$, $\phi_1 = 0.0\pi\pi$, $R_1 = 1$, $R_2 = 0$, $l = 0.0005\,meter$, $l_{ext} = 0.1\,meter$, $\psi = 0\pi$.

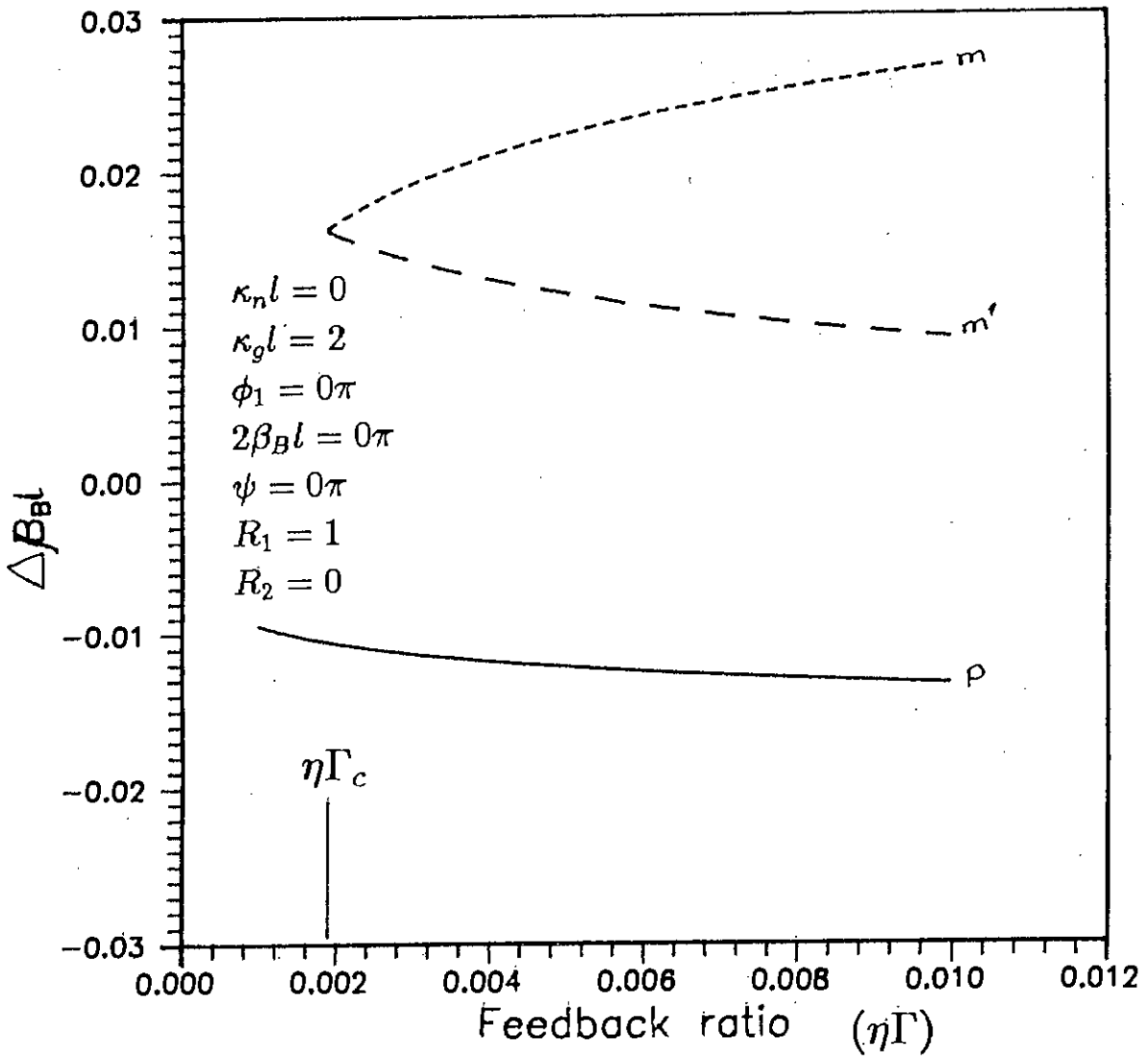

Figure 6.11: Plots of deviation from Bragg condition $\Delta\beta_B l$ vs. feedback ratio for pure gain coupled DFB semiconductor laser indicating the point of critical feedback ratio. Here, $\kappa_n l = 0$, $\kappa_g l = 2$, $\phi_1 = 0.0\pi$, $R_1 = 1$, $R_2 = 0$, $l = 0.0005$ *meter*, $l_{ext} = 0.1$ *meter*, $\psi = 0\pi$.

1, $\kappa_g l = 2$, (iii) $\kappa_n l = 1$, $\kappa_g l = 3$ and (iv) $\kappa_n l = 1$, $\kappa_g l = 4$. For these cases also, we take $R_1 = 1$, $R_2 = 0$, $l = 0.0005\ m$, $2\beta_B l = 0\pi$, $\eta\Gamma = 0$ (i.e., no external reflection). The obtained threshold gain values for each of these cases are plotted against ϕ_1 and the plots are shown in figure 6.5. From figure 6.5 we observe that the lowest gain appears for $\kappa_n l = 1$, $\kappa_g l = 3$ of coupling at $\phi_1 = 0.25\pi$.

We now take $\kappa_n l = 1$, $\kappa_g l = 3$ case with $\phi_1 = 0.25\pi$ and solve the oscillation condition for different values of effective feedback ratio $\eta\Gamma$ assuming l_{ext}=0.1 meter. The plots are presented in figure 6.12. As can be seen from figure 6.12, due to the presence of external feedback, external cavity modes ($m - mode$ and $m' - mode$) appear in addition to the main mode (p-mode) above critical feedback value. From these curves it may be observed that external cavity modes appear when the feedback ratio exceeds 0.010. Therefore, this value is the critical feedback ratio for the above mentioned parameter values of a DFB semiconductor laser. For the main mode the value of relative gain falls by a small amount of 0.65 over the range of feedback ratio of 0 to 0.025. This falls is relatively faster at the beginning of this range.

For the same parameter values curves of $\Delta\beta_B l$ against feedback ratio are also plotted in figure 6.13. Here also, the appearance of external cavity modes can be seen beyond a value of critical feedback ratio of 0.0095. It may be observed that for the main mode the value of $\Delta\beta_B l$ remains constant throughout the range of feedback ratio of 0 to 0.025.

6.5 Effect of reflection at the right facet on the performance of a DFB semiconductor laser

In this section, we will vary the power reflection coefficient R_2 at the right facet (transmitting facet) of a DFB semiconductor laser and obtain the solutions of the oscillation condition to observe the effect of R_2 on the performance of such a laser. The solutions will be obtained only for critical values of feedback ratio (i.e., Γ_c). Since a highly polished $GaAs$ semiconductor structure has a reflection coefficient as high as 0.3 [38], we will vary the reflection coefficient from zero to 0.3. We shall study the effects of variation of R_2 on three types of DFB lasers e.g., (i)

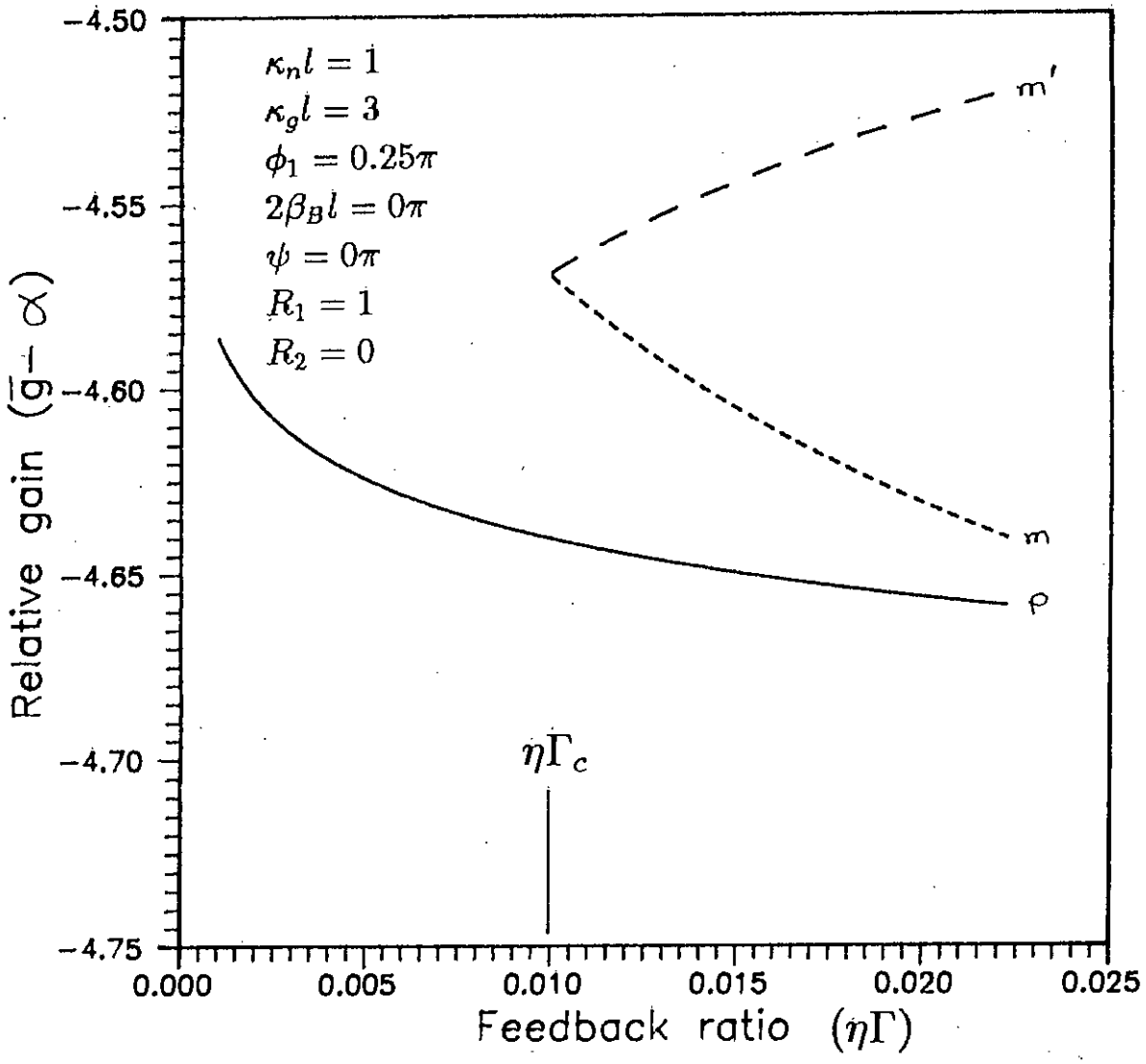

Figure 6.12: Plots of relative gain vs. feedback ratio for 'gain plus index' coupled DFB semiconductor laser indicating the point of critical feedback ratio. Here, $\kappa_n l = 1$, $\kappa_g l = 3$, $\phi_1 = 0.25\pi$, $R_1 = 1$, $R_2 = 0$, $l = 0.0005$ *meter*, $l_{ext} = 0.1$ *meter*, $\psi = 0\pi$.

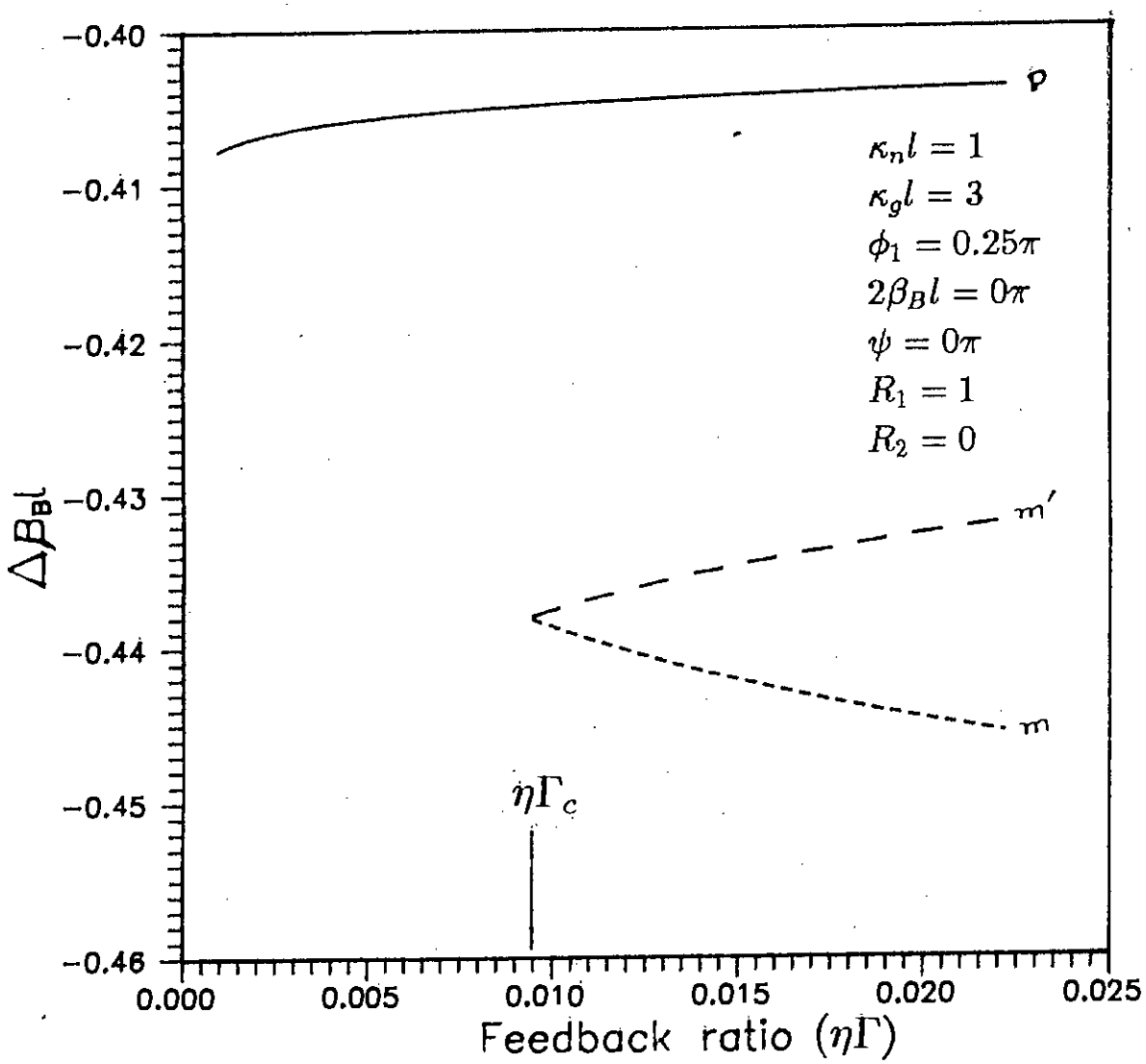

Figure 6.13: Plots of deviation from Bragg condition vs. feedback ratio for 'gain plus index' coupled DFB semiconductor laser indicating the point of critical feedback ratio. Here, $\kappa_n l = 1$, $\kappa_g l = 3$, $\phi_1 = 0.25\pi$, $R_1 = 1$, $R_2 = 0$, $l = 0.0005$ *meter*, $l_{ext} = 0.1$ *meter*, $\psi = 0\pi$.

pure index coupled DFB laser, (ii) pure gain coupled DFB laser and (iii) 'gain plus index' coupled DFB laser.

i) Pure index coupled DFB semiconductor laser with external feedback:

In the previous section the value of critical feedback is obtained from computing solutions (for a particular set of parameters values) for a pure index coupled DFB laser producing single mode oscillation at the lowest threshold gain with R_2=0. Following the same procedure we obtain the values of critical feeback ratio for values of R_2 within the range of $R_2 = 0$ to $R_2 = 0.3$ keeping other parameters unchanged. Using these results the plots of critical feedback ratio Γ_c against right facet reflection coefficient R_2 of figure 6.14 is obtained. For this plot the values of other parameters are $\kappa_n l = 3$, $\kappa_g l = 0$, $\phi_1 = 0.75\pi$, $2\beta_B l = 0\pi$, $l = 0.0005$ meter, l_{ext}=0.1 meter, $\psi = 0\pi$, $R_1 = 1$. From this figure we find that this type of laser has a stable operation for values of R_2 within the range from 0.03 to 0.1 with a slight variation of feedback ratio, after which the feedback ratio has a sharp change.

From figure 6.3 we choose another DFB laser having parameters as $\kappa_n l = 2$, $\kappa_g l = 0$ and $R_2 = 0$. For this case figure 6.3 shows a wide gap between its minimum and maximum threshold gain (without external reflection). This case shows that for this laser minimum gain occurs at $\phi_1 = 0.5\pi$. Now, taking $\kappa_n l = 2$, $\kappa_g l = 0$, $\phi_1 = 0.5\pi$, $2\beta_B l = 0\pi$, $l = 0.0005$m, $l_{ext} = 0.1$m, $\psi = 0\pi$, $R_1 = 1$ the critical feedback ratio is found for various values of reflection coefficient R_2. The plot of Γ_c against R_2 for this case is shown in figure 6.15. From this plot we see that the feedback ratio exponentially increases against the reflection coefficient. In this case, for the choosen range of R_2 (i.e., 0 to 0.3) the values of Γ_c are smaller than the example of figure 6.14.

ii) Pure gain coupled DFB semiconductor laser with external feedback:

From figure 6.4, it is seen that the pure gain coupled DFB semiconductor laser with the gain coupling coefficient $\kappa_g l = 2$ has both the lowest threshold gain and the highest gap between its minimum and maximum threshold gain. So only one type

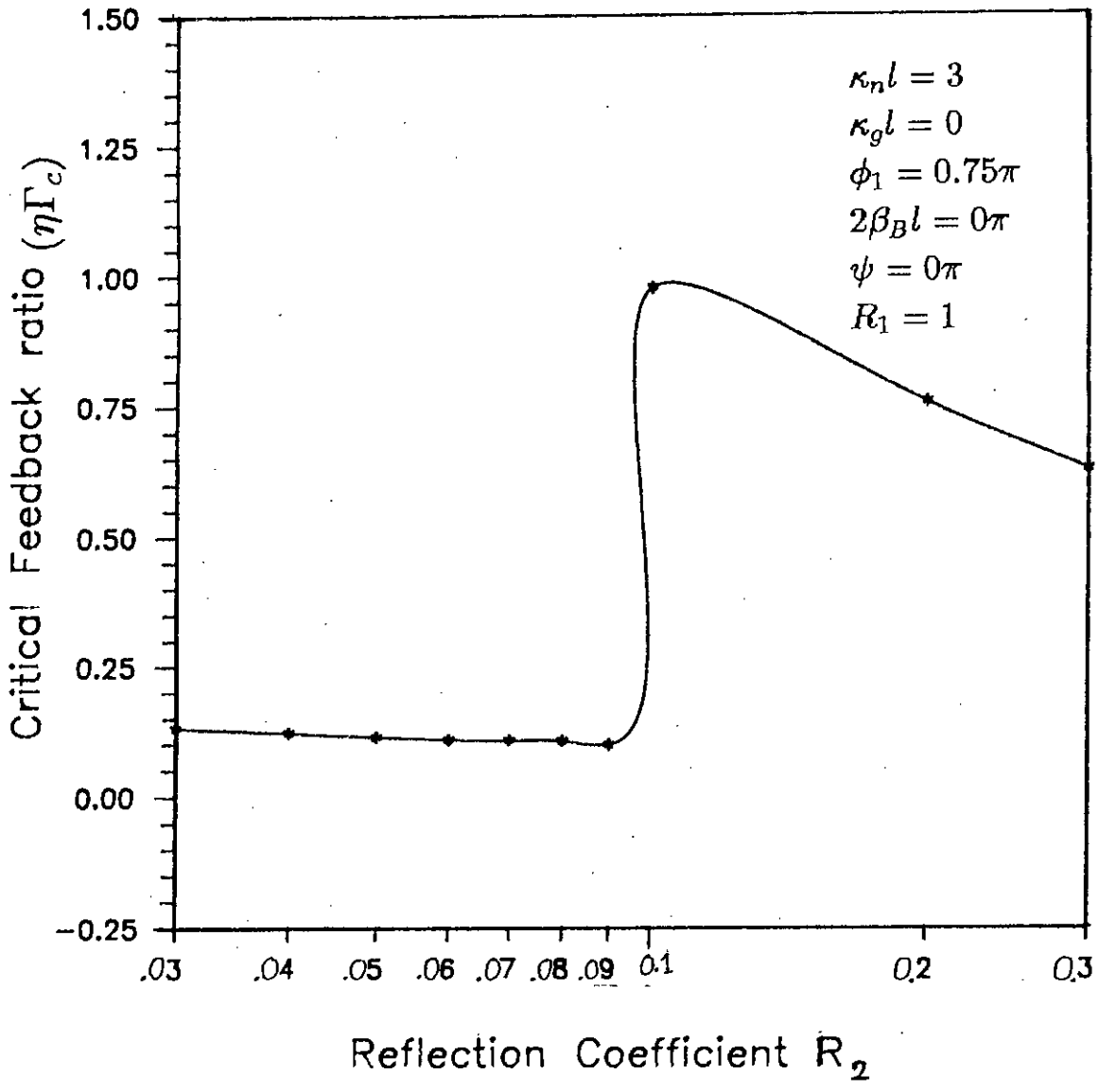

Figure 6.14: Plot of critical feedback ratio against reflection coefficient (R_2) for pure index coupled ($\kappa_n l = 3$, $\kappa_g l = 0$) DFB laser. Here, $\phi_1 = 0.75\pi$, $2\beta_B l = 0\pi$, $\psi = 0\pi$, $R_1 = 1$.

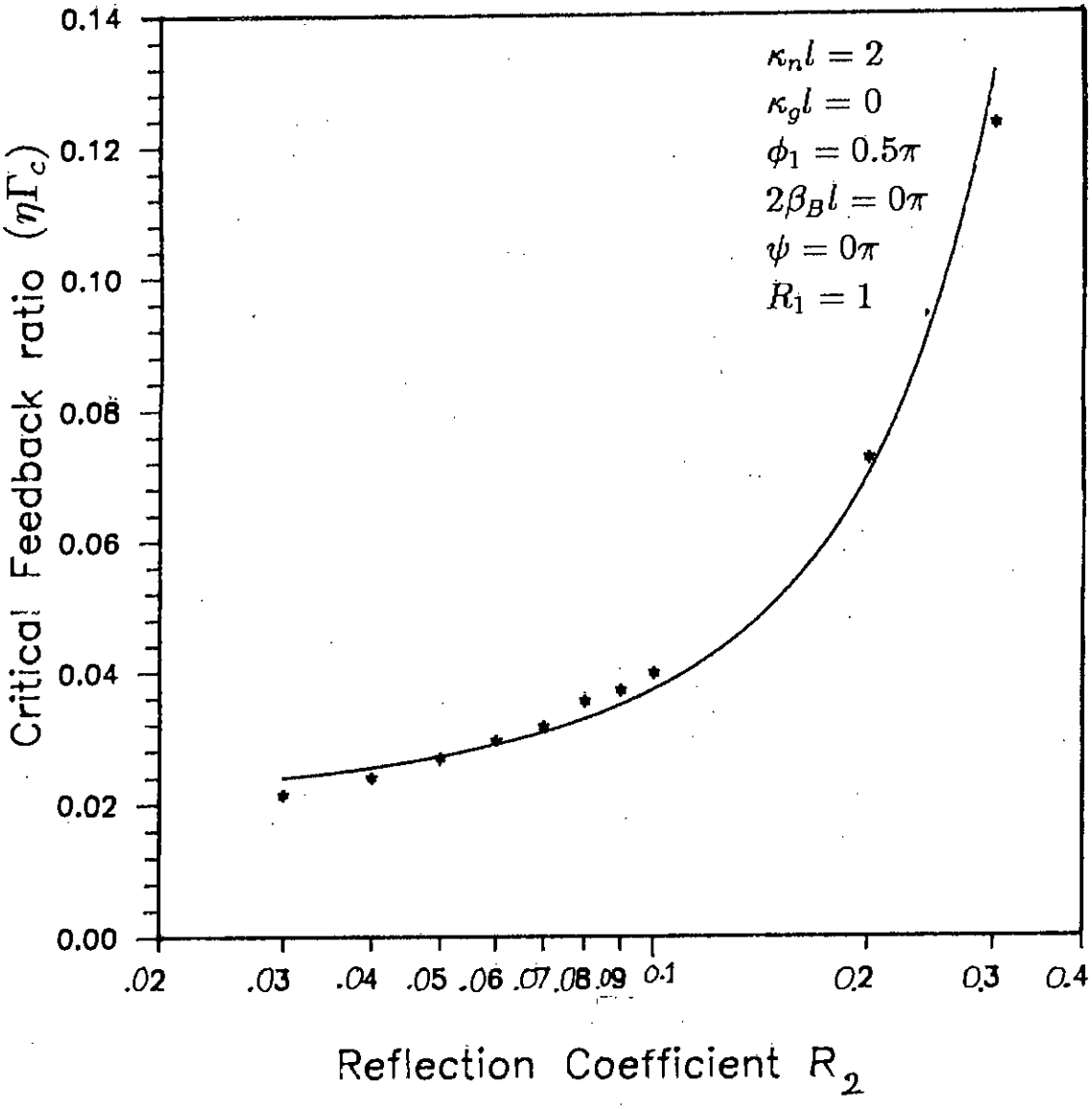

Figure 6.15: Plot of critical feedback ratio against reflection coefficien (R_2) for pure index coupled ($\kappa_n l = 2$, $\kappa_g l = 0$) DFB laser. Here, $\phi_1 = 0.5\pi$, $2\beta_B l = 0\pi$, $\psi = 0\pi$, $R_1 = 1$.

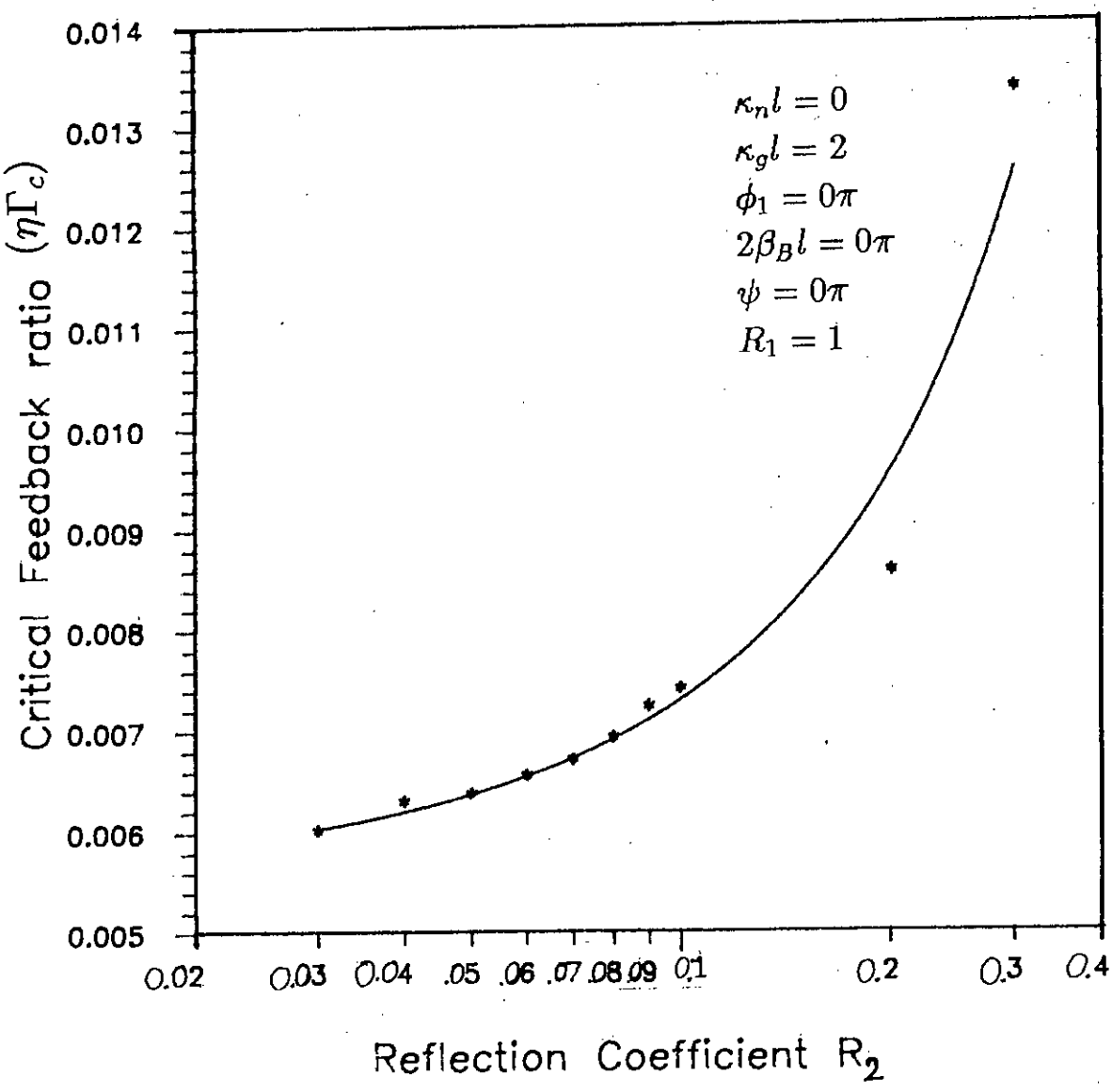

Figure 6.16: Plot of critical feedback ratio against reflection coefficient (R_2) for gain coupled ($\kappa_n l = 0$, $\kappa_g l = 2$) DFB laser. Here, $\phi_1 = 0\pi$, $2\beta_B l = 0\pi$, $\psi = 0\pi$, $R_1 = 1$.

of pure gain coupled DFB laser will be taken for observing the effect of variation of R_2 on Γ_c. Now, taking $\kappa_n l = 0$, $\kappa_g l = 2$, $l = 0.0005$m, $l_{ext} = 0.1$m, $\phi_1 = 0.0\pi$, $2\beta_B l = 0\pi$, $\psi = 0\pi$, $R_1 = 1$ the critical feedback ratio is found for different values of reflection coefficient R_2. The plot is shown in figure 6.16. From this plot we find that the critical feedback ratio increases at a very low rate against R_2. Comparing this case with the two cases of figure 6.14 and 6.15 we observe that the values of Γ_c within the choosen range of R_2 for the present case is much lower than the other two cases of pure index coupling.

iii) 'Gain plus index' coupled DFB semiconductor laser with external feedback:

For complex coupling i.e., 'gain plus index' coupled DFB semiconductor laser a plot of critical feedback ratio against reflection coefficient is presented in figure 6.17 for the combinations of parameters of $\kappa_n l = 1$, $\kappa_g l = 3$, $l = 0.0005$m, $l_{ext} = 0.1$m, $\phi_1 = 0.25\pi$, $2\beta_B l = 0\pi$, $\psi = 0\pi$, $R_1 = 1$. $\phi_1 = 0.25\pi$ value is choosen because for this value minimum threshold gain is obtained (figure 6.5). In this case a dip in Γ_c is observed at R_2=0.5. However, the Γ_c value varies from 10^{-2} to $1.5X10^{-3}$ within the range of R_2.

Similarly, another graph is plotted for 'gain plus index' coupled DFB laser with the following parameters $\kappa_n l = 4$, $\kappa_g l = 1$, $l = 0.0005$m, $l_{ext} = 0.1$m, $\phi_1 = 0.0\pi$, $2\beta_B l = 0\pi$, $\psi = 0\pi$, $R_1 = 1$. The choice of ϕ_1 is made on the same basis of minimum threshold gain (figure 6.6). The plot is shown in figure 6.18. This graph shows a large value of Γ_c at R_2=0.03. The value of Γ_c falls at a fast rate to a low value at 0.04 and after which Γ_c values swing within a small range for the range of values of reflection coefficient from .04 to .3.

Comparing figure 6.5 and 6.6 we find that for 'gain plus index' coupled with coupling coefficients $\kappa_n l$=1, and $\kappa_g l$=4 has the largest gap between its minimum and maximum threshold gain without feedback. The critical feedback ratio against power reflection coefficient for this case with $\kappa_n l$=1, $\kappa_g l$=4, $\phi_1 = 1.75\pi$, $l = 0.0005$m, $l_{ext} = 0.1m$, $2\beta_B l = 0\pi$, $\psi = 0\pi$ is presented in figure 6.19. Here also, the value of ϕ_1 is choosen on the basis of minimum threshold gain (figure 6.5). The plot of figure 6.19 shows that a sudden change of Γ_c occurs for R_2=0.8 to 0.9 and a smooth

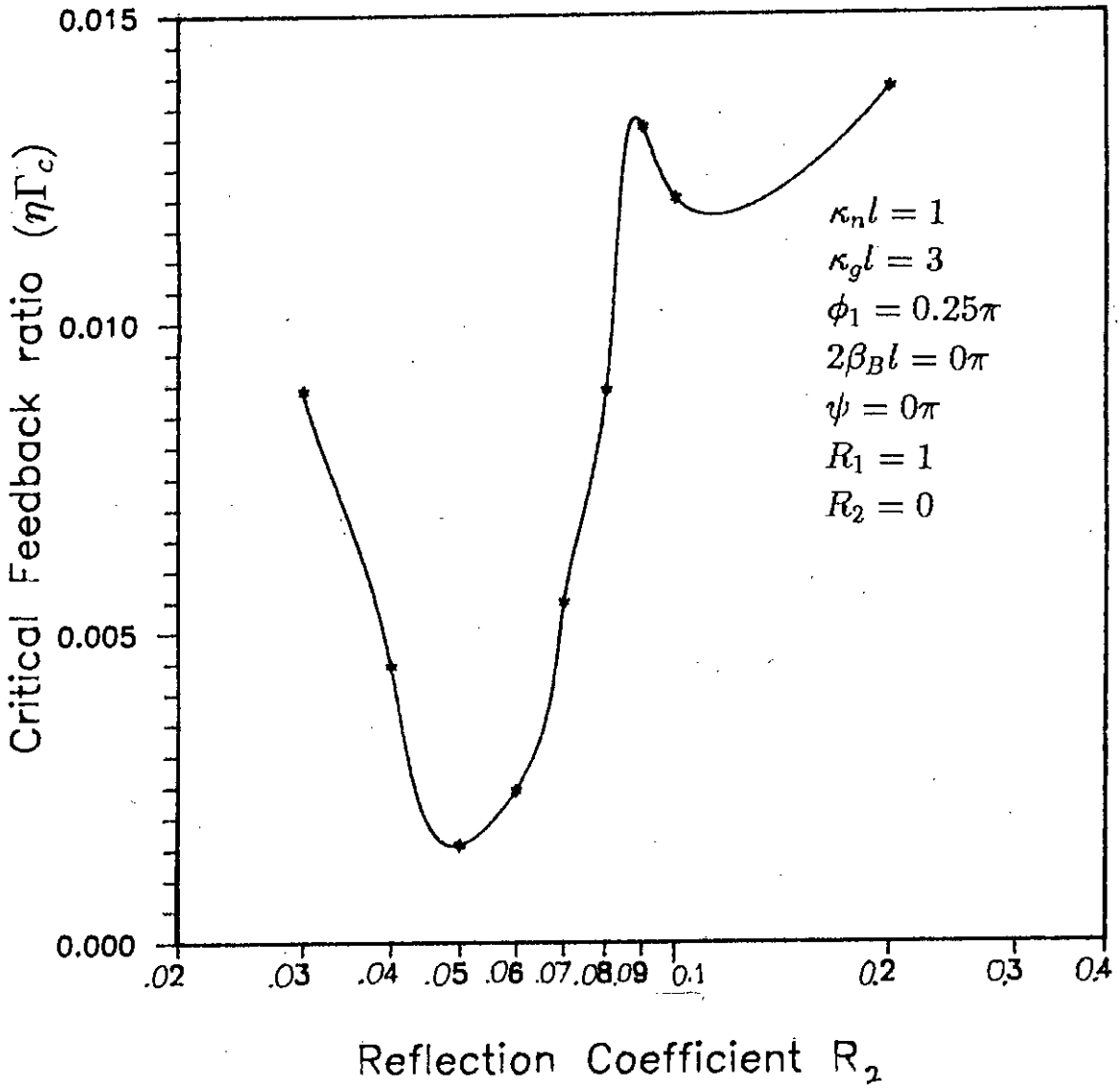

Figure 6.17: Plot of critical feedback ratio against reflection coefficient (R_2) for 'gain plus index' coupled ($\kappa_n l = 1$, $\kappa_g l = 3$) DFB laser. Here, $\phi_1 = 0.25\pi$, $2\beta_B l = 0\pi$, $\psi = 0\pi$, $R_1 = 1$.

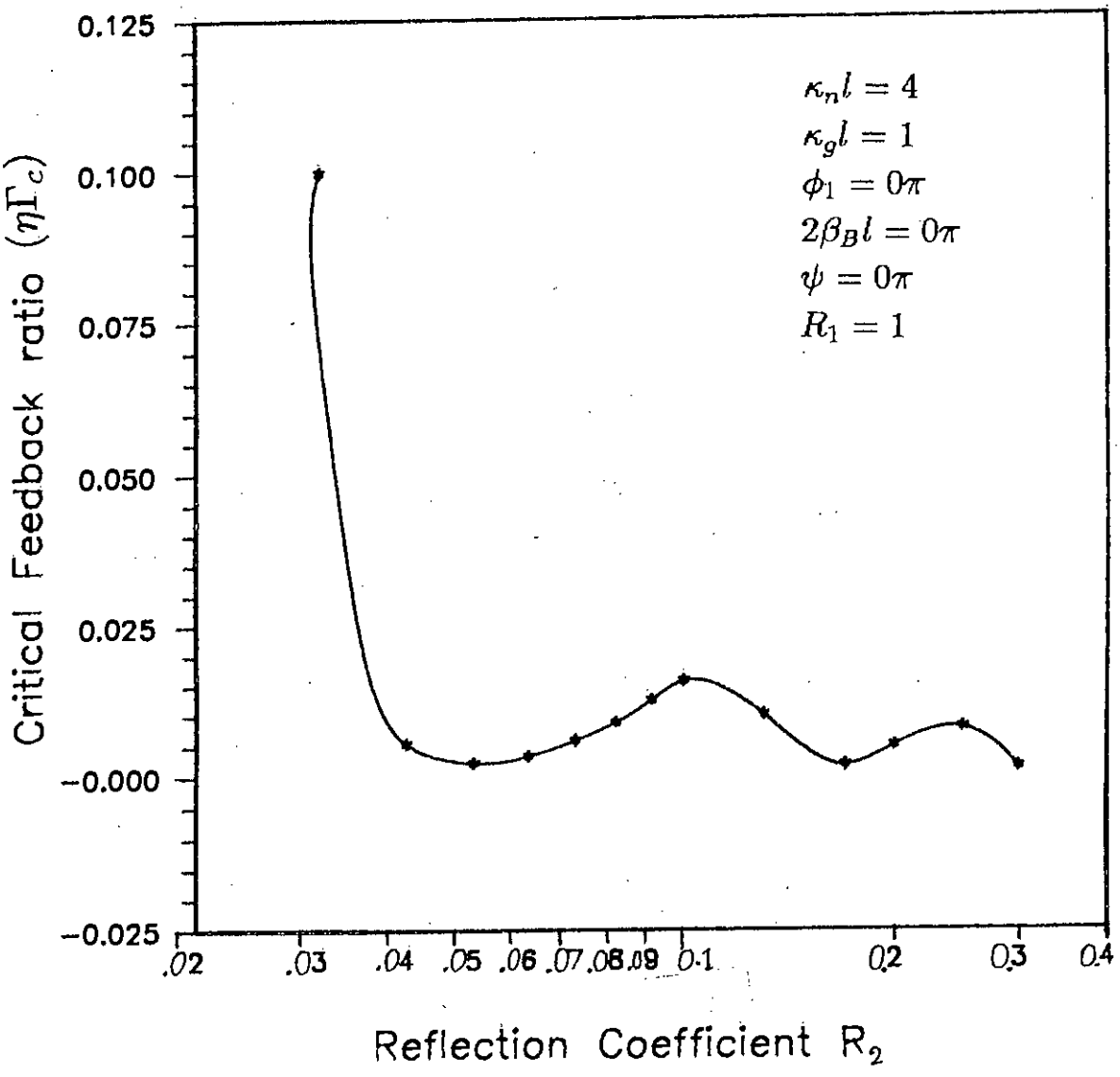

Figure 6.18: Plot of critical feedback ratio against reflection coefficient (R_2) for 'gain plus index' coupled ($\kappa_n l = 4$, $\kappa_g l = 1$) DFB laser. Here, $\phi_1 = 0.0\pi$, $2\beta_B l = 0\pi$, $\psi = 0\pi$, $R_1 = 1$

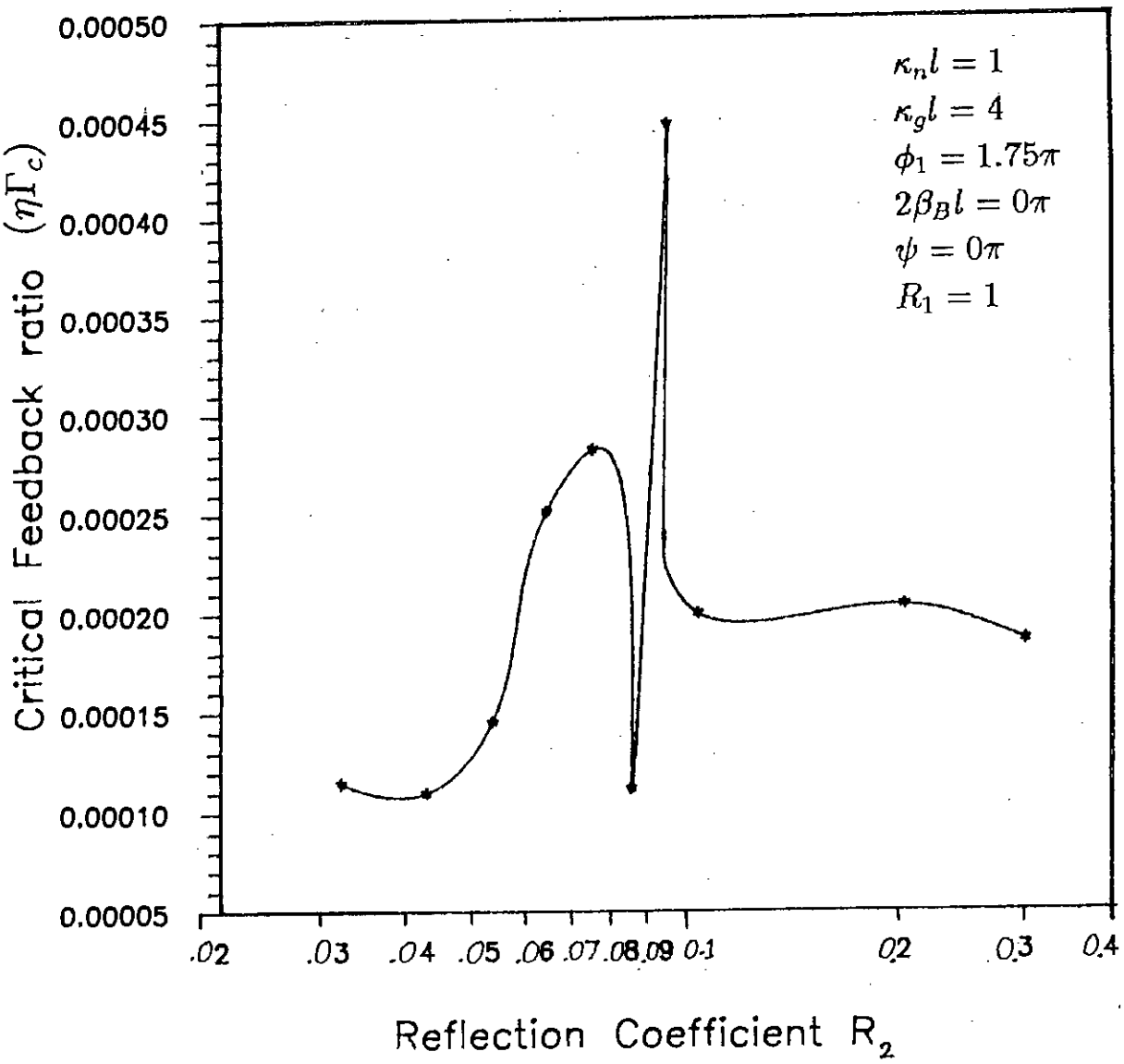

Figure 6.19: Plot of critical feedback ratio against reflection coefficient (R_2) for 'gain plus index' coupled ($\kappa_n l = 1$, $\kappa_g l = 4$) DFB laser. Here, $\phi_1 = 1.75\pi$, $2\beta_B l = 0\pi$, $\psi = 0\pi$, $R_1 = 1$

change occurs within R_2=0.1 to 0.3. This type of laser shows the lowest critical feedback ratio among the types of DFB semiconductor laser considered.

6.6 Summary

Numerical solutions of the oscillation condition for pure index, pure gain and 'gain plus index' coupled DFB semiconductor laser without external feedback have been obtained. The various results have been analyzed. Also, numerical solutions of the oscillation condition for pure index, pure gain and 'gain plus index' coupled DFB semiconductor laser with external feedback have been obtained for various combinations of parameters. The results have been presented in graphical form. The obtained results have been analyzed. Critical feedback ratio values have been obtained for the above mentioned cases and plots of critical feedback ratio against power reflection coefficient at the right facet of a DFB semiconductor laser have been presented.

CHAPTER 7

Discussions and suggestions

7.1 Discussions

Using Maxwell's equations for Electric and Magnetic fields, the equations representing the oscillation condition for a DFB semiconductor laser have been derived following previous publications [14][17][18]. At first, Equations have been derived for pure index coupled DFB semiconductor laser. Then, equations for 'gain plus index' coupled DFB semiconductor laser have been derived by following the same technique used for the above mentioned index coupled case. One of the purpose of this study is to observe the behaviour of a DFB laser under situations when a portion of laser output, after getting reflected from an external surface, enters into the laser. Such a situation has been termed as external reflection. The equations representing the oscillation condition for the 'gain plus index' coupled DFB semiconductor laser have been derived after taking into account of the external reflection. For taking into account of the effect of external feedback the arrangement of external feedback and the method of computation used in [32][33][34][39] have been accepted. Using this method the equations representing the oscillation condition have been modified to take into account of the external feedback. The equations for 'gain plus index' coupled DFB semiconductor laser with external reflection have been taken as general equations since by putting coupling coefficient $\kappa_g l$=0 we can get the equations for pure index coupled case, and by putting $\kappa_n l$=0 we can get the equations for pure gain coupled case from the same generalized equations. If external feedback does not exist then we have to set external reflection coefficient Γ=0.

The equation representing the oscillation condition contains real as well as imaginary terms. As a result it was necessary to split the complex equation into a real

equation and an imaginary equation. Solutions for real and imaginary equations were obtained separately by numerical computations. The intersections of the curves containing real solutions and the curves containing imaginary solutions were taken as the final solutions of the complex equation representing the oscillation condition. Computer programmes have been developed for the generalized 'gain plus index' coupled case and numerical solutions were obtained for different set of parameters. During the computation process we have found that the plots of real solutions and the plots of imaginary solutions sometimes tend to be a touching point rather than a crossing point (figure 6.1). Often, after the magnification of that region, we find that they do not meet at all although the meeting point is also a solution (because both the real and imaginary parts are zero).

Solutions of three types (i.e., (i) pure index coupled, (ii) pure gain coupled and (iii) 'gain plus index' coupled) of DFB semiconductor laser have been obtained using the generalized equations representing the oscillating condition. For each case numerical computations have been performed at first without taking into account of the external feedback and next taking the effect of external feedback into account. The minimum threshold gain for various set of parameters for the above mentioned three types of laser have been obtained with the help of the computer programme mentioned above. The value of minimum threshold gain is important because it indicates which laser will oscillate at the lowest value of injection current.

Kogelnik and Shank [17] showed theoretically that the gain coupled DFB laser would work better than the index coupled DFB laser because the index coupled laser has no oscillation at Bragg frequency but the pure gain coupled laser oscillate at Bragg frequency [17]. This result has been confirmed by Eli Kapon et. al. in [37]. We have also observed the same results during the computation (figure 6.11).

In the operation of a DFB laser in presence of external feedback the critical feedback ratio indicates the highest feedback ratio after which single mode operation is not possible. Therefore, for a DFB laser operation in presence of external feedback, it is necessary to know the value of critical feedback ratio in addition to the lowest threshold gain. A DFB semiconductor laser having a high critical feedback ratio will be very much useful for applications where external feedback exists. It is found that critical feedback ratio changes with the variation of R_2. The sensitivity

of this variation is different for different set of parameters. For observation of this sensitivity we have taken a range of values of the right (front) end facet reflection coefficient R_2 =0.03 to 0.3. A number of combinations of coupling coefficients have been taken for computation of threshold gains. For each set of coupling coefficients the sensitivity due to variation of corrugation phase shift angle ϕ_1 have been computed. From each of these obtained curves the value of ϕ_1 at which minimum value of threshold gain occurs has been obtained. With this value of ϕ_1 critical feedback ratio Γ_c has been computed. The sensitivities of Γ_c due to the variation of the front (right) end facet reflection are then computed and plotted.

Our computations show that for pure index coupled DFB semiconductor laser having the coupling coefficient $\kappa_n l$=3, $R_1 = 1$, $R_2 = 0$, $2\beta_B l = 0$, $\psi = 0$, $l = 0.0005m$ and the lowest value of threshold gain obtained at a value of corrugation phase shift angle of $\phi_1 = 0.75\pi$ (figure 6.3). For this laser the effect of external feedback was taken into consideration and it found that the oscillation frequency has a deviation from the Bragg frequency by about 2.52 radian at lower value of feedback ratio and decreases with the higher of value feedback ratio (figure 6.9) and it has the highest value of deviation from the Bragg frequency among the three examples considered here. Computations also show that for pure gain coupled DFB semiconductor laser with $\kappa_g l = 2$, $R_1 = 1$, $R_2 = 0$, $2\beta_B l = 0$, $\psi = 0$ the value of grating phase shift angle $\phi_1 = 0$ produces lowest possible gain (figure 6.4). Here, for this case the deviation from the Bragg frequency at lower value of feedback ratio is very small around 0.008 and increases to 0.013 for a higher value of feedback ratio (figure 6.11). For a 'gain plus index' coupled DFB semiconductor laser having the parameters as $\kappa_n l = 1$, $\kappa_g l = 3$, $R_1 = 1$, $R_2 = 0$, $2\beta_B l = 0$, $\psi = 0$ the lowest threshold gain is obtained at a grating phase shift angle of $\phi_1 = 0.25\pi$ (figure 6.5). This 'gain plus index' coupled laser has a deviation from the Bragg frequancy by about .408 radian. It appears from these examples that the pure gain coupled DFB laser will have minimum deviation between the oscillation frequency and the Bragg frequency. This deviation has significant value for pure index and 'gain plus index' coupled DFB lasers. For some combinations of parameters the deviation may be higher in index coupled case and for another combination (assuming same value of $\kappa_n l$ for both index coupled and 'gain plus index' coupled cases) this deviation may

be higher in 'gain plus index' coupled lasers.

Among the three types of laser considered here the pure index coupled DFB laser shows the highest critical feedback ratio over the selected variation range of R_2=0.03 to 0.3, but a highest critical feedback ratio is not the only criterion for the selection of a laser. The range of variation of critical feedback ratio with the change in reflection coefficient of the transmitting (front) end facet of the laser is also a significant factor. It is desirable that due to the variation of transmitting end facet reflection the changes in critical feedback ratio should be very small. Therefore, a DFB laser having high values of critical feedback ratio and very small changes in critical feedback values should be a good choice. From this view point, for pure index coupled DFB laser having $\kappa_n l = 3$, $\kappa_g l = 0$, $\phi_1 = 0.75\pi$, $2\beta_B l = 0$, $\psi = 0$, $l = 0.0005m$, $l_{ext} = 0.1m$ has a minimum value of $\Gamma_c = 0.1$ over the range of R_2=0.03 to 0.3 and appears to give good results (figure 6.14). Following the above guide line, the pure gain coupled DFB laser having $\kappa_g l = 2$, $\kappa_n l = 0$, $\phi_1 = 0$, $2\beta_B l = 0$, $\psi = 0$, $l = 0.0005m$, $l_{ext} = 0.1m$ has a minimum value of $\Gamma_c = 0.006$ over the range of R_2=0.03 to 0.3 and appears to give good results (figure 6.16). On the same basis the 'gain plus index' coupled laser having $\kappa_n l = 4$, $\kappa_g l = 1$, $\phi_1 = 0$, $2\beta_B l = 0$, $\psi = 0$, $l = 0.0005m$, $l_{ext} = 0.1m$ has a minimum value of $\Gamma_c = 0.002$ over the range of R_2=0.03 to 0.3 and appears to give good performance over the range of R_2=0.04 to 0.3. At this stage it seems that further computations need to be done with the help of the same computer programme and by varying the coupling coefficients as well as the remaining parameters to search for better set of parameters. During computations it has been observed that using the developed computer program on a 486 microcomputer approximately 15 sec is required (2min by a 286 microcomputer) for obtaining the complete plot including the computations for real and imaginary parts of the equation.

7.2 Suggestions for future work

In the present work an analytical expression for critical feedback could not be presented. An analytical expression for critical feedback ratio will be very useful for studying the effects of various parameters e.g., $\kappa_g l$, $\kappa_n l$, ϕ_1, r_1, r_2, $(\overline{g}-\alpha)$ etc. on

the critical feedback ratio. With the help of such an expression it is expected that computation time can be reduced significantly. Therefore, deducing an analytical expression for critical feedback ration can be done in future.

We have studied the 'gain plus index' coupled DFB semiconductor laser having the coupling coefficient (i) $\kappa_n l$=1, $\kappa_g l$=1, 2, 3, 4 and (ii) $\kappa_g l$=1, $\kappa_n l$=1, 2, 3, 4. The other combinations of coupling coefficients may be studied for a better DFB laser. Instead of selecting individually κ_n and κ_g for searching a good and useful combination it might be worthwhile treating $\kappa_n + j\kappa_g$ as $|\kappa|e^{j\theta}$ and varying both $|\kappa|$ and θ. The obtained results may be presented in some other forms for easy interpretation and analysis.

In the present work, sinusoidal variation has been assumed for both index and gain corrugations. It may be worthwhile studying a sawtooth wave type of periodic variation of corrugations and square wave type of periodic variation of corrugations. The effect of having sinusoidal variation for index corrugation and square wave variation for gain corrugation, and square wave variation for index corrugation and sinusoidal variation for gain corrygation may be studied. Similarly, other combinations may also be studied.

It is expected that by using a different algorithm for the complete solutions of real and imaginary parts of the generalized equation representing the oscillation condition of a DFB semiconductor laser computation time could be minimized. Thus some work on the development of a new computer programme for this purpose needs to be done.

REFERENCES

[1] A. L. Schawlow and C. H. Townes, "Infrared and optical masers," Physical Review vol. 112, December 1958, pp. 1940-1949.

[2] T. H. Maiman, "Stimulated optical radiation in ruby masers," Nature, vol. 187, August 1960, pp. 493-494.

[3] A. Javan, W. R. Benette Jr. and D. R. Herriott, "Population inversion and continuous optical maser oscillation in a gas discharge containing a He - Ne mixture," Physical Review Letters, vol. 6, February 1961, pp. 106-110.

[4] Jeff Hecht, "The laser guide book", Mc Graw-Hill book company, contributed edition 1986, pp. 9-16.

[5] L. P. Johnson, "Optically pumped pulsed crystal laser other than ruby," A. K. Levin, editor, Lasers, vol. 1, Morsel Dekker, New york, 1966, pp. 137-180.

[6] Z. J. Kiss and R. J. Pressley, "Crystalline Solid lasers," Proc. IEEE vol. 54, October 1966, pp. 1236-1248.

[7] D. W. Goodwin and O. S. Heavens, "Doped crystal and gas laser," Rep. Prog. Phys., vol. 31, pt. 2, 1968, pp. 777-859.

[8] L. F. Johnson, G. D. Boyd, K. Nassau, and R. R. Soden, "Continuous operation of a $CaWO_4$: Nd^{3+} optical maser," Proc. IRE, correspondance, vol. 50, February 1962, P. 213.

[9] V. Evtuhov and J. K. Neeland, "Continuous operation of a ruby laser at room temperature," Applied Physics Letters, vol. 6, February 1965, pp. 75-76.

[10] D. Ross, "Room temperature ruby CW laser," Microwaves, vol. 3, April 1965, p. 29.

[11] C. G. Yang, "Continuous glass laser," Applied Physics Letters, vol. 2, April 1963, pp. 151-152.

[12] R. C. Duncan Jr., "Continuous room temperature $Nd : CaMO_4$ laser," Journal of Applied Physics, vol. 36, March 1965, pp. 874-875.

[13] T. Kushida, H. M. Marcos and J. E. Gausic, "Laser transition crosssection and flurescence branching ratio for Nd in Yattrium Aluminium Garnet," Physical review, vol. 157, March 10, 1968, pp. 289-291.

[14] Amon Yariv, "Optical Electronics," 4th edition, Saunders College Publishing, Holt, Rinehart and Winston Inc., Philadelphia, USA, 1991, pp. 565-572, 174-181.

[15] Tsukada T., "$GaAs - Ga_{1-x}Al_xAs$ buried heterostructure injection laser," Journal of Applied Physics, vol. 45, 1974, p. 4899.

[16] A. Yariv, "Quantum Electronics," Wiley, New York, 1967, pp. 242-243.

[17] H. Kogelnik and C.V. Shank, "Coupled wave theory of distributed feedback laser," Journal of Applied Physics, vol. 43, 1972, pp. 2327-2335.

[18] H. Kogelnik and C. V. Shank, "Stimulated emission in a periodic structure," Applied Physics Letters, vol. 18, February 1971, pp. 152-154.

[19] K. Aiki, M. Nakamura, J. Umeda, A. Yariv, A. Katzir and H. W. Yen, "GaAs-GaAlAs Distributed feedback diode lasers with seperate optical and Carrier confinement," Applied Physics Letters, vol. 27, No. 3, August 1975, pp. 145-146.

[20] A. Yariv, "Quantum Electronics," New York, Wiley, 1975, Section 19.6.

[21] K. O. Hill and A. Watanabe, "Envelope gain saturation in distributed feedback lasers," Applied Optics, vol 14, 1975, pp. 950-961.

[22] H. A. Haus, "Gain saturation in distributed feedback lasers," Applied Optics, vol. 14, 1975, pp. 2650-2652.

[23] S. Solimeno and G. Mastrocique, "Gain saturation and output power of distributed feedback lasers," Juornal of Physics, vol. A9, 1976, pp. 1309-1321.

[24] D. C. Flanders, H. Kogelnik, R. V. Schmidt and C. V. Shank, "Grating filters for thin film optical wave guides," Applied Physics Letters, vol. 24, February 1974, pp. 194-196.

[25] Amon Yariv and Michihara Nakamura, "Periodic structures for integrated optics," IEEE Journal of Quantum Electronics, vol. QE-13, No. 4, April, 1977, pp. 233-253.

[26] E. J. Steples, J. S. Schoenwald, R. C. Rosenfield and C. S. Hartmann, "UHF surface accoustic wave resonators," in Proc., IEEE Ultrasonic Symp., 1974, November 11-14, 1974, pp. 245-252.

[27] J. S. Schoenwald, R. C. Rosenfield and E. J. Steples, "Surface wave cavity and resonance characteristics VHF and L-band," in Proc. IEEE, Ultrasonic Symp., 1974, Nov. 11-14, pp. 253-256.

[28] P. P. Sorokin and J. R. Lankard, "Stimulated emission observed from an organic dye, chloroaluminium phtatocyanine," IBM Journal of Research and Development, vol. 10, September 1966, p. 401.

[29] R. Lang and K. Kobayashi, "External Optical Feedback Effects on Semiconductor Injection Laser Properties," IEEE Journal of Quantum Electronics, vol. QE-16, No. 3, March 1980, pp. 347-355.

[30] M. Yamada and M. Suraha, "Analysis of Excess Noise induced by Optical Feedback in Semiconductor Lasers Based on Mode Competition Theory," The transactions of the IEICE, vol. E 73, No. 1, January 1990, pp. 77-82.

[31] H. A. Haus, "Waves and Fields in Optoelectronics," Prentice-Hall Inc., New Jersey, 1984, p. 15.

[32] Saiful Islam, Michihiko Suhara and Minoru Yamada, "The effect of optical feedback on pure gain and 'gain plus index' corrugated DFB semiconductor lasers, "Fellowship research report 1991, the Matsumae International Foundation, Tokyo, Japan, 1991, 1991-43p.

[33] Michihiko Suhara, Saiful Islam and Minoru Yamada, "Criterion of external feedback sensitivity in DFB semionductor lasers to be free from induced excess intensity noise," Conference on lasers and electro-optics CLEO 1992, held in Anaheim, California, 10-15 May 1992, Technical digest series, vol. 12, pp. 304-306.

[34] Michihiko Suhara, Saiful Islam and Minoru Yamada, "Criterion of external feedback sensitivity in index coupled and gain coupled DFB semiconductor lasers to be free from excess intensity noise," Accepted for publication in IEEE journal of Quantum Electronics.

[35] Yoshika Nakano and Kunio Tada, "Short-wavelength, distribute-feedback semiconductor lasers, including those based on gain coupling," Asia-Pacific Engineering Journal (Part A), vol. 1, No. 1 (1991) pp. 37-58.

[36] Minoru Yamada, "Theoretical analysis of line-broadening due to mode competition and optical feedback in semiconductor injections lasers'" The transactions of the IEICE, vol. E 71, No. 2, February 1988, pp. 152-160.

[37] Eli Kapon, A. Hardy and Abraham Katzir, "The effect of complex coupling coefficients on distributed feedback lasers," IEEE Journal of Quantum Electronics, vol. QE-18, No. 1, January 1982, pp. 66-71.

[38] Francois Favre, "Theoretical analysis of external optical feedback on DFB semiconductor lasers," IEEE Journal of Quantum Electronics, vol. QE-23, No. 1, January 1987, pp. 81-88.

[39] Yi Luo, Yoshiaki Nakano, Kunio Tada, Takeshi Inoue, Haruo Hosomatsu, Hideto Iwaoka, "Fabrication and Characteristics of Gain-Coupled Distributed Feedback Semiconductor Lasers with a Corrugated Active Layer," IEEE Journal of Quantum Electronics, vol. QE-27, No. 6, June 1991, pp. 1724-1731.

[40] G. Morthier, P. Vankwikelberge, K. David and R. Baets, "Improved Performance of AR-Coated DFB Lasers by the Introduction of Gain Coupling," IEEE Photonics Technology Letters, vol. 2, No. 3, March 1990, pp. 170-172.

[41] John Allison, "Electronic Engineering Semiconductors and Devices," International Edition, McGraw-Hill Book Co., Singapore, 1990, pp. 313-316.

APPENDIX A

List of the computer programme

```
1110 SCREEN 12 'CONSOLE,,0,1
1120 '-------------------------CONSTANTS-----------------------
1130 'COLF = 5: COLG = 1
1140 L2 = .0005
1150 LMD = .0000008 / 2
1160 BB = 3.141592654# / LMD
1170 L = .1
1180 NR = 3
1190 DIM DBINI(21)
1200 '*START
1210 'LOCATE 1, 2: INPUT "CLS(Y/N)"; A$
1220 IF A$ = "Y" OR A$ = "y" THEN CLS 2
1230 'COLOR 7
1240 'If you would like to see dispersion relations.
1250 ' remove a single-quotation mark in the next line!
1260 'GOSUB 4390: END'*DISPERSION
1270 LOCATE 1, 2: INPUT "Keep parameters (y/n)"; B$
1280 IF B$ = "Y" OR B$ = "y" THEN GOTO 1360'*START2
1290 LOCATE 2, 1: INPUT "k nL,k gL"; KNL, KGL: KP = KNL / L2:
                                    KG = KGL / L2
1300 INPUT "R1,R2"; R1, R2
1310 INPUT "ϕ1 (AT LEFT FACET) Xπ "; xxx: TH1 = xxx *
                                    3.141592654#
1320 INPUT "2β BL (AT RIGHT FACET) Xπ "; xxx: TH2 = xxx *
                                    3.141592654#
1330 ' ϕ ;Phase difference between index and gain
1340 INPUT "ϕ   Xπ"; xxx: TH3 = xxx * 3.141592654#
1350 '*START2
1360 INPUT "XMIN,XMAX,YMIN,YMAX"; XMIN, XMAX, YMIN, YMAX
1370 INPUT "Γ eff=10^X  X"; GAMEFF: GAM = 10 ^ GAMEFF
1380 CLS 1
1390 LOCATE 2, 7: PRINT YMAX: LOCATE 26, 7: PRINT YMIN
1400 LOCATE 27, 12: PRINT XMIN: LOCATE 27, 76: PRINT XMAX
1410 LOCATE 16, 6: PRINT "(g-α)": LOCATE 27, 40: PRINT "δ β L"
1420 LOCATE 28, 6: PRINT "R1="; R1; "R2="; R2; "k nL="; KP * L2; "k gL=";
                                                    KG * L2;
1430 PRINT USING "&   &"; " ϕ1=";
1440 PRINT USING "#.##"; TH1 / 3.141592654#;
1450 PRINT "π  ";
1460 PRINT USING "&    &"; "2β BL=";
1470 PRINT USING "#.##"; TH2 / 3.141592654#;
1480 PRINT "π  ";
1490 LOCATE 29, 25: PRINT USING "&   &"; " ϕ=";
1500 PRINT USING "#.##"; TH3 / 3.141592654#;
1510 PRINT "π  ";
```

```
1520 PRINT USING "&   &"; "Γ eff=";
1530 PRINT USING "##.##^^^^"; GAM;
1540 PRINT "(=10^"; GAMEFF; ")"
1550 '  (XMIN,-YMAX)
1560 '
1570 '
1580 ' ( g-α)
1590 '   (DG)
1600 '
1610 '
1620 '                                          (XMAX,-YMIN)
1630 '                    δ β L
1640 '                    (DB)
1650 '
1660 '
1670 WINDOW (XMIN, YMAX)-(XMAX, YMIN): VIEW (91, 1)-(618,
                                    400), , 7
1680 FOR J = XMIN TO XMAX STEP (XMAX - XMIN) / 10
1690    LINE (J, YMIN)-(J, YMAX), , , &H8888
1700 NEXT J
1710 FOR J = YMIN TO YMAX STEP (YMAX - YMIN) / 10
1720    LINE (XMIN, J)-(XMAX, J), , , &H8888
1730 NEXT J
1740 LINE (XMIN, 0)-(XMAX, 0)
1750 LINE (0, YMIN)-(0, YMAX)
1760 LINE (XMIN, YMAX)-(XMAX, YMIN), , B
1770 'CCOL = 2: CCOL2 = 1
1780 '////////////////////////////////////////////
1790 'Find the solution of G(DB,DG)=0
1800 '////////////////////////////////////////////
1810 FOR Y = YMIN TO YMAX STEP (YMAX - YMIN) / 50
1820 DG = Y / L2
1830 NUM = 0
1840   FOR X = XMIN TO XMAX STEP (XMAX - XMIN) / 50
1850           DB = X / L2
1860            GOSUB 2440 '*FUNC
1870            IF X = XMIN THEN GOTO 1940'*ZZ1
1880            IF SGN(GG) = SGN(OLDGG) THEN GOTO 1940'*ZZ1
1890                    'FOR X=XMIN TO XMAX STEP (XMAX-XMIN)/50
1900                    '       IF DB=DBINI(I) THEN GOTO *ZZ1
1910                    'NEXT
1920            NUM = NUM + 1
1930            DBINI(NUM) = DB
1940    '*ZZ1
1950            OLDGG = GG
1960    NEXT X
1970    '
1980    FOR i = 1 TO NUM
1990            DB1 = DBINI(i)
2000            GOSUB 3850 '*HALF.G
2010    NEXT
2020 NEXT Y
```

```
2030 '////////////////////////////////////////
2040 'Find the solution of F(DB,DG)
2050 '////////////////////////////////////////
2060 FOR Y = YMIN TO YMAX STEP (YMAX - YMIN) / 50
2070 DG = Y / L2

2080 NUM = 0
2090    FOR X = XMIN TO XMAX STEP (XMAX - XMIN) / 50
2100            DB = X / L2
2110            GOSUB 2440 '*FUNC
2120            IF X = XMIN THEN GOTO 2190'*Z1
2130            IF SGN(FF) = SGN(OLDFF) THEN GOTO 2190'*Z1
2140                    'FOR X=XMIN TO XMAX STEP (XMAX-XMIN)/50
2150                    '       IF DB=DBINI(I) THEN GOTO *ZZ1
2160                    'NEXT
2170            NUM = NUM + 1
2180            DBINI(NUM) = DB
2190    '*Z1
2200            OLDFF = FF
2210    NEXT X
2220 '
2230    FOR i = 1 TO NUM
2240    '
2250            DB1 = DBINI(i)
2260            GOSUB 3320 '*HALF.F
2270    NEXT
2280 NEXT Y
2290 '*AXIS
2300 JJJ = JJJ + 1: BEEP: BEEP
2310 LOCATE 30, 1: INPUT "(x/y)"; X, Y
2320 IF X = -1 THEN GOTO 1200'*START
2330 'COLOR (JJJ MOD 6) + 1
2340 LOCATE 30, 15: PRINT "("; XMIN + X * (XMAX - XMIN) / 10;
                                                    ",";
2350 PRINT YMIN + Y * (YMAX - YMIN) / 10; ")"
2360 GOTO 2290 '*AXIS
2370 END
2380 '
2390 '########################################
2400 '# SUB ROUTINES
2410 '########################################
2420 '
2430 '////////////////////////////////////
2440 '  *FUNC
2450 '////////////////////////////////////
2460 'Calculation of the function F(DB,DG),G(DB,DG)
2470 '----------------------------------
2480 'Γ^2= P+jQ.  Γ= C+jD
2490 '----------------------------------
2500 P = KP * KP - KG * KG - DB * DB + DG * DG / 4
2510 Q = -DG * DB + 2 * KP * KG * COS(TH3)
2520 '
```

```
2530 IF P = 0 THEN GOTO 2600'*T1
2540    IF Q = 0 AND P < 0 THEN C = 0: D = SQR(-P): GOTO 2640'*T2
2550    IF Q = 0 AND P > 0 THEN C = SQR(P): D = 0: GOTO 2640'*T2
2560    C = SQR(ABS(P + SQR(P * P + Q * Q)) / 2)
2570    IF C = 0 AND P < 0 THEN D = SQR(-P): GOTO 2640'*T2
2580    D = Q / 2 / C
2590    GOTO 2640 '*T2
2600 '*T2
2610    IF Q = 0 THEN C = 0: D = 0: GOTO 2640'*T2
2620    IF Q < 0 THEN C = SQR(-Q / 2): D = Q / 2 / C: GOTO 2640'*T2
2630    IF Q > 0 THEN C = SQR(Q / 2): D = Q / 2 / C: GOTO 2640'*T2
2640 '*T2
2650 COSH = (EXP(-C * L2) + EXP(C * L2)) / 2
2660 SINH = (EXP(C * L2) - EXP(-C * L2)) / 2
2670 '
2680 'sinh
2690 '
2700 S1 = SINH * COS(D * L2)
2710 S2 = COSH * SIN(D * L2)
2720 '----------------------------------------
2730 'cosh(Γ L2 )=S1+jS2
2740 '----------------------------------------
2750 C1 = COSH * COS(D * L2)
2760 C2 = SINH * SIN(D * L2)
2770 '----------------------------------------
2780 U1 = 1 - SQR(R1 * R2) * COS(TH2) - SQR(R1 * GAM) * (1 -
       R2) * COS(TH2 + 2 * (BB + DB) * L / NR)
2790 V1 = SQR(R1 * R2) * SIN(TH2) + SQR(R1 * GAM) * (1 - R2) *
      SIN(TH2 + 2 * (BB + DB) * L / NR)
2800 U2 = C
2810 V2 = D
2820 U3 = C1
2830 V3 = C2
2840 GOSUB 3250 '*PRODUCT
2850 RR1 = PROR
2860 II1 = PROI
2870 '----------------------------------------
2880 U1 = -DG / 2
2890 V1 = DB
2900 U2 = 1 + SQR(R1 * R2) * COS(TH2) + SQR(R1 * GAM) * (1 -
     R2) * COS(TH2 + 2 * (BB + DB) * L / NR)
2910 V2 = -SQR(R1 * R2) * SIN(TH2) - SQR(R1 * GAM) * (1 - R2)
     * SIN(TH2 + 2 * (BB + DB) * L / NR)
2920 U3 = S1
2930 V3 = S2
2940 GOSUB 3250 '*PRODUCT
2950 RR2 = PROR
2960 II2 = PROI
2970 '----------------------------------------
2980 U1 = -KG * COS(TH3)
2990 V1 = KP + KG * SIN(TH3)
```

```
3000 U2 = SQR(R2) * COS(TH1 + TH2) + (1 - R2) * SQR(GAM) * COS(TH1 + TH2 +
                                                    2 * (BB + DB) * L / NR)
3010 V2 = -SQR(R2) * SIN(TH1 + TH2) - (1 - R2) * SQR(GAM) *
          SIN(TH1 + TH2 + 2 * (BB + DB) * L / NR)
3020 U3 = S1
3030 V3 = S2
3040 GOSUB 3250 '*PRODUCT
3050 RR3 = PROR
3060 II3 = PROI
3070 '-----------------------------------------
3080 U1 = -KG * COS(TH3)
3090 V1 = KP - KG * SIN(TH3)
3100 U2 = SQR(R1) * COS(TH1)
3110 V2 = SQR(R1) * SIN(TH1)
3120 U3 = S1
3130 V3 = S2
3140 GOSUB 3250 '*PRODUCT
3150 RR4 = PROR
3160 II4 = PROI
3170 '-----------------------------------------
3180 FF = RR1 + RR2 + RR3 + RR4
3190 GG = II1 + II2 + II3 + II4
3200 RETURN
3210 '*T4
3220 RETURN
3230 '
3240 '////////////////////////////////
3250 '*PRODUCT
3260 '////////////////////////////////
3270 PROR = U1 * U2 * U3 - U1 * V2 * V3 - U2 * V1 * V3 - U3 *
                                          V1 * V2
3280 PROI = U1 * U2 * V3 + U1 * U3 * V2 + U2 * U3 * V1 - V1 *
                                          V2 * V3
3290 RETURN
3300 '
3310 '////////////////////////////////
3320 '*HALF.F
3330 'Half devided search along X axis to solve F=0
3340 '////////////////////////////////
3350 WX = (XMAX - XMIN) / 200 / L2
3360 COUNT = 0
3370 DB2 = DB1 + WX
3380 '*ML1
3390 COUNT = COUNT + 1
3400 IF COUNT = 20 THEN GOTO 3800'*ML5
3410 DB = DB1
3420 GOSUB 2440 '*FUNC
3430 F1 = FF
3440 '
3450 DB = DB2
```

```
3460 GOSUB 2440 '*FUNC
3470 F2 = FF
3480 IF DB2 * L2 > XMAX OR DB2 * L2 < XMIN THEN GOTO 3800'*ML5
3490 IF F1 * F2 < 0 THEN GOTO 3520'*ML2
3500 IF ABS(F1) > ABS(F2) THEN DB1 = DB2: DB2 = DB1 + WX: GOTO 3380'*ML1
3510 IF ABS(F1) < ABS(F2) THEN DB2 = DB1: DB1 = DB2 - WX: GOTO 3380'*ML1
3520 '*ML2
3530 COUNT = COUNT + 1
3540 IF COUNT = 20 THEN GOTO 3800'*ML5
3550 DB3 = (DB1 + DB2) / 2
3560 DB = DB3
3570 GOSUB 2440
3580 F3 = FF
3590 '
3600 IF (F1 * F3) < 0 THEN GOTO 3700'*ML3
3610 '
3620 DB1 = DB3
3630 DB = DB1
3640 GOSUB 2440
3650 F1 = FF
3660 '////////////////Judgement of convergence//////////////////
3670    IF ABS(F1 - F2) < 10 THEN GOTO 3780'ML4
3680 GOTO 3520 'ML2
3690 '
3700 '*ML3
3710 DB2 = DB3
3720 DB = DB2
3730 GOSUB 2440 '*FUNC
3740 F2 = FF
3750 IF ABS(F1 - F2) < 10 THEN GOTO 3780 *ML4
3760 GOTO 3520 '*ML2
3770 '
3780 '*ML4
3790    CIRCLE (DB3 * L2, DG * L2), (XMAX - XMIN) / 300 '
                                   CCOL2 ', , F
3800 '*ML5
3810 RETURN
3820 '
3830 '
3840 '////////////////////////////////////////
3850    '*HALF.G
3860 'Half devided search along X axis to solve G=0
3870 '////////////////////////////////////////
3880 WX = (XMAX - XMIN) / 200 / L2
3890 COUNT = 0
3900 DB2 = DB1 + WX
3910 '*MN1
3920 COUNT = COUNT + 1
3930 IF COUNT = 20 THEN GOTO 4340'*MN5
3940 DB = DB1
3950 GOSUB 2440 '*FUNC
```

```
3960 G1 = GG
3970 '
3980 DB = DB2
3990 GOSUB 2440 '*FUNC
4000 G2 = GG
4010 IF DB2 * L2 > XMAX OR DB2 * L2 < XMIN THEN GOTO 4340'*MN5
4020 IF G1 * G2 < 0 THEN GOTO 4060'*MN2
4030 IF ABS(G1) > ABS(G2) THEN DB1 = DB2: DB2 = DB1 + WX: GOTO 3910'*MN1
4040 IF ABS(G1) < ABS(G2) THEN DB2 = DB1: DB1 = DB2 - WX: GOTO 3910
4050 '
4060 '*MN2
4070 COUNT = COUNT + 1
4080 IF COUNT = 20 THEN GOTO 4340'*MN5
4090 DB3 = (DB1 + DB2) / 2
4100 DB = DB3
4110 GOSUB 2440
4120 G3 = GG
4130 '
4140 IF G1 * G3 < 0 THEN GOTO 4240'MN3
4150 '
4160 DB1 = DB3
4170 DB = DB1
4180 GOSUB 2440 'FUNC
4190 G1 = GG
4200 '////////////////JUDGEMENT OF CONVERGENCE/////////////
4210 IF ABS(G1 - G2) < 10 THEN GOTO 4320'*MN4
4220 GOTO 4060 '*MN2
4230 '
4240 '*MN3
4250 DB2 = DB3
4260 DB = DB2
4270 GOSUB 2440 '*FUNC
4280 G2 = GG
4290 IF ABS(G1 - G2) < 10 THEN GOTO 4320'*MN4
4300 'LOCATE 23, 1: PRINT ABS(G1 - G2): GOTO 4060'*MN2
4310 '
4320 '*MN4
4330    CIRCLE (DB3 * L2, DG * L2), (XMAX - XMIN) / 200 '
                                        CCOL' 1
4340 '*MN5
4350 RETURN
4360 '
4370 '
4380 '////////////////////////////////////////
4390      '*DISPERSION
4400 '
4410 '////////////////////////////////////
4420 INPUT "XMIN,XMAX"; XMIN, XMAX
4430 WINDOW (XMIN, -XMAX)-(XMAX, -XMIN)
4440 VIEW (1, 1)-(300, 300), , 7
4450 FOR X = XMIN TO XMAX
```

```
4460    LINE (X, -XMIN)-(X, -XMAX), , , &H8888
4470    LINE (XMIN, -X)-(XMAX, -X), , , &H8888
4480 NEXT X
4490 LINE (XMIN, 0)-(XMAX, 0): LINE (0, -XMIN)-(0, -XMAX)
4500 '
4510 VIEW (310, 1)-(610, 300), , 7
4520 FOR X = XMIN TO XMAX
4530    LINE (X, -XMIN)-(X, -XMAX), , , &H8888
4540    LINE (XMIN, -X)-(XMAX, -X), , , &H8888
4550 NEXT X
4560 LINE (XMIN, 0)-(XMAX, 0): LINE (0, -XMIN)-(0, -XMAX)
4570 LOCATE 1, 19
4580 'INPUT "Select a color number from 1 to 6."; col
4590 INPUT "Input a value (g-α)L ="; idg: DG = idg / L2
4600 INPUT "Input a value k iL"; ikp: KP = ikp / L2
4610 INPUT "              k gL"; ikg: KG = ikg / L2
4620 INPUT "              ϕ Xπ"; xxx: TH3 = xxx * 3.141592654#
4630 FOR X = XMIN TO XMAX STEP (XMAX - XMIN) / 400
4640 DB = X / L2
4650 GOSUB 2440 '*func
4660 '
4670 VIEW (1, 1)-(300, 300)
4680 PSET (X, -D * L2): PSET (X, D * L2)
4690 '
4700 VIEW (310, 1)-(610, 300)
4710 PSET (X, -C * L2): PSET (X, C * L2)
4720 NEXT X
4730 '
4740 RETURN
```